



UNIVERSIDAD NACIONAL DE COLOMBIA

Validation of the Square Wave Anodic Stripping Voltammetry methodology for cadmium quantification in *Theobroma cacao* L. beans

Maria Camila González Basto

Universidad Nacional de Colombia
Facultad de Ciencias, Departamento de Química
Bogotá D.C., Colombia
2023

Validation of the Square Wave Anodic Stripping Voltammetry methodology for cadmium quantification in *Theobroma cacao* L. beans

Maria Camila González Basto

Thesis submitted in partial fulfilment of the requirements for the Degree of:
Master of Science in Chemistry

Director:

Dr. Andrea Del Pilar Sandoval Rojas

Co-Director:

MSc. Carlos Andrés España Sánchez

Advisor:

Dr. Jesús Alberto Ágreda Bastidas

Lines of Investigation:

Analytical Electrochemistry

Research Groups:

Grupo de Estudios para la Remediación y Mitigación de Impactos Negativos al Ambiente -
GERMINA

Grupo de investigación en Electroquímica y Termodinámica Computacional

Grupo de investigación en Metrología Química y Bioanálisis - GIMQB

Universidad Nacional de Colombia
Facultad de Ciencias, Departamento de Química
Bogotá D.C., Colombia

2023

To my family

Acknowledgment

I extend my sincere thanks to my family: my mother, my father, my aunt, and my sisters. To Felipe for his unwavering support and belief in me.

I want to express my gratitude to all the people who were with me, supporting me during my master's studies, especially:

To Dr. Andrea del Pilar Sandoval Rojas for successfully directing this work.

To Dr. Jesús Alberto Ágreda Bastidas for his advice at every stage of the research project.

To MSc. Carlos Andrés España Sánchez for the co-direction of this work.

To my research group partner Jessica Smith for her friendship and support.

To the institutions:

To the Instituto Nacional Metrología de Colombia (INM) and the Universidad Nacional de Colombia - sede Bogotá for allowing the development of this research under the project - 9932100271370 "Plan de Fortalecimiento del Instituto Nacional de Metrología como centro de investigación" funded by the Ministerio de Ciencia, Tecnología e Innovación de Colombia (MINCIENCIAS).

Abstract

Cadmium is toxic to humans. It accumulates in the body, causing kidney, lung, and bone damage. The new European Union (EU) regulation No 488/2014 on maximum cadmium levels in different types of chocolate and cocoa powder entered into force in January 2019. Its main aim is to address high levels of food safety in these foodstuffs. Therefore, cadmium quantification in cocoa beans has become a need for producers. They must guarantee consistently high-quality products and, at the same time, compliant with the maximum levels of Cd^{2+} that oscillate between 0.1 and 0.8 mg kg^{-1} for the different types of chocolate and 0.6 mg kg^{-1} in cocoa powder. Considering the previous facts, this study presents the development and validation of a reliable electroanalytical method for Cd^{2+} determination in cocoa by Square Wave Anodic Stripping Voltammetry (SWASV) with bismuth film on glassy carbon electrodes as working electrodes (BiFE). The study was carried out in conjunction with the Instituto Nacional de Metrología de Colombia (INM) under the “Plan de Fortalecimiento” project.

The first step of the study was the characterization of the bismuth reduction process on glassy carbon using Cyclic Voltammetry, Chronoamperometry, and Electrochemical Impedance Spectroscopy. The bismuth film deposited over a working glassy carbon electrode showed an increment of the electrode area and the heterogeneous charge transfer rate constant value. These improvements help us to understand the enhancement in the voltammetric signal of cadmium obtained by anodic stripping voltammetry, validating the selection of this modified working electrode in the present investigation. On the other hand, combining the internal standard *in situ* calibration with the single-point standard addition method is proposed as a useful and faster alternative to the traditional multi-point calibration method. The performance parameters of the developed method, precision, and trueness were tested for cadmium quantification in a reference material NIST 3108 in solution. Levels of RSD = 6.77 % and bias = 5.16 % were achieved, showing the capability of the electrochemical method to provide accurate results for determinations in standard solutions. The developed methodology achieves detection and quantification levels suitable for the quantification of Cd^{2+} in cocoa, limit of detection (LOD) 0.45 $\mu\text{g kg}^{-1}$, and limit of quantification (LOQ) 1.60 $\mu\text{g kg}^{-1}$. Additionally, the square wave anodic stripping voltammetry optimal experimental conditions obtained by the simplex method were founded to be: pH 4.3, deposition potential (E_d) -1.2 V vs. Ag/AgCl, and deposition time (t_d) 198 s. Moreover, the acid microwave-assisted digestion of cocoa powder was selected as the most appropriate in terms of repeatability (RSD = 22 %) and trueness ($\text{recovery}_{\text{average}} = 92 \%$) for cadmium determination in a synthetic cocoa matrix. We also have found that the high concentrations of copper in cocoa interfere with cadmium quantification by SWASV with BiFE. Two procedures, one including the use of the chelating resin Chelex 100 by the batch method and the other one employing the electroseparation by constant potential electrolysis, were found suitable for the selective removal of copper from the digested extract in a reference material of cocoa

powder and allowed the determination of Cd^{2+} .

With this investigation, the INM, as a research center, has developed an electrochemical method to quantify cadmium that meets the requirements for intra-laboratory validation in standard solution and synthetic cocoa matrix. Additional studies will improve the performance of the proposed method in real cocoa samples and allow further research in portable systems for field studies.

Keywords: Cadmium quantification, Cocoa analysis, Anodic Stripping Voltammetry, Bismuth film electrode, Copper interference, Microwave digestion.

Título en español: Validación de la metodología de voltamperometría de redisolución anódica de onda cuadrada para la cuantificación de cadmio en granos de *Theobroma cacao* L.

Resumen

El cadmio posee una alta toxicidad para el ser humano al ser bioacumulado y causar daños en órganos internos, como el riñón, pulmones y huesos. En enero de 2019 entró en vigor el nuevo reglamento de la Unión Europea (UE) N.º 488/2014 sobre niveles máximos de cadmio en diferentes tipos de chocolate y cacao en polvo. Su objetivo principal es regular los altos niveles de seguridad alimentaria en estos productos alimenticios. Por lo tanto, la cuantificación de cadmio en granos de cacao se ha convertido en una necesidad para los productores. Ellos deben garantizar productos de alta y constante calidad, que cumplan con los niveles máximos de Cd^{2+} que oscilan entre 0,1 y 0,8 mg kg^{-1} para los diferentes tipos de chocolate y 0,6 mg kg^{-1} en cacao en polvo. Teniendo en cuenta lo anterior, este estudio presenta el desarrollo y validación de un método electroanalítico confiable para la determinación de Cd^{2+} en cacao mediante voltamperometría de redisolución anódica de onda cuadrada (SWASV) con electrodos de película de bismuto sobre carbono vítreo (BiFE) como electrodos de trabajo. El estudio se realizó en conjunto con el Instituto Nacional de Metrología de Colombia (INM) en el marco del proyecto “Plan de Fortalecimiento”. Así, en primer lugar, la voltamperometría cíclica, cronoamperometría y espectroscopía de impedancia electroquímica fueron utilizadas para caracterizar el proceso de reducción de bismuto sobre un electrodo de trabajo de carbono vítreo. Dicho estudio demostró que la película de bismuto aumenta el área del electrodo y la constante de transferencia de carga heterogénea. Estas mejoras nos ayudan a comprender el incremento en la señal voltamperométrica del cadmio obtenida por voltamperometría de redisolución anódica, validando la selección de este electrodo de trabajo modificado para la cuantificación de cadmio. Por otra parte, hemos desarrollado un método de cuantificación

de cadmio combinando la calibración con estándar interno *in situ* y el método de adición de estándar de un solo punto. El método desarrollado es una alternativa útil y más rápida respecto de los métodos tradicionales de calibración multipunto. Los parámetros del método desarrollado, rendimiento, precisión y veracidad, se evaluaron para la cuantificación de cadmio en un material de referencia NIST 3108 en solución. Así, se lograron niveles de RSD = 6,77 % y sesgo = 5,16 %, lo que demuestra la capacidad del método electroquímico para proporcionar resultados precisos y veraces para determinaciones de cadmio en soluciones estándar. La metodología desarrollada logró niveles de detección y cuantificación adecuados para la cuantificación de cadmio, límite de detección (LOD) $0,45 \mu\text{g kg}^{-1}$, y límite de cuantificación (LOQ) $1,63 \mu\text{g kg}^{-1}$. Además, se optimizó la cuantificación del cadmio mediante SWASV, usando el método simplex, obteniendo como las mejores condiciones: pH = 4,3, potencial de reducción (E_d) -1,2 V vs. Ag/AgCl y tiempo de reducción (t_d) 198 s. También, se encontró que la digestión ácida asistida por microondas fue el procedimiento más apropiado en términos de repetibilidad (RSD = 22 %) y veracidad (Porcentaje de recuperación = 92 %) para la determinación de cadmio en una matriz sintética de cacao. Finalmente, se halló que las altas concentraciones de cobre presente en el cacao son la principal interferencia para la cuantificación de cadmio por SWASV con BiFE. Dos procedimientos, uno que incluye el uso de la resina quelante Chelex 100 por el método discontinuo (batch) y el otro que emplea la electroseparación por electrólisis a potencial constante, resultaron adecuados para la eliminación selectiva de cobre del extracto digerido de un material de referencia de cacao en polvo, con lo cual se logró la determinación del Cd^{2+} en el mencionado material de referencia de cacao en polvo.

Con esta investigación, el INM, como centro de investigación, ha logrado desarrollar un método electroquímico para la cuantificación de cadmio que cumple con los requisitos para la validación intra-laboratorio en solución patrón y en matriz sintética de cacao. Se espera que estudios posteriores mejoren el método propuesto y lo hagan aplicable a muestras reales de cacao, así como su extrapolación a sistemas portátiles que permitan medir el cadmio directamente en los campos en donde se cultiva el cacao.

Palabras clave: Cuantificación de cadmio, Análisis de cacao, Voltamperometría de Redisolución Anódica, Electrodo de Película de Bismuto, Interferencia de cobre, Digestión asistida por microondas.

Contents

Acknowledgment	vii
Abstract	ix
List of abbreviations	xv
List of Figures	xvii
List of Tables	xix
1. Introduction	1
1.1. References	4
List of abbreviations	1
2. Electrochemical study of bismuth deposition on the glassy carbon electrode	5
2.1. Introduction	5
2.2. Experimental section	8
2.2.1. Reagents	8
2.2.2. Instrumentation, electrochemical cell and electrodes	8
2.3. Results	9
2.3.1. Cyclic voltammetry	9
2.3.2. Chronoamperometry	12
2.3.3. Electrochemical Impedance Spectroscopy	15
2.4. Conclusions	16
2.5. References	17
3. Implementation of the SWASV using BiFE for Cd quantification	19
3.1. Introduction	19
3.2. Experimental section	21
3.2.1. Reagents	21
3.2.2. Samples	21
3.2.3. Instrumentation, electrochemical cell and electrodes	21
3.2.4. Simplex optimization	22

3.3. Results	22
3.3.1. Calibration methodology development: <i>in situ</i> internal standard and single-point standard addition calibration	22
3.3.2. Simplex optimization of SWASV methodology	32
3.4. Conclusions	34
3.5. References	34
4. Digestion methods for electrochemical analysis of cadmium in <i>Theobroma cacao L.</i>	38
4.1. Introduction	38
4.2. Experimental section	40
4.2.1. Reagents	40
4.2.2. Samples	40
4.2.3. Instrumentation, electrochemical cell and electrodes	41
4.2.4. Dry ashing digestion	41
4.2.5. Alkali microwave-assisted digestion	41
4.2.6. Acid microwave-assisted digestion	42
4.3. Results	42
4.3.1. Dry ashing	42
4.3.2. Microwave assisted digestion	44
4.4. Conclusions	50
4.5. References	51
5. Validation of SWASV for cadmium quantification in <i>Theobroma cacao L.</i>	54
5.1. Introduction	54
5.2. Experimental section	57
5.2.1. Reagents	57
5.2.2. Samples	57
5.2.3. Instrumentation, electrochemical cell and electrodes	57
5.2.4. Chelating Ion Exchange Resin	58
5.2.5. Constant potential electrolysis (CPE)	58
5.3. Results	58
5.3.1. Linearity	58
5.3.2. Limit of detection and limit of quantification	59
5.3.3. Selectivity: Copper interference	61
5.3.4. Precision and Trueness	71
5.4. Conclusions	76
5.5. References	76
6. Conclusions and Recommendations	79

A. Appendix: Portable potentiostat experiment	81
A.1. Introduction	81
A.2. Experimental	82
A.2.1. Reagents	82
A.2.2. Samples	82
A.2.3. Instrumentation, electrochemical cell and electrodes	82
A.3. Results	84
A.4. Conclusions	85
A.5. References	85
B. Appendix: Published article	87
C. Appendix: Participation in academic events	88

List of abbreviations

Abbreviation	Definition
ACS	American Chemical Society
A	Electrode area
AAS	Atomic absorption spectroscopy
Amp	Pulse amplitude
Area _{Cd} /Area _{Bi}	Normalized Cd peak area with respect to the Bi peak area
ASV	Anodic stripping voltammetry
BiFE	Bismuth film onto glassy carbon electrode
C _{dl}	Double-layer capacitance
CA	Chronoamperometry
CPE	Constant Potential Electrolysis
CV	Cyclic voltammetry
E _d	Deposition potential
E _f	Final scan potential
E _i	Initial scan potential
EIS	Electrochemical impedance spectroscopy
ESC	Multi-point external standard calibration
ESC-IS	Multi-point standard addition with internal standard calibration
EU	European Union
FAAS	Flame atomic absorption spectroscopy
GCE	Glassy carbon electrode
GFAAS	Graphite furnace atomic absorption spectrometry
ICP - MS	Inductively coupled plasma mass spectrometry
ICP - OES	Inductively coupled plasma optical emission spectroscopy
ICP	Inductively coupled plasma spectroscopy
INM	Instituto Nacional de Metrología de Colombia
IS	Internal standard
ISC	Internal standard calibration
k ⁰	Heterogeneous charge rate constant
LOD	Limit of detection
LOQ	Limit of quantification
MFEs	Mercury film electrodes

Abbreviation	Definition
MINCIENCIAS	Ministerio de Ciencia, Tecnología e Innovación de Colombia
NIST	National Institute of Standards and Technology
OLS	Least Squares regression
Q	Constant phase element
R_{ct}	Charge transfer resistance
R_S	Solution resistance
RM	Standard reference material
RSD	Relative standard deviation
SM	Synthetic cocoa matrix
SM-B	Synthetic cocoa matrix blank
SM-Cd	Fortified synthetic cocoa matrix
SSA	Single-point standard addition
SSA-IS	Standard addition calibration with the internal standard
SWASV	Square Wave Anodic Stripping Voltammetry
t_d	Deposition time
t_{rest}	Rest time
u_c	Combined standard uncertainty
u_{hom}	Uncertainty due to homogeneity
U	Expanded uncertainty
W	Warburg coefficient

List of Figures

1-1. Sources of human exposure to cadmium	1
1-2. Maximum permissible levels of cadmium in cocoa products	2
2-1. Voltammograms using SWASV $6 \mu\text{g kg}^{-1}$ of Cd^{2+} , comparison working electrodes: GCE and BiFE	7
2-2. Voltammograms using CV oxygen effect	10
2-3. Cyclic voltammetry at different scan rates and Bi^{3+} concentrations	11
2-4. Cyclic voltammetry at different potential windows at two Bi^{3+} concentrations	12
2-5. Experimental and Normalized current transients for bismuth electrodeposition on GCE	13
2-6. Nyquist plot ferri/ferrocyanide redox couple, comparison working electrodes: GCE and BiFE	15
3-1. Voltammograms using SWASV of a calibration curve by ESC and calibration curves ESC and ESC-IS	23
3-2. Cadmium peak voltammograms using SWASV, comparison acetate buffer 0.1 M and 0.5 M	26
3-3. Normalized areas of a cadmium solution $30.68 \mu\text{g kg}^{-1}$ with and without cleaning the GCE between measurements	27
3-4. Calibration curve ESC-IS cleaning between calibration levels and Calibration curves SSA-IS without cleaning	28
3-5. Mean response $\text{Area}_{\text{Cd}}/\text{Area}_{\text{Bi}}$ and RSD values vs. vertex number of the simplex optimization	33
4-1. Voltammograms using SWASV of the SM blank (SM-B) and fortified samples (SM-Cd) obtained by dry ashing	43
4-2. Calibration curves SSA-IS for the SM-Cd treated by dry ashing	44
4-3. Voltammograms using SWASV of the SM-B and SM-Cd samples obtained by alkali microwave-assisted digestion	45
4-4. Voltammograms using SWASV of the SM-B and SM-Cd obtained by acid microwave-assisted digestion	47
4-5. Calibration curves of SM fortified samples (SM-Cd) obtained by alkali and acid microwave-assisted digestion	48

4-6. Comparison of the SM-Cd cadmium concentration and expanded uncertainty determined by SWASV and ICP-MS	50
5-1. Hierarchical levels of validation	55
5-2. LOD - LOQ calibration curve	60
5-3. Voltammograms using SWASV of cocoa RM, copper interference	61
5-4. Copper interference study	62
5-5. Voltammograms using SWASV of a cadmium and copper standard solution for Chelex 100 batch method	64
5-6. Voltammograms using SWASV of a cadmium and copper standard solution for Chelex 100 column method	66
5-7. Comparison voltammograms and signal recovery percentages for replicates treated by the Chelex 100 batch and column methods	67
5-8. Voltammograms using SWASV of cocoa powder RM Chelex 100 improved treatment	69
5-9. Voltammograms using SWASV of cocoa powder RM CPE improved treatment	71
5-10. Voltammograms using SWASV of cocoa powder RM Chelex 100 improved treatment - precision and trueness experiments	72
5-11. Calibration curves SSA-IS of cocoa powder RM. Chelex 100 and CPE procedures	73
5-12. Voltammograms using SWASV of cocoa powder RM constant potential electrolysis improved treatment - precision and trueness experiments	75
A-1. Experimental setup for SWASV measurement using Sensit BT electrochemical sensor and ItalSens Sensors.	83
A-2. Voltammograms using SWASV of a calibration curve by SSA-IS using the Sensit BT electrochemical sensor and ItalSens Sensors.	84

List of Tables

2-1. Electrochemical parameters for EIS measurements	9
2-2. Electrochemical parameters estimated using the Nyquist plots for GCE and BiFE	16
3-1. Electrochemical parameters for SWASV	22
3-2. Regression parameters for ESC and ESC-ISC	24
3-3. Cadmium concentration results for the RM in solution obtained by ESC, ESC-IS and SSA-IS	25
3-4. Comparison of the normalized areas at different concentrations of the supporting electrolyte	26
3-5. Cadmium concentrations and estimated expanded uncertainty of the RM NIST 3108	31
3-6. Simplex information for the 11 vertexes	32
4-1. Synthetic cocoa matrix composition	41
4-2. Cadmium concentrations and estimated expanded uncertainty for the SM-Cd replicas	49
4-3. Performance parameters recovery and repeatability of the digestion methods	49
5-1. Studies of copper interference in cadmium determination by ASV	56
5-2. Chelex 100 resin selectivity factors	56
5-3. t-Student tests for linearity assessment	59
5-4. Recovery percentage obtained by the Chelex 100 batch and column methods	67
5-5. Comparison of cadmium concentrations and performance parameters of the RM cocoa powder obtained by Chelex 100 and CPE	73
A-1. Electrochemical parameters for SWASV	83

1. Introduction

Cadmium (Cd, atomic number 48, atomic weight $122.414 \text{ g mol}^{-1}$) makes up about 0.1 mg kg^{-1} of Earth's crust, and the most significant cadmium mineral is greenockite (CdS) (Wedepohl, 1995). Cadmium is often found in zinc ores, zinc-bearing lead ores, or complex copper-lead-zinc ores, forming an isomorphic impurity in sphalerite (ZnS), a zinc mineral (Morrow, 2000). Therefore, cadmium is commonly isolated during the production of zinc by vacuum distillation or precipitated as cadmium sulfate from the electrolysis solution (Scoullou et al., 2012). Some applications of cadmium are pigments (Sarkar et al., 2013), coatings, and electroplating (Morrow, 2000). The most common cadmium ingestion is through foodstuffs, and cigarette smoking since plants take up cadmium from contaminated soil or water (Figure 1-1).

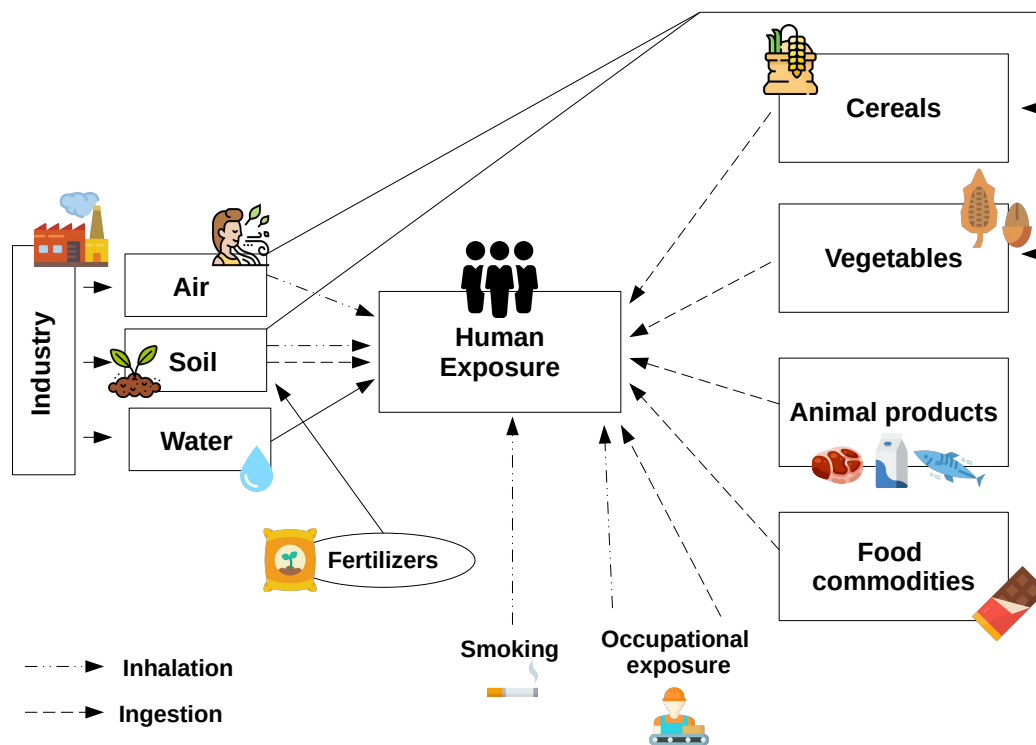


Figure 1-1.: Sources of human exposure to cadmium. [Adapted from The EFSA Journal (2009) 980, 1-139. Scientific Opinion of the Panel on Contaminants in the Food Chain].

Cadmium has been dispersed into the environment by human-made routes like mining, smelting, using phosphate fertilizers, and industrial uses such as plating and pigments. Once in the ground, cadmium moves easily through soil layers and enters the food chain by plant uptake, cereals, and grains (Genchi et al., 2020). In humans, oral ingestion of high cadmium levels causes irritation in the stomach, leading to vomiting and diarrhea and, in the worst cases, death. The ingestion of lower levels of cadmium over a long period has a mainly toxic effect on kidneys and bones, causing renal failure and demineralization (Genchi et al., 2020). Consequently, different health agencies have set maximum limits for this element in various sources.

New maximum permissible levels have been established for food commodities, such as chocolate, seeking the protection of infants and young children. The European regulation No. 488/2014 established the maximum permissible levels of cadmium that different types of chocolate and cocoa powder could contain (Commission Regulation, 2014). The legislation entered into force in January 2019 and established maximum permissible levels between 0.1 and 0.8 mg kg⁻¹ of Cd²⁺ for different types of chocolate and 0.6 mg kg⁻¹ in cocoa powder (Commission Regulation, 2014)(Figure 1-2).

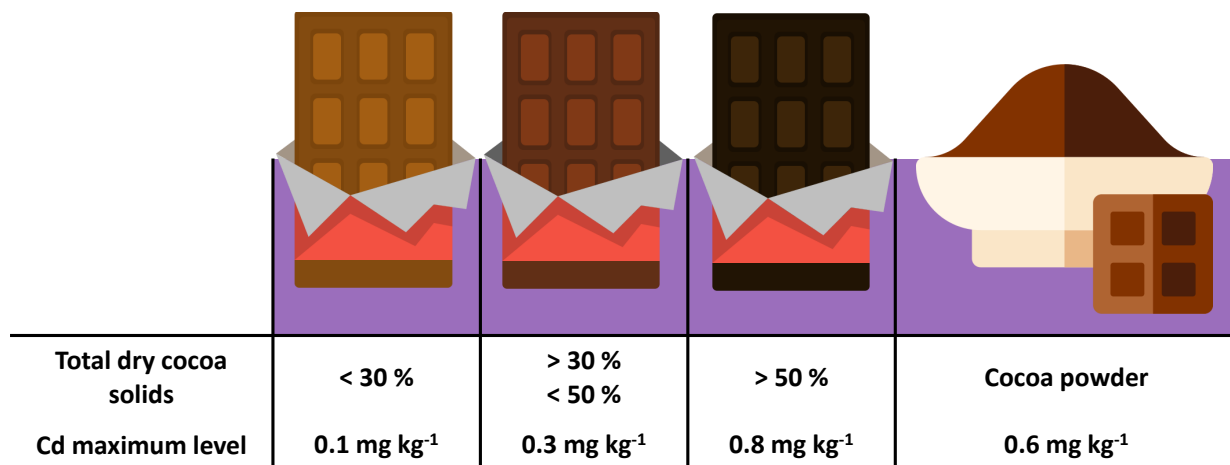


Figure 1-2.: Maximum permissible levels of cadmium in cocoa products from European regulation No. 488/2014.

Cocoa farming is led by West Africa, Southeast Asia, and Latin America (ICCO, 2017). Colombia has a promising potential for cocoa production since it has a competitive advantage over other countries, owing to its optimal climatic conditions for cocoa production (García et al., 2012). With a strategic geographical position and a tropical climate, Colombia benefits from the luminosity and availability of hydric resources throughout the year. The main cocoa-producing areas in Colombia are Santander, Norte de Santander, Tolima, Nariño, Antioquia, and Arauca. Colombia produces 70 % of the world's fine and aroma cocoa (ICCO,

2017).

Even though Colombia has considerable potential in cocoa production, the presence of cadmium in cocoa beans by uptake from plantations soils causes concern among producers. Firstly, being a toxic metal, cadmium accumulation compromises the health and well-being of cocoa-derived product consumers. In addition, since Europe is responsible for 50 % of chocolate consumption worldwide and is not a cocoa producer, the Europe market is one of the most important for Colombian producers. Hence, it is crucial to comply with the requirements of the new regulation No. 488 / 2014. Considering the previous facts, producers need to determine cadmium levels and classify the different batches of cocoa beans to comply with the maximum permissible levels allowed for exportation and national production and also need to support research to reduce the Cd content in Colombian cocoa.

Analytical methods for the determination of cadmium in cocoa recommended by the Codex Alimentarius according to the CODEX STAN 228-2001 standard are inductively coupled plasma optical emission spectroscopy (ICP - OES), inductively coupled plasma mass spectrometry (ICP - MS), graphite furnace atomic absorption spectrometry (GFAAS), flame atomic absorption spectroscopy (FAAS) and anodic stripping voltammetry (ASV). The latter spectrophotometric methodologies for this type of analysis require high-cost equipment and reagents. In contrast, ASV is a faster, less expensive, and more accessible alternative with the low limit of detection required to quantify cadmium in cocoa. However, the main disadvantage of electrochemical techniques is the lack of robustness and poorly reproducible results.

Accordingly, a deep and detailed study of the square wave anodic stripping voltammetry (SWASV) as a technique for quantifying cadmium in cocoa is relevant. In this work, we have started such study through the characterization of the working electrode and the optimization of the electrochemical parameters: pH, deposition potential, and time deposition. In addition, the optimization of the sample digestion is necessary, particularly the digestion of cocoa beans and cocoa-derived products. In this work, we have focused only on cocoa powder digestion. Also, it is important to mention that the scope of this research is not to achieve the same performance of techniques such as AAS, GFAAS, or ICP but to establish a more straightforward and cheaper methodology projecting its possible contribution to field measurements.

On the other hand, to our knowledge, electrochemical methods using bismuth film electrodes for cadmium detection in cocoa beans matrix have not been reported. Therefore, in this investigation, we present the optimization and validation of an electrochemical method for Cd^{2+} determination in cocoa, using SWASV with bismuth film electrodes (BiFE) as a working electrode.

This document was organized into chapters to present the results of this work. The second chapter shows the results of the study of the bismuth film formation on glassy carbon electrodes using cyclic voltammetry, chronoamperometry, and electrochemical impedance spectroscopy. The third chapter presents the implementation and optimization of the quantification methodology (SWASV-BiFE) for the determination of cadmium, and the optimization of the experimental parameters, pH of the supporting electrolyte, deposition potential, and deposition time, of the analytical methodology SWASV. The fourth chapter presents the selection and optimization of the digestion method for determining cadmium in the synthetic matrix of cocoa using dry and wet digestion methodologies. Finally, the fifth chapter shows the intra-laboratory validation, called methodology's level two validation.

1.1. References

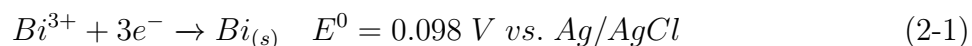
- Comission Regulation, E. (2014). Commission regulation (eu) no 488/2014 amending regulation (ec) no 1881/2006 as regards maximum levels of cadmium in foodstuffs. *off. j. eur. union* 138, 75. *Official Journal of the European Union*, pages 75–79.
- García, M., Quintero, L. F. M., and Montoya, A. (2012). Análisis comparativo de competitividad de las cadenas productivas de cacao de colombia y ecuador. *Revista de Ciencias Agrícolas*, 29(1):99–112.
- Genchi, G., Sinicropi, M. S., Lauria, G., Carocci, A., and Catalano, A. (2020). The effects of cadmium toxicity. *International journal of environmental research and public health*, 17(11):3782.
- ICCO, I. C. O. (2017). Fine or flavour cocoa. <https://www.icco.org/about-cocoa/fine-or-flavour-cocoa>.
- Morrow, H. (2000). Cadmium and cadmium alloys. *Kirk-Othmer Encyclopedia of Chemical Technology*, pages 1–36.
- Sarkar, A., Ravindran, G., and Krishnamurthy, V. (2013). A brief review on the effect of cadmium toxicity: from cellular to organ level. *International Research Journal of Biotechnology*, 3(1):17–36.
- Scoullou, M. J., Vonkeman, G. H., Thornton, I., and Makuch, Z. (2012). *Mercury—cadmium—lead handbook for sustainable heavy metals policy and regulation*, volume 31. Springer Science & Business Media.

2. Electrochemical study of bismuth deposition on the glassy carbon electrode

2.1. Introduction

The proper performance of any electrochemical analysis relies mainly on the correct choice of electrodes. An ideal electrode should be mechanically stable, chemically inert, have a wide range of useful potentials, and easily reproducible surface (Economou, 2005). Film electrodes are electrodes with a thin metal coating, liquid or solid, deposited on an electric conductor support. The elements that can be used to form this film are restricted. Over the years, mercury film electrodes (MFEs) have shown excellent electro-analysis behavior, mainly for anodic stripping and adsorptive stripping voltammetry (Yang and Hu, 2005). Given the high toxicity of mercury and mercury salts in our environment, other metals have been proposed as alternatives to MFEs. Since 2000, bismuth film electrode (BiFE) has received considerable attention as a working electrode, as it is environmentally friendly and possesses a wide potential window for anodic stripping voltammetry, similar to mercury (Economou, 2005).

Usually, bismuth is plated on the same substrates as mercury, mainly different forms of carbon, such as glassy carbon (Yang and Hu, 2005; Zhou et al., 2012; Vladislavic et al., 2014), graphite electrodes and carbon fiber microelectrodes (Vladislavic et al., 2014). The reduction reaction of Bi^{3+} possesses a standard potential of 0.098 V vs. Ag/AgCl (reaction 2-1).



There are two general methods of coating the substrate with bismuth, and selecting one of these is critical for the correct performance of the BiFE (Economou, 2005).

***Ex situ* coating**

The first method is an *ex situ* deposition, where the bismuth film is generated in a separate solution and then placed in the solution containing the analyte of interest. Usually, an acidic media is recommended as Bi^{3+} is easily hydrolyzed at higher pH, following the reaction 2-2.



In general, a solution containing 5 to 200 mg L⁻¹ of Bi³⁺ with a deposition potential in the range of -0.50 to -1.20 V vs. Ag/AgCl and a deposition time of 1 to 8 min under conditions of forced convection (rotating electrode or magnetic stirring) is used for this type of coating (Economou, 2005). For anodic stripping voltammetry, after the stripping step, the surface of the electrode should be reactivated by applying a potential to oxidize any remaining species avoiding the dissolution of the bismuth film. Therefore, the cleaning potential must be more positive than the oxidation potential of metal ions and more negative than the oxidation potential of bismuth. Commonly, a short cleaning step of 10 to 30 s at -0.35 V vs. Ag/AgCl in stirred solution is sufficient (Economou, 2005).

***In situ* coating**

The second coating method, *in situ* deposition, uses the same solution for the deposition of bismuth and to preconcentrate the analyte. As a general practical rule, the concentration of Bi³⁺ must be at least 10-fold higher than the expected analyte concentration, normally the concentration range is 400 to 1000 μg L⁻¹ of Bi³⁺ (Economou, 2005). For the cleaning step, the bismuth film is removed completely after each measurement at a potential more positive than the oxidation potential of bismuth. Usually, a potential between 0.0 and 0.3 V vs. Ag/AgCl for 30 s (Economou, 2005) is applied.

Since no additional bismuth-coating step is required, the main advantage of *in situ* coating is the simplification and time reduction of the experimental procedure. However, *in situ* coating is limited to anodic stripping analysis where negative polarization of the electrode is employed for the electrolytic preconcentration of metal ions. On the other hand, *ex situ* coating is more versatile as the bismuth-coating process can be independently controlled by varying the chemical and instrumental conditions in the bismuth plating solution and can be used for any analysis. Nevertheless, it is more complicated and time-consuming than *in situ* plating (Economou, 2005).

Enhancing the voltammetric signal intensity using BiFE is well established (Economou, 2005). Figure 2-1 shows the voltammograms obtained in this work for a 6 μg kg⁻¹ cadmium solution, using the unmodified glassy carbon electrode (GCE) and the same electrode modified with a bismuth film. Effectively, there is an increase in the cadmium current when there is a bismuth film over the glassy carbon electrode. However, it is essential to understand why this improvement happens.

Several studies have been carried out on bismuth film electrodes; some of them discussed the nucleation and growth mechanisms that occur over different electrodes, including glassy

carbon electrodes (Ismail et al., 1993; Zhou et al., 2012; Youbi et al., 2020; Ramirez et al., 2017; Yang and Hu, 2005).

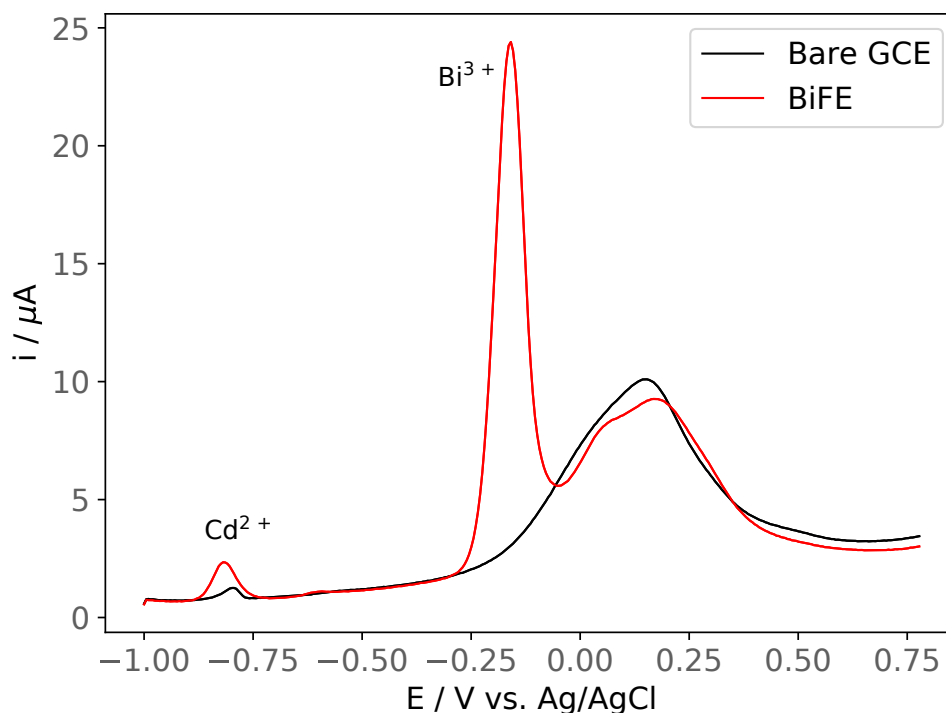


Figure 2-1.: Voltammograms using SWASV of a $6 \mu\text{g kg}^{-1}$ of Cd^{2+} in acetate buffer 0.1 M and pH 4.5. Deposition potential (E_d) -1 V, deposition time (t_d) 120 s, rest time (t_{rest}) 20 s, initial scan potential (E_i) -1.0 V, final scan potential (E_f) 0.8 V, pulse amplitude (Amp) 20 mV, pulse frequency (freq) 25 Hz, step pulse (Step) 5 mV, and bismuth concentration ($[\text{Bi}^{3+}]$) $500 \mu\text{g kg}^{-1}$. Working electrode: GCE (black line) and BiFE (red line).

The mentioned studies use cyclic voltammetry (CV) and chronoamperometry (CA) to characterize the process of bismuth reduction on the electrode surface. Chronoamperometry, alongside the Scharifker-Hills models, is a useful electrochemical technique for studying bismuth electrodeposition on different electrode surfaces. Furthermore, electrochemical impedance spectroscopy (EIS) has been used as a characterization technique for bismuth film-modified electrode interfaces (Ouyang et al., 2013a).

According to the above, within the specific objectives of this research project, this chapter presents an electrochemical study of the deposition of bismuth on the GCE. CV and CA techniques were used to understand the bismuth nucleation and growth mechanism. Moreover, the surface of the glassy carbon electrode with (BiFE) and without the bismuth film (GCE) was studied using EIS and $[\text{Fe}(\text{CN})_6]^{3-}/[\text{Fe}(\text{CN})_6]^{4-}$ as a probe redox couple.

2.2. Experimental section

2.2.1. Reagents

Standard solutions, samples, and the supporting electrolyte were prepared using type I water. Analytical grade sodium acetate ($\geq 99\%$, w/w) and glacial acetic acid (Merck, 100%, w/w) were used to prepare the supporting electrolyte in a total acetate concentration of 0.1 M. For the CV and CA measurements, the pH of the solution was adjusted to a value equal to 4.5 and 2.0, respectively, with a 1 M NaOH solution. The pH value of the supporting electrolyte used in our study was selected from the literature review (Economou, 2005) and previous exploratory experiments. The Bi^{3+} stock solutions were prepared gravimetrically using $\text{Bi}(\text{NO}_3)_3 \cdot 5\text{H}_2\text{O}$ (PanReac AppliChem, $\geq 98\%$, w/w) and the supporting electrolyte as the solvent. The $[\text{Fe}(\text{CN})_6]^{3-}/[\text{Fe}(\text{CN})_6]^{4-}$ solution was prepared gravimetrically using $\text{K}_3\text{Fe}(\text{CN})_6$ and $\text{K}_4\text{Fe}(\text{CN})_6 \cdot 3\text{H}_2\text{O}$ (PanReac AppliChem, $\geq 99\%$, w/w) and a solution of 0.1 M KCl as the solvent.

The laboratory glassware was cleaned, before every experiment, by immersion in a solution containing 2.5 mM of KMnO_4 and 22.4 mM H_2SO_4 solution for at least 24 h. Then, it was washed with 0.03 M H_2O_2 and 4.6 mM H_2SO_4 solution. Subsequently, it was washed and boiled with type I water. This operation was repeated at least three times, and finally, the glassware was allowed to dry at room temperature.

2.2.2. Instrumentation, electrochemical cell and electrodes

All measurements were carried out using the Metrohm Autolab PGSTAT128N potentiostat and NOVA software (version 2.1, Metrohm Autolab B.V). The working electrode was a glassy carbon voltammetric disk (GCE - 3 mm diameter). The reference electrode was Ag/AgCl, KCl (sat). The counter electrode was a platinum wire. Ar 99.999% pure was bubbled into the solution 5 min before beginning an experiment, and an atmosphere of Ar was maintained during the whole experiment. Before modification, the GCE was polished with a 0.3 μm (one time) and 0.05 μm (three times) gamma alumina suspension and washed in a type I ultrasound water bath between polishes. Then, an electrochemical cleaning was carried out with 20 cycles of CV in 0.1 M KOH, between -0.60 and 1.80 V at 0.10 V s^{-1} ; followed by 15 cycles of CV in the supporting electrolyte, between -1.00 and 0.80 V at 0.10 V s^{-1} .

Cyclic voltammetry was used to characterize the electrochemical behavior of bismuth deposition on the glassy carbon electrode. It was performed in the presence and absence of oxygen in a potential window between 0.80 and -0.80 V and a scan rate of 0.10 V s^{-1} in a solution containing 0.50 mg kg^{-1} of Bi^{3+} . The analysis was performed at different scan rates 0.05, 0.10, 0.25, 0.50, 0.75, and 1.00 V s^{-1} , different potential windows between 0.80 and -0.25, -0.38, -0.43, -0.60, -1.00 V, and at two bismuth concentrations, 2.0 and 7.0 mg kg^{-1} .

Chronoamperometry was used to determine the mechanism of nucleation and growth of the bismuth film on the glassy carbon electrode. The electrode potential was stepped from 300 mV vs. Ag/AgCl to different potentials, -76, -78, -80, -82, -84, -86, -88, -90, -94, and -96 mV, in a solution containing 1.10×10^3 mg kg⁻¹ of Bi³⁺.

The bismuth film was formed by the *ex situ* method using 0.5 mg kg⁻¹ of Bi³⁺ for the EIS experiment. The *ex situ* deposition of the bismuth film on the GCE was performed at -1.00 V for 120 s under magnetic stirring (500 rpm) and a rest time of 20 s. These parameters were selected from the literature review (Mirceski et al., 2012). Finally, the BiFE was carefully rinsed with type I water, and the electrode was used for the subsequent EIS experiments. The experimental parameters for EIS are shown in Table 2-1. They were selected from the literature review (Ouyang et al., 2013b).

Table 2-1.: Electrochemical parameters used in the EIS measurements.

Parameter	Value
First applied frequency	25000 Hz
Last applied frequency	0.1 Hz
Number of frequencies	10 per decade
Frequency step type	Points per decade
Amplitude	0.01 V

2.3. Results

2.3.1. Cyclic voltammetry

The oxygen effect. The CV measurements of Bi³⁺ in the presence and absence of oxygen are shown in Figure 2-2.

The voltammograms revealed well-defined cathodic (E_p^{C1}) and anodic peaks (E_p^{A1} and E_p^{A2}), which correspond to bismuth deposition and dissolution. The multiple oxidation signals can be associated with the formation of different bismuth hydroxides (Ismail et al., 1993). It has been found that bismuth hydroxides can be formed at neutral and basic pH. Even though our supporting electrolyte buffer solution has a pH = 4.5, the pH of the interface is not necessarily the same as that of the bulk dissolution. Therefore, more than one species that can be oxidized may coexist if the interface has a pH more basic than the bulk. The same oxidation peaks have been reported before, and the authors attribute these signals to the presence of multiple bismuth species (reaction 2-3, reaction 2-4 and reaction 2-5) (Ismail et al., 1993; Espinosa et al., 1991), that we have adapted and presented as a general

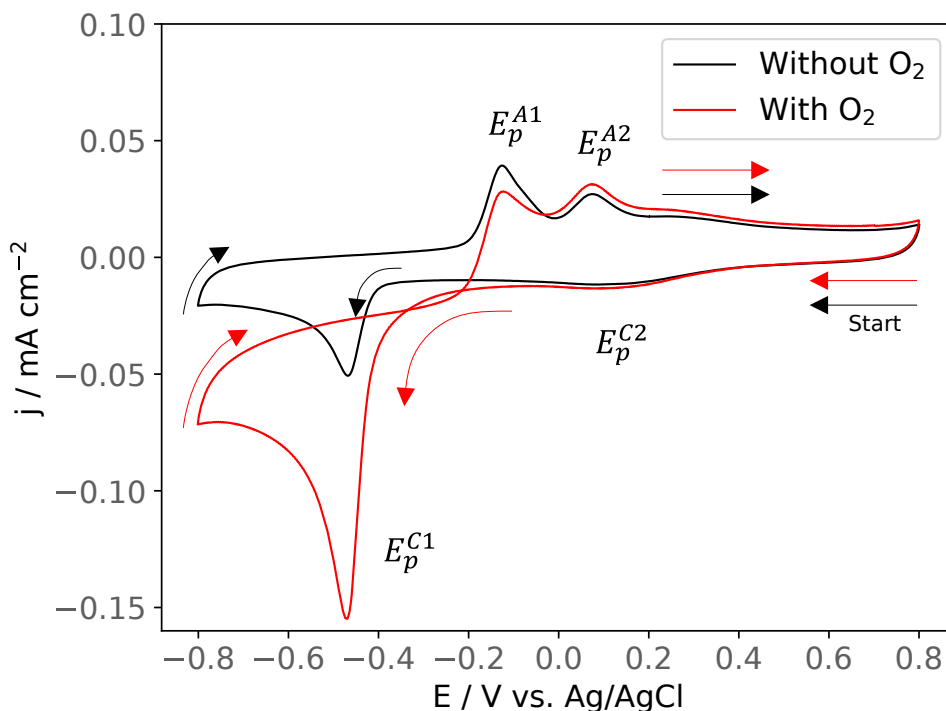
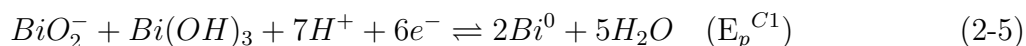
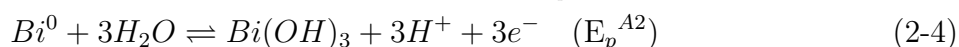
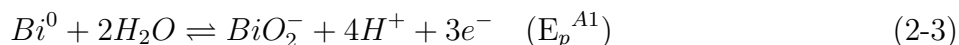


Figure 2-2.: Voltammograms using CV on the GCE in acetate buffer 0.1 M and pH 4.5. $[Bi^{3+}] = 0.5 \text{ mg kg}^{-1}$ with (red line) and without (black line) oxygen.

mechanism with no other intention than to give a global panorama of the phenomenon. Of course, more detailed studies will be required to verify or reject the presented hypothesis. However, those studies are beyond the objectives of this work.



Both anodic peaks E_p^{A1} and E_p^{A2} produce only one peak in the negative scan, the global process that generates the E_p^{C1} . Previous studies proposed a hypothesis that envisages a chemical reduction of E_p^{A2} to E_p^{A1} to explain this observation (Ismail et al., 1993).

The E_p^{C2} reduction signal is attributed to the adsorption of acetates from the supporting electrolyte on the surface of the working electrode. In the presence of oxygen, significant reduction currents at potentials lower than 0.00 V vs Ag/AgCl associated with oxygen reduction are observed (Figure 2-2, red line). Therefore, the formation of the film can be affected when oxygen is present and so, to avoid reproducibility problems, it is essential to eliminate the oxygen in the solution.

System response to scan rate variation. Figure 2.3(a) shows a series of cyclic voltammograms for bismuth film formation on GCE from a 2 mg kg^{-1} of Bi^{3+} solution at different scan rates. As the scan rate increases, a negative shift in the cathodic peak potential is observed. This behavior is typically attributed to quasi-reversible electrochemical reactions (Zhou et al., 2012; Sandnes et al., 2007). Diffusion-limited and kinetically controlled processes influence CV. The peak potential should be independent of the scan rate if the studied redox process is influenced exclusively by diffusion. On the contrary, when the electrode kinetics is the main factor, the scan rate affects the entire voltammetric response. If the system is kinetically limited, the peak potential will shift away from the nominal potential when the scan rate increases (Bard and Faulkner, 2001). The same behavior has been reported in previous studies of bismuth deposition on different electrodes (Zhou et al., 2012; Vladislavic et al., 2014; Sandnes et al., 2007). In addition, the separation of the cathodic and anodic peaks exceeds $59/n \text{ mV}$ and increases with the scan rate. Given these characteristics, it is possible to affirm that the bismuth film formation process on GCE is not electrochemically reversible.

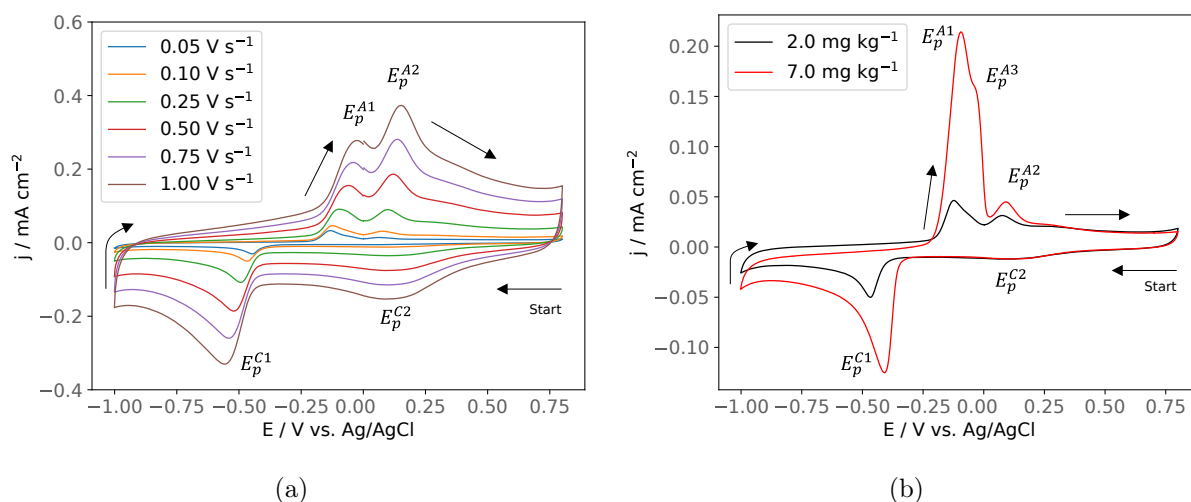


Figure 2-3.: Cyclic voltammetry on GCE in acetate buffer 0.1 M, pH 4.5, and without oxygen. **(a)** $[\text{Bi}^{3+}] = 2.0 \text{ mg kg}^{-1}$ at different scan rates, and **(b)** $[\text{Bi}^{3+}] = 2.0 \text{ mg kg}^{-1}$ (black line) and $[\text{Bi}^{3+}] = 7.0 \text{ mg kg}^{-1}$ (red line) at 0.10 V s^{-1} .

System response to bismuth concentration variation. Figure 2.3(b) shows the CV measurements at different bismuth concentrations. At 2.0 mg kg^{-1} , two oxidation peaks are observed again, but when the concentration was increased to 7.0 mg kg^{-1} an additional shoulder appears (E_p^{A3}). The same behavior was also observed in a previous investigation, where the number of anodic peaks increased with the thickness of the bismuth films (Ismail et al., 1993).

System response to potential window variation. Varying the potential window for the same two concentrations as above, Figure 2.4(a), and Figure 2.4(b), it is possible to observe a “nucleation loop” for the CV at higher bismuth concentration, the inset in Figure 2.4(b). The same characteristic behavior has been found in metal deposition studies from dilute solutions onto a foreign substrate (Zhou et al., 2012; Vladislavic et al., 2014; Ismail et al., 1993; Grujicic and Pesic, 2002).

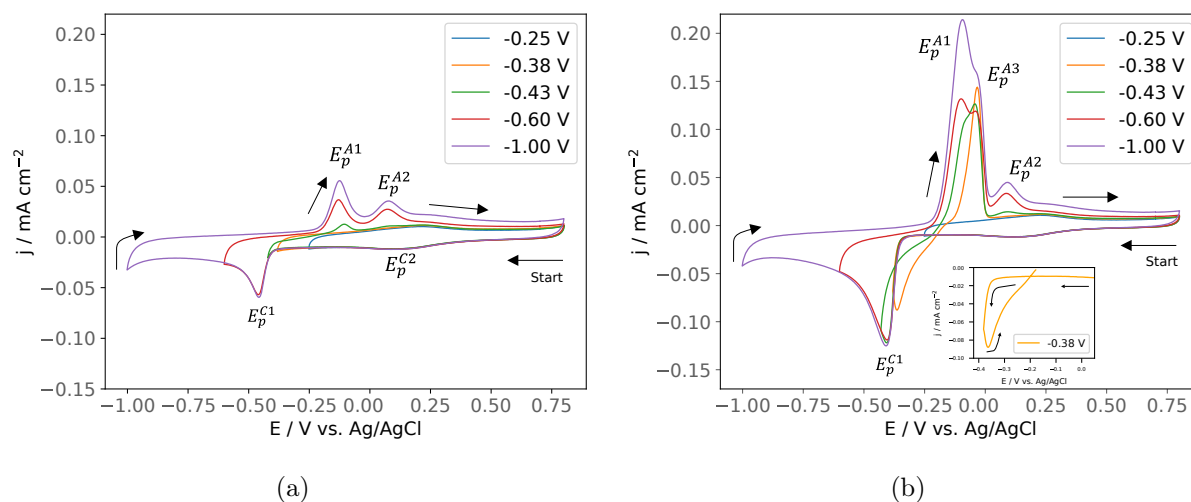


Figure 2-4.: Cyclic voltammetry on the GCE in acetate buffer 0.1 M and pH 4.5 at different potential windows without oxygen. **(a)** $[\text{Bi}^{3+}] = 2.0 \text{ mg kg}^{-1}$, and **(b)** $[\text{Bi}^{3+}] = 7.0 \text{ mg kg}^{-1}$. Inset: close-up of the nucleation loop.

A crossover between the cathodic and anodic current traces, or nucleation loop, is attributed to the formation of thermodynamically stable bismuth nuclei on glassy carbon. The deposition potential of metal ions on a foreign substrate is usually greater than the potential required to reduce the metal ion on an electrode of the same metal due to crystallographic substrate/metal misfit (Vladislavic et al., 2014). Therefore, deposition of bismuth on GCE requires a more negative potential than the equilibrium potential to reduce Bi^{3+} over Bi^0 . It was also found that depending on the potential window, the oxidation of one bismuth species or another (E_p^{A1} , E_p^{A2} or E_p^{A3}) is favored.

2.3.2. Chronoamperometry

The concentrations of bismuth used for *in situ* coating (400 to $1000 \mu\text{g kg}^{-1}$) during the SWASV experiments are too low to evidence nucleation by Chronoamperometry. In the mentioned conditions, the influence of capacitive currents is mostly observed instead of the nucleation. To accelerate the electrodeposition process and analyze the kinetics of nucleation,

the bismuth concentration was increased to $1.10 \times 10^3 \text{ mg kg}^{-1}$. Thus, we expect to have some ideas about what happens in micro-currents when the SWASV experiments are done. The electrode potential was stepped from 300 mV vs. Ag/AgCl at different potentials, among which the nucleation loop is observed in CV, -76, -78, -80, -82, -84, -86, -88, -90, -94, and -96 mV vs. Ag/AgCl. The sets of current transients in the previously mentioned conditions are shown in Figure 2.5(a). The increase in the potentiostatic transient current is due to the growth of independent nuclei alone and the simultaneous increase in the number of nuclei. The current increases until the growth centers begin to overlap. A decrease in the current starts due to a decrease in the effective electrode surface area when the diffusion zones around the nuclei overlap, and the growth centers impinge on each other (Paunovic and Schlesinger, 2006).

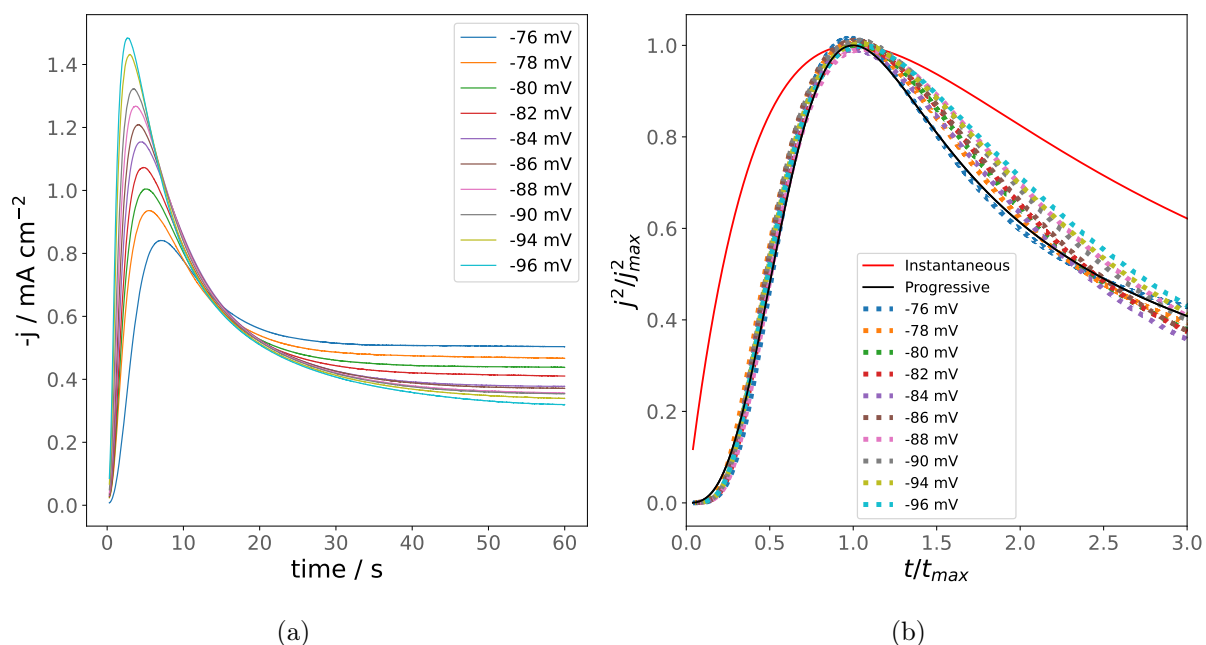


Figure 2-5.: (a) Experimental current transients for bismuth electrodeposition on GCE in acetate buffer 0.1 M and pH 2.0. $[\text{Bi}^{3+}] = 1.10 \times 10^3 \text{ mg kg}^{-1}$. Sample interval 10 ms. (b) Normalized potentiostatic transients from (a) and theoretical curves for the 3D instantaneous (red line) and progressive (black line) nucleation and growth.

Two and three-dimensional nucleation processes associated with the early stages of electrochemical deposition strongly depend on the overpotential. It is possible to find the relationship between the overpotential and the nucleation kinetics by relating the current to the electroactive surface area (Scharifker and Hills, 1983). Scharifker and Hills' models (Eq. 2-6 and Eq. 2-7) for the three-dimensional (3D) multiple nucleation and growth can be used to define the nucleation mechanism of the bismuth deposition as an instantaneous or a progres-

sive nucleation (Scharifker and Hills, 1983).

Instantaneous nucleation:

$$\left(\frac{I^2}{I_{max}^2}\right) = \frac{1.9542}{t/t_{max}} \left[1 - \exp\left(-1.2564 \left(\frac{t}{t_{max}}\right)\right)\right]^2 \quad (2-6)$$

Progressive nucleation:

$$\left(\frac{I^2}{I_{max}^2}\right) = \frac{1.2254}{t/t_{max}} \left[1 - \exp\left(-2.3367 \left(\frac{t}{t_{max}}\right)^2\right)\right]^2 \quad (2-7)$$

The nucleation process of bismuth on the electrode surface can be described by a first-order kinetic equation (Paunovic and Schlesinger, 2006) described by Eq. 2-8.

$$N = N_0[1 - \exp(-At)] \quad (2-8)$$

where N represents the number of nuclei formed, N_0 is the maximum number of nuclei that can be formed on the surface of the electrode, t the conversion time, and A the nucleation rate constant.

The nucleation rate constant, A , will determine two possible cases, the first for large nucleation constant A .

$$N = N_0 \quad (2-9)$$

Eq. 2-9 indicates that all electrode sites become nuclei instantaneously. Thus, this is referred to as **instantaneous nucleation**. In a second case, for a small A and small t

$$N \approx AN_0t \quad (2-10)$$

In this case, Eq. 2-10 indicates that the number of nuclei N is a function of time t , and the nucleation is termed **progressive nucleation**.

The non-dimensional plot of the experimental current transients obtained for Bi electrodeposition onto GCE at different deposition potentials is shown in Figure 2.5(b). At all the applied potential steps, the normalized currents clearly suggest that the bismuth deposition on the glassy carbon electrode is given by a progressive nucleation process because the experimental data better fit the progressive theoretical curve (Figure 2.5(b), black line). This result agreed with previously reported bismuth deposition studies (Ramirez et al., 2017; Vladislavic et al., 2014; Grubač and Metikoš-Huković, 1998; Yang and Hu, 2005).

2.3.3. Electrochemical Impedance Spectroscopy

The EIS results for the redox probe $[\text{Fe}(\text{CN})_6]^{3-}/[\text{Fe}(\text{CN})_6]^{4-}$ are shown in Figure 2-6.

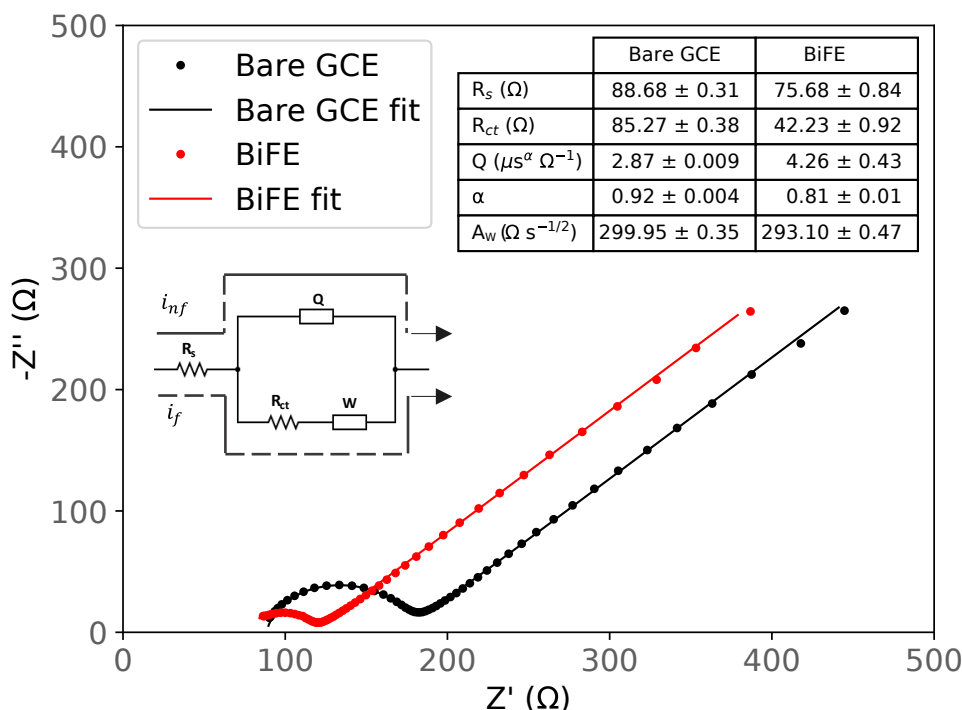


Figure 2-6.: EIS measurements and fitting of 0.0106 M $[\text{Fe}(\text{CN})_6]^{3-}$ and 0.0101 M $[\text{Fe}(\text{CN})_6]^{4-}$ in 0.1 M KCl at bare GCE (black) and BiFE (red) in the impedance range of 25 kHz to 0.1 Hz at OCP = 0.234 V. Fitting using modified Randles equivalent circuit with a CPE (Q) as shown in the inset. (AtherMath 1.6.10513 Software)

The EIS data was fitted with a modified Randles equivalent circuit (inset Figure 2-6) composed by a solution resistance (R_s) in series with the parallel combination of the charge transfer resistance (R_{ct}), the Warburg diffusional impedance (W), and a constant phase element (Q) replacing the double-layer capacitance (C_{dl}). Q represents a non-ideal capacitor, which affects the flattening level of the semicircle. R_{ct} corresponds to the diameter of the semicircle in the Nyquist plot. R_{ct} value decreases when the working electrode is modified with the bismuth film, from 85.27 to 42.23 Ω . The decrease in the R_{ct} value indicates that the presence of the bismuth film improves the electron transfer over the electrode surface (higher k^0) according to Eq. 2-11.

$$R_{ct} = \frac{RT}{n^2 F^2 A C k^0} \quad (2-11)$$

where $C_O = C_R = C$. Estimating the electrochemical parameters k^0 and the electrode

area (A) can help to understand the improvement in the electrocatalytic performance of the working electrode with the formation of the bismuth film. The fitting values from the modified Randles circuit (Figure **2-6**), Eq. 2-11 and Eq. 2-12

$$A_W = \frac{RT}{n^2 F^2 A \sqrt{2}} \left(\frac{1}{D_O^{1/2} C_O^*} + \frac{1}{D_R^{1/2} C_R^*} \right) \quad (2-12)$$

allowed us to calculate the parameters k^0 and A in the absence and presence of the bismuth film on GCE. The calculations used the following constants and parameters: $F = 96485.33212 \text{ C mol}^{-1}$, $R = 8.314462618 \text{ J mol}^{-1}\text{K}^{-1}$, $T = 293.15 \text{ K}$, $n = 1$, $D_O = 6.09 \times 10^{-10} \text{ m}^2\text{s}^{-1}$, and $D_R = 5.54 \times 10^{-10} \text{ m}^2\text{s}^{-1}$ taken from (Haynes et al., 2016). As expected, a higher k^0 and area were obtained using the BiFE (Table **2-2**). However, it is important to notice that the increase in the area is not significant and could be in the measurement error range.

Table 2-2.: Electrochemical parameters estimated using the Nyquist plots measurements and fitting of $0.0106 \text{ M } [\text{Fe}(\text{CN})_6]^{3-}$ and $0.0101 \text{ M } [\text{Fe}(\text{CN})_6]^{4-}$ in 0.1 M KCl at bare GCE and BiFE.

Parameter	bare GCE	BiFE
$k^0 / \text{cm s}^{-1}$	5.56×10^{-3}	1.10×10^{-2}
A / cm^2	3.96×10^{-2}	4.05×10^{-2}

Nevertheless, the significant increase in k^0 explains the improvement in the current intensity observed for the SWASV measurements in determining cadmium (Figure **2-1**). In addition, it has been found that the bismuth film increased the hydrophilicity of the electrode surface (Ouyang et al., 2013a). Thence, the electronic transfer in aqueous determinations is favored, which will increase the electrochemical rate constant (Table **2-2**) and, consequently, the current intensity obtained by SWASV.

2.4. Conclusions

The bismuth reduction process on glassy carbon, supporting electrolyte of buffer acetic acid/sodium acetate pH 4.5, is a non-reversible complex process with several signals. The multiple oxidation signals of bismuth may be related to surface different pH values. On the other hand, the presence of oxygen in the synthesis of the film affects its reproducibility, properties, and, consequently, its performance in SWASV measurements. Therefore, it is recommended to remove oxygen before making any measurements. In our case, Ar will be bubbled into the solution 5 min before starting an experiment, and Ar atmosphere will be maintained throughout the experiment.

Using Scharifker-Hills' models, the nucleation mechanism of bismuth deposition in GCE has been shown to occur via progressive nucleation and 3D growth mechanism. Hence, under these experimental conditions, the number of bismuth nuclei formed onto GCE is a function of time. Therefore, in order to use the BiFE electrodes to determine cadmium by SWASV, the deposition time (t_d) will be a factor to consider when developing and improving the SWASV method.

Furthermore, by using EIS, it was possible to estimate the heterogeneous charge rate constant k^0 for the $[\text{Fe}(\text{CN})_6]^{3-}/[\text{Fe}(\text{CN})_6]^{4-}$ redox couple, and to compare their values when using glassy carbon electrodes with and without bismuth film modification. A larger k^0 when using the bismuth film electrode is attributed to an increase in hydrophilicity. The above allows us to understand the improvement in the current intensity observed in the determinations of cadmium in an aqueous medium by anodic stripping voltammetry using bismuth film electrodes. In addition, it justifies using this type of modified working electrode in this research.

2.5. References

- Bard, A. J. and Faulkner, L. R. (2001). *Electrochemical methods. Fundamentals and applications*. John Wiley & Sons, Inc.
- Economou, A. (2005). Bismuth-film electrodes: recent developments and potentialities for electroanalysis. *TrAC Trends in Analytical Chemistry*, 24(4):334–340.
- Espinosa, A., San José, M., Tascón, M., Vázquez, M., and Batanero, P. S. (1991). Electrochemical behaviour of bismuth (v) and bismuth (iii) compounds at a carbon paste electrode. application to the study of the superconductor bisrcaquo. *Electrochimica acta*, 36(10):1561–1571.
- Grubač, Z. and Metikoš-Huković, M. (1998). Nucleation and growth of anodic oxide films on bismuth. *Electrochimica acta*, 43(21-22):3175–3181.
- Grujicic, D. and Pesic, B. (2002). Electrodeposition of copper: the nucleation mechanisms. *Electrochimica acta*, 47(18):2901–2912.
- Haynes, W. M., Lide, D. R., and Bruno, T. J. (2016). *CRC handbook of chemistry and physics*. CRC press.
- Ismail, J., Ahmed, M., and Kamath, P. V. (1993). Cyclic voltammetry studies of electrodeposited thin films of bismuth in 1 m koh. *Journal of Electroanalytical Chemistry*, 354(1-2):51–58.

- Mirceski, V., Hocevar, S. B., Ogorevc, B., Gulaboski, R., and Drangov, I. (2012). Diagnostics of anodic stripping mechanisms under square-wave voltammetry conditions using bismuth film substrates. *Analytical chemistry*, 84(10):4429–4436.
- Ouyang, R., Zhang, W., Zhou, S., Xue, Z.-L., Xu, L., Gu, Y., and Miao, Y. (2013a). Improved bi film wrapped single walled carbon nanotubes for ultrasensitive electrochemical detection of trace cr (vi). *Electrochimica acta*, 113:686–693.
- Ouyang, R., Zhang, W., Zhou, S., Xue, Z.-L., Xu, L., Gu, Y., and Miao, Y. (2013b). Improved bi film wrapped single walled carbon nanotubes for ultrasensitive electrochemical detection of trace cr (vi). *Electrochimica acta*, 113:686–693.
- Paunovic, M. and Schlesinger, M. (2006). *Fundamentals of electrochemical deposition*. john wiley & sons.
- Ramirez, D. P., Álvarez-Romero, G. A., Huizar, L. H. M., and Corona-Avenidaño, S. (2017). Electrochemical characterization of the electrocrystallization of bismuth on a graphite electrode. *ECS Transactions*, 76(1):161.
- Sandnes, E., Williams, M. E., Bertocci, U., Vaudin, M. D., and Stafford, G. R. (2007). Electrodeposition of bismuth from nitric acid electrolyte. *Electrochimica acta*, 52(21):6221–6228.
- Scharifker, B. and Hills, G. (1983). Theoretical and experimental studies of multiple nucleation. *Electrochimica acta*, 28(7):879–889.
- Vladislavic, N., Brinic, S., Grubac, Z., and Buzuk, M. (2014). Study of bi film formation on different carbon based electrodes for possible applicability in electroanalytical determination of cysteine. *Int. J. Electrochem. Sci*, 9:6020.
- Yang, M. and Hu, Z. (2005). Electrodeposition of bismuth onto glassy carbon electrodes from nitrate solutions. *Journal of electroanalytical chemistry*, 583(1):46–55.
- Youbi, B., Lghazi, Y., El Bachiri, A., Himi, M. A., Elibrizy, O., and Bimaghra, I. (2020). Investigation of nucleation and growth mechanism of bismuth electrodeposited on its substrate in nitric acid medium. *Materials Today: Proceedings*, 22:6–11.
- Zhou, L., Dai, Y., Zhang, H., Jia, Y., Zhang, J., and Li, C. (2012). Nucleation and growth of bismuth electrodeposition from alkaline electrolyte. *Bulletin of the Korean Chemical Society*, 33(5):1541–1546.

3. Implementation of the Square Wave Anodic Stripping Voltammetry methodology using bismuth film electrodes for cadmium quantification

3.1. Introduction

Square wave anodic stripping voltammetry (SWASV) has been used in the determination of cadmium and other toxic metals at trace levels in matrices such as milk, drinking and mineral water, aqueous solutions, urine, soils, wastewater, and seawater (Palisoc et al., 2019a; Chen et al., 2016; Palisoc et al., 2019b; Zhao et al., 2016; Fang et al., 2019; Pauliukaite et al., 2002). As seen in the previous chapter, bismuth film electrodes (BiFE) have been one of the most commonly used working electrodes for SWASV measurements. Nevertheless, the BiFE can be easily affected by variations in the experimental conditions between measurements (Brown et al., 2009; Fernando and Kratochvil, 1991; Pratt and Koch, 1988; Liu et al., 1997; Wang et al., 2001). **Internal standard calibration (ISC)** is one of the strategies to minimize the influence of these variations (Worsfold et al., 2019). This calibration method normalizes the target analyte's response to a reference's standard response, providing a correction factor for any fluctuation that may occur in the analysis routine. For electrochemical determinations of Zn^{2+} , Cd^{2+} , Pb^{2+} and Cu^{2+} in water samples, a substantial improvement in precision and trueness was achieved using the analytes under investigation as internal standards among themselves (Brown et al., 2009). In the same way, Pb^{2+} and Cd^{2+} have been used as internal standards of each other in the electrochemical determination of these toxic metals in biological materials and soils (Fernando and Kratochvil, 1991). Bismuth *in situ* plated film electrodes have also been used as a "built-in" internal standard (Wang, 2005), as the deposition of both analyte and electrode material are subject to the same variations. The bismuth oxidation signal has been used as an internal standard for trace measurements of Pb^{2+} . This strategy dramatically simplifies the analysis protocol and improves precision by minimizing the influence of uncontrolled conditions, which can cause random errors in

the measurement (Wang et al., 2001).

Multi-point and **single-point standard addition calibrations** are used to overcome matrix effects (analyte's signal intensity affected by other components present in the solution) in analytical measurements (Ellison and Thompson, 2008). Once linearity has been verified within the concentration range analyzed, the **single-point standard addition (SSA)** is a fast and efficient methodology for metal trace analysis in diverse matrices (Ellison and Thompson, 2008).

Furthermore, to improve the performance of the SWASV methodology in the determination of cadmium, the experimental parameters of SWASV need to be optimized. Simplex is an optimization technique that does not require the use of complex mathematical and statistical tools and can be useful in developing analytical methods (Bezerra et al., 2016; Rutten et al., 2014). A simplex is a geometric figure with $(k + 1)$ vertexes where k equals the number of variables in a k -dimensional experimental domain (Lundstedt et al., 1998). Simplex optimization is performed by the displacement of this geometric figure in the experimental region studied in order to avoid regions with undesirable responses (Michalowski et al., 2008). Simplex is a sequential optimization method where the experiments are performed a few at a time. Then, a response is assigned to each vertex. Finally, one of the vertexes is discarded in favor of a new one that must be evaluated. The results obtained in each stage are used to support decisions regarding experiments to be conducted later until the optimum is reached or a response good enough is obtained (Bezerra et al., 2016).

This chapter introduces the combination of **single-point standard addition calibration (SSA)** and the use of the bismuth oxidation signal as an *in situ* **internal standard (IS)** to obtain a practical and functional protocol that provides accurate results in the quantification of Cd^{2+} by SWASV. The latter calibration method aims to compensate for the variation identified in the electrochemical system, specifically in forming the BiFE working electrode. To validate this methodology, a NIST reference material of Cd^{2+} in solution was used as the sample to be tested. The results of the first Section 3.3.1 were published in (González-Basto et al., 2022). Finally, the simplex method was employed to optimize the SWASV parameters: pH of the supporting electrolyte, deposition potential, and deposition time.

3.2. Experimental section

3.2.1. Reagents

Standard solutions, samples, and the supporting electrolyte were prepared using type I water. Analytical grade sodium acetate ($\geq 99\%$, w/w) and glacial acetic acid (Merck, 100%, w/w) were used to prepare the supporting electrolyte in total acetate concentrations of 0.1 or 0.5 M. The pH of the solution was adjusted to a value equal to 4.5 with a solution of 1 M NaOH. The pH value selected for the supporting electrolyte used in our study was selected from the literature review (Economou, 2005) and preliminary experiments. The Cd^{2+} and Bi^{3+} stock solutions were prepared gravimetrically using a Cd^{2+} standard solution of $1.000 \pm 0.002 \text{ g L}^{-1}$ (Sigma-Aldrich Inc.), $\text{Bi}(\text{NO}_3)_3 \cdot 5\text{H}_2\text{O}$ (PanReac AppliChem, $\geq 98\%$, w/w) and the supporting electrolyte as the solvent. The standard reference material (RM) NIST 3108 (Cadmium $10.007 \pm 0.027 \text{ mg g}^{-1}$ in 1.3 M HNO_3 solution) was used to evaluate the proposed electroanalytical method in terms of repeatability and trueness. The solutions of the calibration curves were prepared gravimetrically in Falcon® tubes (50 mL). The laboratory glassware was cleaned as described in Section 2.2.1.

3.2.2. Samples

The RM, certified concentration of $10.007 \pm 0.027 \text{ mg g}^{-1}$ of Cd^{2+} , was used to prepare a sample in concentration of $15 \mu\text{g kg}^{-1}$ of Cd^{2+} . The latter required two intermediate solutions, one of $221.32 \text{ mg kg}^{-1}$ and the other of 4.01 mg kg^{-1} of Cd^{2+} . The cadmium concentration is reported with its uncertainty, using the GUM-2008 recommendations (JCGM, 2008).

Simplex experiments were performed in triplicate using a standard solution in concentration of $30 \mu\text{g kg}^{-1}$ of Cd^{2+} . Before measuring each vertex and each triplicate, the GCE was cleaned and polished as described in Section 2.2.2. The response variable chosen was the Cd peak area normalized to the Bi peak area. The R package `labsimplex` (Paredes and Ágreda, 2020) was used to generate and visualize the coordinates of the experimental variables and the evolution in the response as a function of the number of experiments.

3.2.3. Instrumentation, electrochemical cell and electrodes

The electrochemical system used and the cleaning procedure for the GCE are the same as described in Section 2.2.2. The bismuth film was formed by the *in situ* method using $500 \mu\text{g kg}^{-1}$ of Bi^{3+} in the electrochemical cell. The experimental parameters for SWASV are shown in Table 3-1. They were selected from the literature review (Mirceski et al., 2012) and preliminary studies.

Table 3-1. Electrochemical parameters used in the determination of cadmium using SWASV.

Parameter	Value
Deposition potential	-1.00 V vs. Ag/AgCl
Deposition time	120 s
Rest time	20 s
Agitation rate	500 rpm
Pulse amplitude	20 mV
Pulse frequency	25 Hz
Square wave voltammetry potential limits	-1.00 to 0.80 V
Cleaning step (agitation on)	90 s at 0.80 V
pH supporting electrolyte	4.5

3.2.4. Simplex optimization

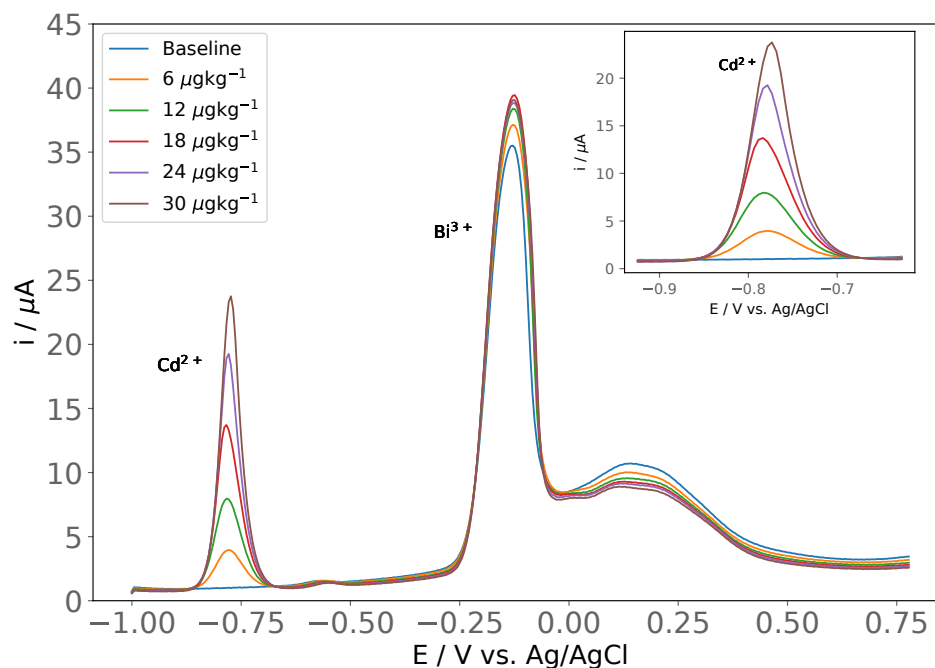
The set of critical parameters to be optimized were selected according to the literature review (Zhao et al., 2016; Palisoc et al., 2019a; Chen et al., 2016; Fang et al., 2019; Kava et al., 2020; Ping et al., 2014) and preliminary studies. The values reported in Table **3-1** for the parameters to be optimized, pH, deposition potential (E_d), and deposition time (t_d), were the values used to generate the initial simplex. The step size, in the simplex, selected for each variable were pH = 0.2, E_d = -0.2, t_d = -25 s. The optimization criterion was selected as a maximum in the response, and the variable size algorithm was used to generate a new vertex. The simplex will contract into the optimal point until the difference between two vertices becomes too small to be experimentally practical (Paredes and Ágreda, 2020).

3.3. Results

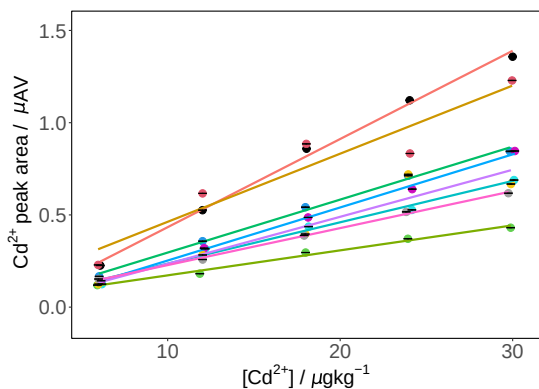
3.3.1. Calibration methodology development: *in situ* internal standard and single-point standard addition calibration

The implementation of the SWASV methodology began with selecting the most appropriate calibration method for its use in the determination of cadmium. Figure 3.1(a) shows the voltammograms obtained by SWASV of an **multi-point external standard calibration (ESC)** curve with five calibration levels.

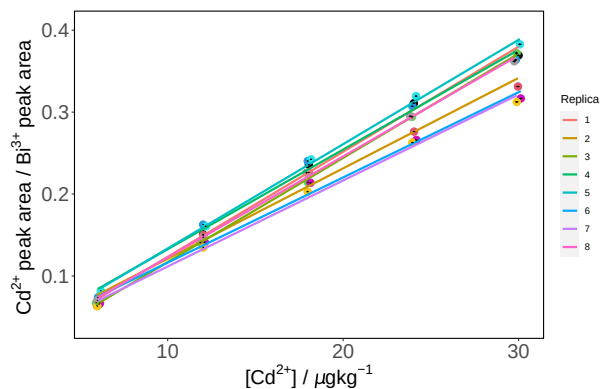
A close-up of the Cd^{2+} signal is shown in the inset. Cadmium and bismuth oxidation signals are observed at approximately -0.80 and -0.15 V, respectively. The response variable chosen to construct the **ESC** curve was the peak area of the cadmium oxidation since the peak potential shifts to less negative potentials as the concentration increases. Meaning that some



(a)



(b)



(c)

Figure 3-1.: (a) Voltammograms using SWASV of a calibration curve by external standard calibration method from $6 \mu\text{g kg}^{-1}$ to $30 \mu\text{g kg}^{-1}$ of Cd^{2+} in acetate buffer 0.1 M and $\text{pH } 4.5$. $[\text{Bi}^{3+}] = 500 \mu\text{g kg}^{-1}$. Inset: close-up of the cadmium peak. (b) Calibration curves Cd^{2+} peak area vs. $[\text{Cd}^{2+}]$. (c) Calibration curves Cd^{2+} peak area / Bi^{3+} peak area vs. $[\text{Cd}^{2+}]$.

charge transfer effect is being involved in the measurement which should ideally be controlled entirely by diffusion. Eight replicates of this calibration curve were constructed, and a linear model was adjusted using Ordinary Least Squares regression (OLS). Table 3-2 shows regression parameters in columns two to four. Figure 3.1(b) presents the high variability

between the responses at each calibration level.

Table 3-2.: Regression parameters obtained for the multi-point external standard calibration without internal standard (ESC) and multi-point standard addition with internal standard calibration method (ESC-IS).

Replica	ESC			ESC-IS		
	slope ($\mu\text{AVkg } \mu\text{g}^{-1}$)	y-intercept (μAV)	r^2	slope ($\mu\text{AVkg } \mu\text{g}^{-1}$)	y-intercept (μAV)	r^2
1	0.0478	-0.0443	0.9958	0.0128	-0.0048	0.9947
2	0.0369	0.0936	0.9041	0.0110	0.0109	0.9867
3	0.0135	0.0370	0.9892	0.0127	-0.0101	0.9995
4	0.0287	0.0089	0.9959	0.0122	0.0111	0.9928
5	0.0224	0.0117	0.9855	0.0127	0.0064	0.9982
6	0.0288	-0.0348	0.9977	0.0104	0.0124	0.9912
7	0.0255	-0.0197	0.9057	0.0105	0.0067	0.9952
8	0.0200	0.0278	0.9979	0.0123	-0.0005	0.9988
Mean	0.0280	0.0100	0.9715	0.0118	0.0040	0.9946
SD	0.0106	0.0445	0.0413	0.0010	0.0083	0.0043
RSD (%)	37.8	443.51	4.25	8.70	205.78	0.44

Eight RM sample replicates were prepared at $15 \mu\text{g kg}^{-1}$ of Cd^{2+} and measured under the same experimental conditions as the calibration curves. Then, the concentration of cadmium, $[\text{RM}]_{\text{measured}}$, was calculated by interpolation. The $[\text{RM}]_{\text{measured}}$ ranged between 9.81 and 23.97 mg g^{-1} of Cd^{2+} . The precision in the concentration of cadmium found in the samples is poor, with an RSD of 29.71 % (Table 3-3 column two). The low repeatability of the results obtained by the **ESC** method is attributed to uncontrolled variations in the measurement conditions.

Figure 3.1(c) shows the ESC calibration curves constructed using the Bi signal as an *in situ* internal standard (**ESC-IS**), in which the Cd peak area is normalized to the peak area of Bi. Table 3-2 shows its regression parameters, columns five to seven; the improvement, due to the ESC-IS procedure, is evident in the repeatability of the slope, intercept, and correlation coefficient, last row of the table, RSD (%). Consequently, there was an improvement in the repeatability of the $[\text{RM}]_{\text{measured}}$, which now ranged only between 11.79 and 14.41 mg g^{-1} of Cd^{2+} , RSD = 6.88 %, see Table 3-3, column four. Therefore, using the electrode material as an *in situ* internal standard improves the repeatability of the curve compared to the **ESC** method, obtaining a decrease of 22.83 % in the RSD of the calculated concentration of Cd^{2+} in the RM. The above facts confirm that the **ESC-IS** calibration method compensates for the experimental variations between measurements, as was reported previously (Pratt and Koch, 1988; Wang et al., 2001; Fernando and Kratochvil, 1991; Brown et al., 2009). At the same time, using the film electrode material as an internal standard avoids adding another substance, simplifies standards and sample preparation protocols, and avoids

Table 3-3.: Comparison of Cd concentration results for the reference material, $[RM] \pm u_{exp} = 10.007 \pm 0.027$. The calculations were made using the multi-point external standard calibration i-) without (ESC) and ii-) with the internal standard method (ESC-IS). The ESC-IS method was tested at two concentrations of the supporting electrolyte (0.1 and 0.5 M), with cleaning the working electrode between measurements. Also, the single-point standard addition calibration with the internal standard method (SSA-IS) is presented.

Calibration method → [AcCOOH] →	ESC 0.1 M		ESC-IS 0.1 M		ESC-IS 0.5 M*		SSA-IS 0.5 M	
Replica	$[RM]_{measured}$ (mg g ⁻¹)	bias (%)	$[RM]_{measured}$ (mg g ⁻¹)	bias (%)	$[RM]_{measured}$ (mg g ⁻¹)	bias (%)	$[RM]_{measured}$ (mg g ⁻¹)	bias (%)
1	9.81	-1.97	12.46	24.48	9.36	-6.50	9.69	-3.20
2	15.48	54.70	14.41	43.97	8.77	-12.36	9.36	-6.44
3	23.97	139.56	13.03	30.17	8.72	-12.92	8.75	-12.59
4	12.67	26.60	11.79	17.82	8.74	-12.67	9.90	-1.12
5	21.25	112.40	11.99	19.80	9.05	-9.56	11.06	10.57
6	13.08	30.72	13.60	35.86	8.82	-11.86	10.05	0.43
7	13.70	36.90	13.57	35.58	8.72	-12.82	9.51	-4.98
8	16.77	67.59	12.63	26.17	8.48	-15.21	9.81	-1.95
Mean	15.84	58.80	12.93	29.23	8.83	-11.74	9.77	-5.16
SD	4.71	46.33	0.89	8.89	0.26	2.62	0.66	4.46
RSD (%)	29.71	78.78	6.88	30.42	2.97	22.31	6.77	86.37

*Calibration curve with cleaning (polishing and electrochemical cleaning) between measurements.

additional sources of uncertainty.

In addition, the effect of the supporting electrolyte concentration was studied. Normalized areas were calculated for eight replicates of a cadmium standard solution at $30 \mu\text{g kg}^{-1}$ and compared when the supporting electrolyte was 0.1 or 0.5 M acetate buffer, Figure 3.2(a) and 3.2(b).

First, it was observed that the ratio of areas, $\text{Area}_{Cd}/\text{Area}_{Bi}$, was smaller when using the 0.5 M acetate buffer. This is explained by considering that increasing the supporting electrolyte concentration decreases the migration current of the cation during the cation reduction. That is, less Cd^{2+} reaches the electrode surface by migration because more supporting electrolyte is responsible for this migration (Broekaert, 2015). According to the above, migration should affect Cd^{2+} and Bi^{3+} in a similar way. However, it is important to remember that Bi^{3+} is more concentrated than Cd^{2+} (around 16-fold higher); and such concentration would cause the Bi^{3+} current not to decrease as significantly as Cd^{2+} signal does. This leads to a smaller area ratio, $\text{Area}_{Cd}/\text{Area}_{Bi}$, for the 0.5 M acetate buffer experiments when compared to the 0.1 M concentration. The latter will affect the methodology's sensibility (slope of the calibration curves). Thus, to increase sensibility, we must decrease the supporting electrolyte concentration.

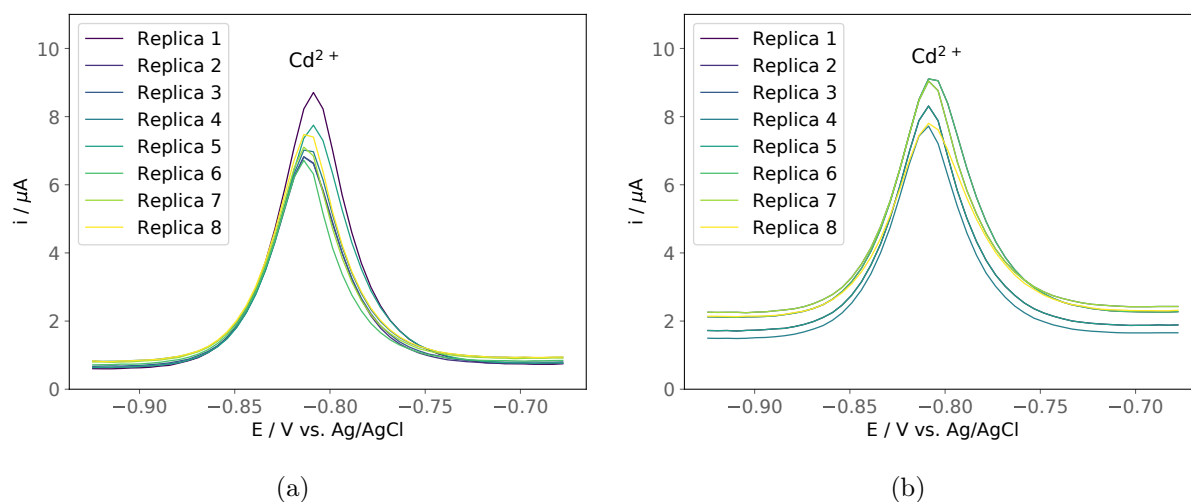


Figure 3-2.: Cadmium peak of eight voltammograms using SWASV for the analysis of a cadmium standard solution containing $30 \mu\text{g kg}^{-1}$ of Cd^{2+} and pH 4.5; **(a)** in acetate buffer 0.1 M, and **(b)** in acetate buffer 0.5 M.

Nevertheless, we found that having a lower supporting electrolyte concentration makes the system more irreproducible. For the calculated areas, the RSD was 2.99 % for 0.1 M acetate buffer and 1.26 % when the acetate buffer was 0.5 M (Table 3-4). The latter is consistent with the basic theory.

Table 3-4.: Comparison of the normalized areas of a cadmium standard solution at different concentrations of the supporting electrolyte.

Replica	$\text{Area}_{\text{Cd}}/\text{Area}_{\text{Bi}}$	$\text{Area}_{\text{Cd}}/\text{Area}_{\text{Bi}}$
[AcCOOH]	0.1 M	0.5 M
1	0.2377	0.0824
2	0.2268	0.0837
3	0.2398	0.0817
4	0.2374	0.0808
5	0.2288	0.0822
6	0.2250	0.0833
7	0.2216	0.0811
8	0.2364	0.0815
Mean	0.232	0.082
SD	0.0069	0.0010
RSD (%)	2.99	1.26

Therefore, the increase in the concentration of the supporting electrolyte decreases the contribution of the analyte to the total migration in the solution, compacts the electric double layer, and thereby, the capacitive currents are higher but more constant (Bard and Faulkner, 2001; Bagotsky, 2005). The latter increases the precision of the current intensity obtained from the cadmium oxidation signal between replications, Table **3-4** and Figure 3.2(b). Thus, it was decided to increase the supporting electrolyte concentration for the following experiments.

The latter results show that the repeatability improves by employing the *in situ* internal standard and buffer acetate 0.5 M. However, the method still fails when trueness is considered. The biases obtained by the **ESC** and **ESC-IS** methods reach considerably high percentages, 59 % and 29 % of bias, see Table **3-3** columns three and five. The lack of trueness in the methodology seems to be related to the low repeatability of the bismuth film after repeated measurements. It has been found that the Cd signal obtained for consecutive replications in the same solution decreases systematically, Figure 3.3(a). During each formation of a new bismuth layer, the layer is not formed in the same way as before. It appears that fewer nuclei are formed, making the new area of the bismuth film smaller than the previous one. This would also be consistent with a smaller heterogeneous charge transfer constant. Resulting in a smaller voltammetric signal.

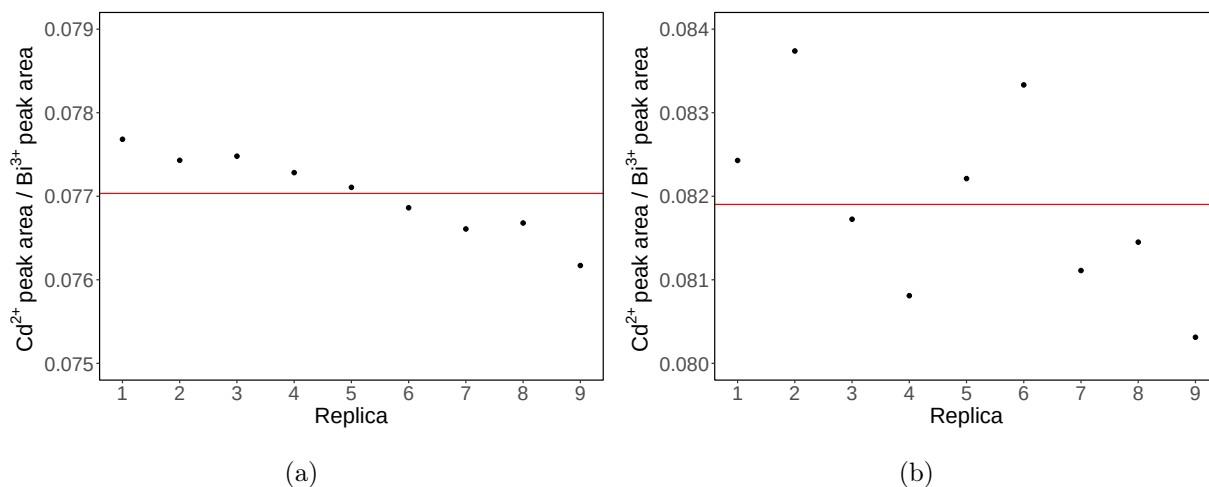


Figure 3-3.: Normalized response Cd^{2+} peak area / Bi^{3+} peak area for nine replicates of a standard solution containing $30.68 \pm 0.02 \mu\text{g kg}^{-1}$ of Cd^{2+} in acetate buffer 0.5 M and pH 4.5. **(a)** Without cleaning the GCE between measurements, and **(b)** with cleaning the GCE between measurements.

The latter means that after several cycles of formation and stripping of the Bi-Cd film, the active surface changes, and its performance declines as the number of measurements increases. On the contrary, when the measurement is performed with a freshly clean electrode

(polishing and electrochemical cleaning as described in Section 2.2.2), the response has no tendency, see Figure 3.3(b). The systematic decrease in current between measurements explains why multi-point calibration curves (**ESC** and **ESC-IS** method) give high percentages of bias. To confirm the effect of the electrode surface condition on the performance of the calibration curves, we prepared new **ESC-IS** calibration curves between concentrations of 5 and 95 $\mu\text{g kg}^{-1}$ of Cd^{2+} and performed a cleaning step of the GCE surface (polishing and electrochemical cleaning) between calibration levels, Figure 3.4(a).

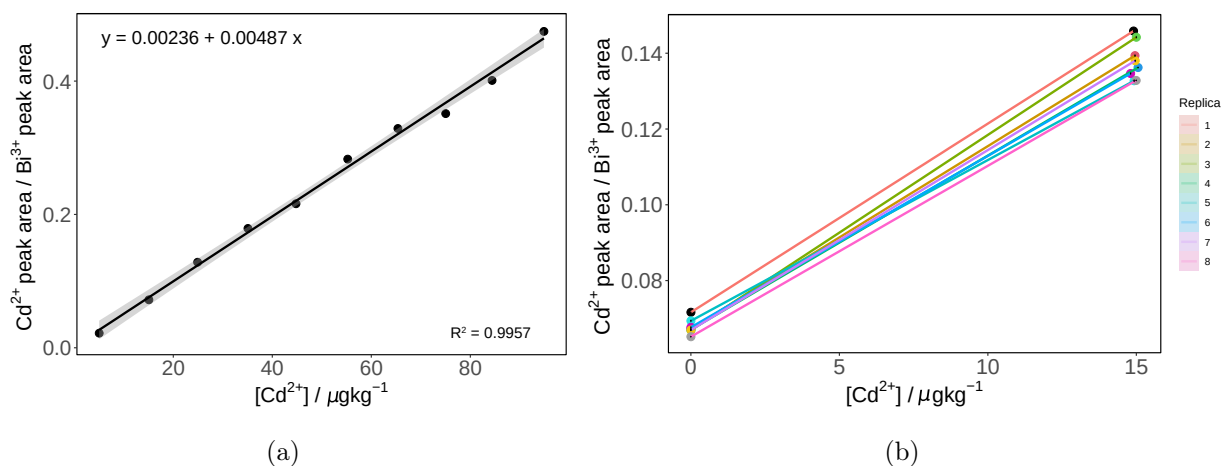


Figure 3-4.: (a) Calibration curve Cd^{2+} peak area / Bi^{3+} peak area vs. $[\text{Cd}^{2+}]$ by external standard calibration with the internal standard method (ESC-IS) and cleaning between calibration levels. (b) Calibration curve Cd^{2+} peak area / Bi^{3+} peak area vs. $[\text{Cd}^{2+}]$ by single-point standard addition with the internal standard method (SSA-IS) without cleaning the BiFE between the two levels.

Using the mentioned calibration curve, the $[\text{RM}]_{\text{measured}}$ ranged between 8.48 and 9.36 mg g^{-1} of Cd^{2+} . The RSD was 2.97%, and the bias was 11.74%, which are lower than the results obtained without the cleaning step, Table 3-3, columns six and seven. This result confirms that the surface of the electrode is affected as the calibration curve is built; therefore, cleaning between concentration levels is necessary to obtain reliable results.

Despite the improvements due to the cleaning step, this procedure involves a considerable amount of time, about one hour for each calibration level, which makes the construction of a calibration curve a tedious and impractical procedure for a routine calibration and quantification method. Thus, to reduce the RSD and bias while maintaining the simplicity and practicality of the methodology, the **single-point standard addition method (SSA)** was implemented together with the *in situ* **internal standard (IS)** procedure presented before. Observe that we confirm the linearity of the method over the whole relevant concentration range of Cd^{2+} , **ESC-IS** with cleaning experiment, Figure 3.4(a), before using the

SSA method.

The **SSA** method is an excellent analytical alternative because the calculations are simplified by eliminating the need for regression, retaining similar results as would be provided by regression (Ellison and Thompson, 2008). In addition, **SSA** reduces the number of operations needed per measurement, decreasing the GCE surface passivation effect on the results. Therefore, with this methodology, cleaning between the two calibration points is unnecessary to obtain reliable results with high trueness levels, Table **3-3**, column nine.

Figure 3.4(b) shows eight **SSA-IS** calibration curves. The RM solution and the single spiked solution measurements were made without cleaning the working electrode between the two levels. The $[RM]_{measured}$ ranged between 8.75 and 11.06 mg g⁻¹ of Cd²⁺. An RSD of 6.77 % and bias of 5.16 % were obtained for the cadmium quantification in the RM, see the last two columns of Table **3-3**. Therefore, it can be said that with the **SSA-IS** calibration method and the use of a supporting electrolyte concentration of 0.5 M, the problems of the poor repeatability and passivation of the GCE are surpassed. At the same time, it is possible to maintain the practicality of the measurement protocol (no cleaning is necessary) without sacrificing the required levels of precision and trueness.

Uncertainty estimation for the single-point standard addition calibration method

Eq. 3-1 represents the mathematical model used to calculate the Cd²⁺ concentration, $[RM] \left(\frac{mg}{g} \right)$, by the **SSA-IS** method, which includes the extrapolation of the calibration curve to the x-intercept (s_1), the dilution factors W (s_2) and the repeatability P (s_3).

$$[RM] \left(\frac{mg}{g} \right) = C_s \underbrace{\frac{A_{RM}}{(A_{RM+C}) - A_{RM}}}_{s_1} \cdot \underbrace{\frac{W_{f3}}{W_{al3}} \cdot \frac{W_{f2}}{W_{al2}} \cdot \frac{W_{f1}}{W_{al1}}}_{s_2} \cdot \underbrace{P}_{s_3} \quad (3-1)$$

The meaning of each symbol in Eq. 3-1 is presented below.

- C_s : Cd²⁺ concentration of the spike in $\mu g kg^{-1}$.
- A_{RM} : Normalized area of the sample in the non-spiked mixture.
- A_{RM+C} : Normalized area of the sample in the spiked mixture.
- W_{al1} : Aliquot weight of the starting stock solution in g.
- W_{f1} : Final weight of the starting stock solution in g.
- W_{al2} : Aliquot weight of the second intermediate solution in g.
- W_{f2} : Final weight of the second intermediate solution in g.
- W_{al3} : Aliquot weight of the third intermediate solution in g.
- W_{f3} : Final weight of the third intermediate solution in g.
- P : Repeatability factor. $P = 1$.

The uncertainty budget for the measurand is composed of uncertainty contributions that correspond to all variables of the model equation. In our case, we identify three main sources of uncertainty (s_1, s_2, s_3) in the Cd^{2+} quantification by our proposed **SSA-IS** method (Eq. 3-1). We use the three uncertainty sources to calculate the combined standard uncertainty $u_{c(RM)}$ as reported in the GUM - 2008 (JCGM, 2008), and according to Eq. 3-2.

$$\frac{u_{c(RM)}}{[RM] \left(\frac{mg}{g} \right)} = \sqrt{(u_{s_1})^2 + (u_{s_2})^2 + (u_{s_3})^2} \quad (3-2)$$

The first contribution to the combined uncertainty comes from the calculations implicit in the single-point standard addition calibration curves (Eq. 3-3).

$$u_{s_1} = RSD(T) = \frac{Q}{Q-1} \left[2A^2 + \frac{1}{4k^2} \left(1 + \frac{1}{Q^2} \right) \right]^{1/2}, \quad (3-3)$$

where:

- T : Cd^{2+} concentration of the non-spiked solution in $\mu\text{g kg}^{-1}$.
- $k = T/c_L$: Generalized concentration with c_L the detection limit.
- $Q = C_s/T$: Ratio concentrations of the Cd^{2+} concentration of the spike (C_s) and the Cd^{2+} concentration of the non-spiked solution (T).
- A : asymptotic RSD of the response.

The extrapolation uncertainty, u_{s_1} , is the relative standard deviation, $RSD(T)$, of the concentration value estimated for the single-point standard addition case (Eq. 3-1, s_1) as previously reported by (Ellison and Thompson, 2008; Thompson, 2009). The deduction of this expression considers two facts, the detection limit and the heteroscedasticity of analytical calibrations. This standard deviation is calculated by error propagation, and it is expressed in terms of k , the generalized concentration (relative to the detection limit), Q , the concentration ratio between the single standard addition over the sample, and A , the asymptotic RSD of the answer.

The second contribution is the uncertainty arising from the preparation of the RM solutions (u_{s_2}), including the uncertainty of the balance (u_W) used for the preparation of the solutions and the uncertainty reported (u_{stock}) of the NIST 3108 RM used (Eq. 3-4).

$$\begin{aligned} u_{s_2}^2 = & \left(\frac{u_W}{W_{al3}} \right)^2 + \left(\frac{u_W}{W_{f3}} \right)^2 + \left(\frac{u_W}{W_{al2}} \right)^2 + \left(\frac{u_W}{W_{f2}} \right)^2 \\ & + \left(\frac{u_W}{W_{al1}} \right)^2 + \left(\frac{u_W}{W_{f1}} \right)^2 + \left(\frac{u_{stock}}{W_{stock}} \right)^2 \end{aligned} \quad (3-4)$$

The last contribution, the uncertainty associated with the repeatability (u_{s3}), is given by Eq. 3-5 and Eq. 3-6.

$$u_{s3}^2 = \left(\frac{u_{rep}}{[RM]} \right)^2 \quad (3-5)$$

$$u_{rep} = \frac{SD}{\sqrt{n}} \quad (3-6)$$

Finally, the expanded uncertainty (U) is calculated with the combined uncertainty values and using Eq. 3-7 with 95 % confidence.

$$U = u_{c(RM)} \cdot 1.962 \quad (3-7)$$

Following the above, the concentration and the expanded uncertainties were estimated for each analyzed replica of the RM. The concentration values are reported along with its expanded uncertainty in Table 3-5.

Table 3-5.: Cadmium concentrations and estimated expanded uncertainty of the RM NIST 3108 measured by SWASV and the SSA-IS methodology developed in this work.

Replica	$[RM]_{measured} / \text{mg g}^{-1}$	$U_{(k=1.962)} / \text{mg g}^{-1}$
1	9.69	0.95
2	9.36	0.92
3	8.75	0.86
4	9.89	0.97
5	11.10	1.10
6	10.05	0.99
7	9.51	0.93
8	9.81	0.96
Mean	9.77	0.96
SD	0.66	0.06
RSD(%)	6.77	6.62

The One-Sample t-test was used to compare the mean of the eight experimental results (m) to the certificated cadmium concentration ($\mu = 10.007 \pm 0.027 \text{ mg g}^{-1}$). The t-test result, with a p-value of 0.2758 greater than the significance level of 0.05, fails to reject the null hypothesis ($H_0: m = \mu$). In other words, the sample mean calculated with the calibration method proposed in this work is not statistically different from the reported value.

3.3.2. Simplex optimization of SWASV methodology

According to the literature, optimization studies of SWASV parameters in determining cadmium using bismuth film electrodes on different substrates use the cadmium stripping peak current or peak area as the response variable to be optimized (Zhao et al., 2016; Lazanas et al., 2020; Kava et al., 2020; Zhang et al., 2020; Palisoc et al., 2019a; Ping et al., 2014). However, considering the experiments carried out previously in this work (Section 3.3.1), we find that to obtain acceptable repeatability ($RSD \approx 7\%$), it is necessary to employ and evaluate the normalized Cd peak area with respect to the Bi peak area ($Area_{Cd}/Area_{Bi}$). Thus, the changes in the peak area ratio will be due to the changes in the signal obtained for each element (Cd and Bi), and these changes will depend on the selected parameters (pH, E_d , t_d). Table 3-6 presents the vertexes generated by the variable step-size simplex optimization for pH, E_d , and t_d SWASV parameters.

Table 3-6.: Simplex information for the 11 vertexes of the variable step-size simplex optimization for pH, E_d , and t_d SWASV parameters, generated with the R package `labsimplex`. The mean response $Area_{Cd}/Area_{Bi}$ obtained from a triplicate measurement of a solution $30 \mu\text{g kg}^{-1}$ of Cd^{2+} is presented alongside its % RSD.

Current Simplex:							
	pH	E_d (V)	t_d (s)	label	nature	$Area_{Cd}/Area_{Bi}$	% RSD
9	4.3	-1.15	162	N	R	0.16638	2.8
7	4.4	-0.95	153		R	0.16933	2.2
10	4.3	-1.20	198		R	0.19054	5.4
11	4.2	-1.30	238		E	0.18522	6.9
Historical Vertexes:							
	pH	E (V)	t (s)	label	nature	$Area_{Cd}/Area_{Bi}$	% RSD
6	4.5	-1.20	162	W	E	0.15345	2.3
1	4.5	-1.00	120	W	S	0.15088	1.2
4	4.7	-0.95	128	N	S	0.14776	1.2
2	4.7	-1.15	120	W	S	0.12452	3.4
3	4.7	-0.95	103	W	S	0.12006	5.4
5	4.6	-1.12	142	D	R	0.15274	0.7
8	4.3	-0.85	170	D	E	0.01074	11.5

Labels: W: Worst or Wastebasket, N: Next to the worst, B: Best, D: Disregarded.

Nature: S: Starting, R: Reflected, E: Expanded.

The simplex examined the pH value from 4.2 to 4.7, the deposition potential from -1.30 to -0.85 V, and the deposition time from 103 to 238 s. The mean response $Area_{Cd}/Area_{Bi}$ (obtained from each vertex triplicate) alongside its % RSD were used as a quality criterion.

It was found that the $\text{Area}_{\text{Cd}}/\text{Area}_{\text{Bi}}$ increased by applying a more negative potential for a longer deposition time and a decreasing pH value. Deposition potential dramatically influences the sensitivity and selectivity of the determination. Low deposition potential ($E_d > -0.95$ V) is not enough to reduce cadmium ions (vertex 8). Then, more cathodic deposition potentials enhance the stripping currents for cadmium and bismuth ions. However, as the deposition potential becomes more negative, the hydrogen reduction becomes more significant, which could lead to a lower signal for cadmium and bismuth reduction (Lazanas et al., 2020; Fang et al., 2019; Zhang et al., 2020; Chen et al., 2016; Ping et al., 2014). As expected, the time at which the *in situ* bismuth film is deposited together with the cadmium ions greatly influences the response. Both metal stripping signals follow an increasing tendency when increasing the deposition time. This result further agreed with the found in Chapter 2 and the nucleation and growth mechanism of Bi onto GCE. Nevertheless, it should be considered that the goal is to develop a practical and agile quantification methodology. This includes achieving a reasonable time of analysis. Finally, the decrease in stripping currents for bismuth and cadmium at higher pH values may be related to the possibility of hydrolysis reactions of both metals (Fang et al., 2019; Zhang et al., 2020).

After 11 vertexes, the optimal values for the parameters were found to be: pH = 4.3, $E_d = -1.2$ V, and $t_d = 198$ s, values corresponding to the vertex 10, Figure 3.5(a).

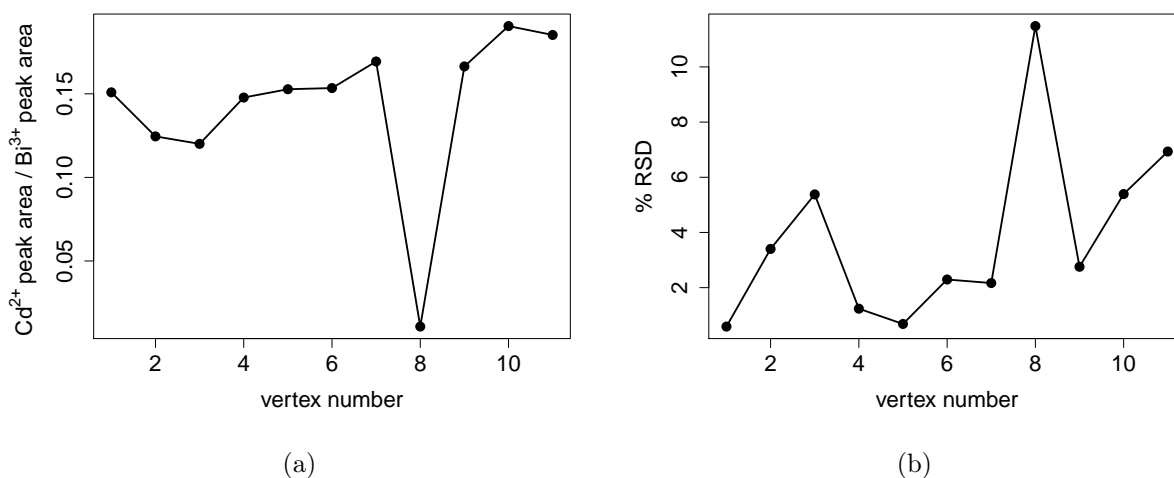


Figure 3-5.: (a) Mean response $\text{Area}_{\text{Cd}}/\text{Area}_{\text{Bi}}$ vs. vertex number for the variable step-size simplex optimization for pH, E_d , and t_d SWASV parameters of a solution $30 \mu\text{g kg}^{-1}$ of Cd^{2+} . (b) % RSD values of the response $\text{Area}_{\text{Cd}}/\text{Area}_{\text{Bi}}$ vs. vertex number.

The simplex movement was stopped when a 26% improvement and a 5% of variability in

the response variable were obtained. A considerable $\text{Area}_{\text{Cd}}/\text{Area}_{\text{Bi}}$ increase is observed in vertex 10; when performing vertex 11, the increase stopped, indicating that an optimum has possibly been reached. In addition, at vertex 11, the % RSD of the results begins to increase see Figure 3.5(b). As mentioned before, more negative deposition potential approaches the functional potential window of the GCE. Therefore, other faradaic reactions interfere with the measurement, and the stripping signals become unstable, increasing the variability of the results. Consequently, the optimized parameters were selected as a compromise to maintain the sensitivity, simplicity, and agility of the technique, one of the main characteristics and desired advantages of the SWASV.

3.4. Conclusions

The surface conditions of the bismuth film/glassy carbon working electrode during the quantification of Cd^{2+} by SWASV directly affect the precision and trueness of the methodology. The combination of the internal standard *in situ* calibration and the single-point standard addition method dramatically improves the precision and trueness compared to the traditional multi-point external standard calibrations without or even with internal standard calibration. Also, increasing the supporting electrolyte concentration from 0.1 M to 0.5 M improves the precision of the measurements. Then, the proposed methodology represents a practical and faster alternative to traditional methods, as no mechanical or electrochemical cleaning is necessary (between calibration patrons) to satisfy the required levels of precision and trueness. The precision, $\text{RSD} = 6.77\%$, and trueness, $\text{bias} = 5.16\%$, of the developed method, the single-point standard addition along with internal standard calibration methodology in acetic acid - sodium acetate buffer at 0.5 M as supporting electrolyte, are acceptable when compared to the reference material NIST 3108 ($\text{Cd}^{2+} 10.007 \pm 0.027 \text{ mg g}^{-1}$). Our result, $\text{Cd}^{2+} 9.77 \pm 0.96 \text{ mg g}^{-1}$, is statistically similar to the certified value. Additionally, the experimental conditions pH, deposition potential, and deposition time for Cd^{2+} detection by SWASV using BiFE were optimized with a simplex method. In this way, the proposed methodology is ready to be tested under the optimal experimental conditions, $\text{pH} = 4.3$, $E_d = -1.2 \text{ V}$, and $t_d = 198 \text{ s}$, in the measurement of trace concentration levels of cadmium in real cocoa samples.

3.5. References

- Bagotsky, V. S. (2005). *Fundamentals of electrochemistry*. John Wiley & Sons.
- Bard, A. J. and Faulkner, L. R. (2001). *Electrochemical methods. Fundamentals and applications*. John Wiley & Sons, Inc.
- Bezerra, M. A., dos Santos, Q. O., Santos, A. G., Novaes, C. G., Ferreira, S. L. C., and

- de Souza, V. S. (2016). Simplex optimization: a tutorial approach and recent applications in analytical chemistry. *Microchemical Journal*, 124:45–54.
- Broekaert, J. A. (2015). Daniel c. harris: Quantitative chemical analysis.
- Brown, R. J., Roberts, M. R., and Brett, D. J. (2009). Stripping voltammetry using sequential standard addition calibration with the analytes themselves acting as internal standards. *Analytica Chimica Acta*, 635(1):1–5.
- Chen, G., Hao, X., Li, B. L., Luo, H. Q., and Li, N. B. (2016). Anodic stripping voltammetric measurement of trace cadmium at antimony film modified sodium montmorillonite doped carbon paste electrode. *Sensors and Actuators B: Chemical*, 237:570–574.
- Economou, A. (2005). Bismuth-film electrodes: recent developments and potentialities for electroanalysis. *TrAC Trends in Analytical Chemistry*, 24(4):334–340.
- Ellison, S. L. and Thompson, M. (2008). Standard additions: myth and reality. *Analyst*, 133(8):992–997.
- Fang, Y., Cui, B., Huang, J., and Wang, L. (2019). Ultrasensitive electrochemical sensor for simultaneous determination of cadmium and lead ions based on one-step co-electropolymerization strategy. *Sensors and Actuators B: Chemical*, 284:414–420.
- Fernando, A. R. and Kratochvil, B. (1991). Internal standards in differential pulse anodic stripping voltammetry. *Canadian journal of chemistry*, 69(4):755–758.
- González-Basto, M. C., España-Sánchez, C. A., Ágreda, J. A., and del Pilar Sandoval-Rojas, A. (2022). Improving precision and trueness in the quantification of cadmium using square wave anodic stripping voltammetry and bismuth film electrodes. *Results in Chemistry*, page 100630.
- JCGM, J. (2008). Joint Committee for Guides in Metrology: Evaluation of measurement data - guide to the expression of uncertainty in measurement. Technical report, JCGM.
- Kava, A. A., Beardsley, C., Hofstetter, J., and Henry, C. S. (2020). Disposable glassy carbon stencil printed electrodes for trace detection of cadmium and lead. *Analytica chimica acta*, 1103:58–66.
- Lazanas, A. C., Tsirka, K., Paipetis, A. S., and Prodromidis, M. I. (2020). 2d bismuthene/graphene modified electrodes for the ultra-sensitive stripping voltammetric determination of lead and cadmium. *Electrochimica Acta*, 336:135726.
- Liu, T. Z., Lai, D., and Osterloh, J. D. (1997). Indium as internal standard in square wave anodic stripping analysis of lead in blood with microelectrode arrays. *Analytical chemistry*, 69(17):3539–3543.

- Lundstedt, T., Seifert, E., Abramo, L., Thelin, B., Nyström, Å., Pettersen, J., and Bergman, R. (1998). Experimental design and optimization. *Chemometrics and intelligent laboratory systems*, 42(1-2):3–40.
- Michalowski, T., Rymanowski, M., and Pietrzyk, A. (2008). A simple approach to the simplex method. *Chem. Anal.(Warsaw)*, 53:743.
- Mirceski, V., Hocevar, S. B., Ogorevc, B., Gulaboski, R., and Drangov, I. (2012). Diagnostics of anodic stripping mechanisms under square-wave voltammetry conditions using bismuth film substrates. *Analytical chemistry*, 84(10):4429–4436.
- Palisoc, S., Gonzales, A. J., Pardilla, A., Racines, L., and Natividad, M. (2019a). Electrochemical detection of lead and cadmium in uht-processed milk using bismuth nanoparticles/nafion®-modified pencil graphite electrode. *Sensing and Bio-Sensing Research*, 23:100–268.
- Palisoc, S., Sow, V. A., and Natividad, M. (2019b). Fabrication of a bismuth nanoparticle/nafion modified screen-printed graphene electrode for in situ environmental monitoring. *Analytical Methods*, 11(12):1591–1603.
- Paredes, C. and Ágreda, J. (2020). *labsimplex: Simplex Optimization Algorithms for Laboratory and Manufacturing Processes*. R package version 0.1.2.
- Pauliukaite, R., Metelka, R., Švancara, I., Królicka, A., Bobrowski, A., Vytřas, K., Norkus, E., and Kalcher, K. (2002). Carbon paste electrodes modified with bi 2 o 3 as sensors for the determination of cd and pb. *Analytical and Bioanalytical Chemistry*, 374(6):1155–1158.
- Ping, J., Wang, Y., Wu, J., and Ying, Y. (2014). Development of an electrochemically reduced graphene oxide modified disposable bismuth film electrode and its application for stripping analysis of heavy metals in milk. *Food Chemistry*, 151:65–71.
- Pratt, K. W. and Koch, W. F. (1988). High-accuracy differential-pulse anodic stripping voltammetry with indium as an internal standard. *Analytica chimica acta*, 215:21–28.
- Rutten, K., De Baerdemaeker, J., and De Ketelaere, B. (2014). A comparison of evolutionary operation and simplex for process improvement. *Chemometrics and Intelligent Laboratory Systems*, 139:109–120.
- Thompson, M. (2009). Standard additions: myth and reality. in 37 ed. *Analytical Methods Committee, Ed. RSC*.
- Wang, J. (2005). Stripping analysis at bismuth electrodes: a review. *Electroanalysis: An International Journal Devoted to Fundamental and Practical Aspects of Electroanalysis*, 17(15-16):1341–1346.

- Wang, J., Kirgöz, Ü. A., and Lu, J. (2001). Stripping voltammetry with the electrode material acting as a built-in internal standard. *Electrochemistry communications*, 3(12):703–706.
- Worsfold, P., Townshend, A., Poole, C. F., and Miró, M. (2019). *Encyclopedia of analytical science*. Elsevier.
- Zhang, Y., Li, C., Su, Y., Mu, W., and Han, X. (2020). Simultaneous detection of trace Cd(II) and Pb(II) by differential pulse anodic stripping voltammetry using a bismuth oxycarbide/NAFION electrode. *Inorganic Chemistry Communications*, 111:107672.
- Zhao, G., Wang, H., Liu, G., and Wang, Z. (2016). Box–Behnken response surface design for the optimization of electrochemical detection of cadmium by square wave anodic stripping voltammetry on bismuth film/glassy carbon electrode. *Sensors and Actuators B: Chemical*, 235:67–73.

4. Digestion methods for electrochemical analysis of cadmium in *Theobroma cacao L.*

4.1. Introduction

Cadmium determination in cocoa beans has been reported mainly using atomic absorption spectroscopy (AAS) and inductively coupled plasma spectroscopy (ICP), and the most common digestion method is an acid microwave-assisted digestion (Gramlich et al., 2017; Romero-Estévez et al., 2019; Mohamed et al., 2020; Engbersen et al., 2019). From preliminary experiments, acid digestion like aqua regia digestion (3:1, v/v, HCl-HNO₃) performed in a graphite digestion block under NTC 3388 standard showed a significant matrix effect in SWASV, probably due to remaining components from the digestion, such as nitrates and chlorides. Therefore, more clean digestion methods must be studied and developed.

Dry ashing techniques seem to be the most suitable and simplest method to digest samples with a high organic matter content, such as foodstuffs, biological, and petroleum-based products (Hu and Qi, 2014; Barnes et al., 2014). Also, the organic matter can be completely converted into CO₂ and H₂O by pyrolysis and combustion using a muffle furnace with temperature control programs from 450 to 600 °C and atmospheric oxygen. The residual ash contains all the associated elements in the samples in the form of carbonates or oxides. The main advantage of dry ashing is the resulting organic matter-free sample matrix. Thus, the influence of residual carbon or some undigested organic molecules on ASV, ICP-MS or ICP-AES measurements is minimized (Mamani et al., 2005; Hu and Qi, 2014). In general, selecting an appropriate ashing temperature and ashing vessels will lead to a complete decomposition procedure without losses by volatilization, formation of refractory oxides, or reactions with the crucible materials. However, some applications, such as trace elements determination, exhibit severe limitations since some elements are more prone to volatilization by being converted into volatile species and can be partially or entirely lost (Barnes et al., 2014).

The microwave-assisted digestion methods were proposed as an alternative to dry ashing methods, aiming to diminish the sample digestion time and the working temperatures and

consequently prevent losses by volatilization, typically occurring in dry ashing procedures (Munoz et al., 2013; Hu and Qi, 2014). Microwave chemistry is based on the efficient heating of materials by dielectric heating effects. Microwave digestion uses electromagnetic radiation with a typical frequency of 2450 MHz. The radiating energy is absorbed by both the digestion medium and the sample molecules, minimizing wall effects, thus, enhancing the chemical reaction that completes the decomposition of the sample, providing a more energy-efficient way of heating. Also, the faster heating of a reaction mixture leads to fewer byproducts, higher yields, and a simplified procedure (Kingston et al., 1988; Munoz et al., 2013). For aqueous solutions of acids, the efficiency of absorption of microwave radiation decreases according to the following series: nitric, hydrofluoric, sulfuric, and hydrochloric acids. In addition, the NaOH–H₂O₂ system has been reported as a media to provide the destruction of the organic matter in microwave digestion (Saihua et al., 2018). However, both alkali and acid wet digestion methods require the use of large amounts of reagents and, therefore, gave higher blank contributions for some elements (Hu and Qi, 2014). Also, possible residual organic matter from wet digestions processes can affect the stripping voltammetric detection of metal cations, such as cadmium and lead (Hu and Qi, 2014; Mamani et al., 2005).

On the other hand, among the most frequent drawbacks in developing a quantitative method, including selecting the appropriate digestion method, is that reference materials or real matrix samples free of the target interferences are difficult to find. For our investigation, the main potential interferences will be other metals that are believed to be present in cocoa beans. After the matrix is digested, other metal ions present in the plant will be extracted alongside cadmium. A multi-elemental analysis via ICP-MS of cocoa beans from Africa, Asia, Central America, and South America had shown that the most abundant macroelement in cocoa beans is K, which presented a content greater than 10 g kg⁻¹. P, Mg, and Ca are presented in a concentration that varied from 10 mg kg⁻¹ to 1 g kg⁻¹; Al and Fe were between 100 mg kg⁻¹ and 1 g kg⁻¹, while Zn, Rb, Mn, B, Cu, Na, and Sr were present in concentrations between 10 and 100 mg kg⁻¹. The content of Cd, Co, Mo, V, Ce, and Se was between 0.1 and 1 mg kg⁻¹, and La, Pb, Nd, Cs, Ga, Y, As, Th, Li, Pr, Tl, Sm, and Gd were found between 0.01 and 0.1 mg kg⁻¹ (Bertoldi et al., 2016).

Specifically for electrochemical determination of Cd²⁺, in other matrices using different working electrodes, it has been found that the presence of Cu²⁺ in the working solution interferes with decreasing the voltammetric signal (Wise et al., 1983; Lin et al., 2019; Yanagisawa et al., 2015; Yang et al., 2013; Babyak and Smart, 2004). As mentioned before, copper is expected to be in a higher concentration than cadmium since copper is an essential metal for plants (Bertazzo et al., 2013). Therefore, no copper-free cocoa matrix can be found. In this sense, copper interference will not allow the assessment of cocoa digestion methods. Implementing synthetic matrices whose nature is closer to real matrices could overcome this analytical issue (Alexandre et al., 2016).

Therefore, this chapter compares three digestion procedures in terms of recovery and repeatability: dry ashing, alkali microwave-assisted digestion, and acid microwave-assisted digestion. The standard to evaluate the performance of the three mentioned digestions will be a synthetic cocoa matrix at a concentration of 3.20 mg kg^{-1} of Cd^{2+} . The cadmium quantification will be made by SWASV using BiFE and the SSA-IS calibration methodology developed in the previous chapter. Also, this work includes a homogeneity study carried out using ICP-MS as a reference technique. A homogeneity study refers to the variation in a property's value within the reference material. The latter means that when the intended use of the material allows taking subsamples, it must be ensured that each subsample taken from the material will have the same property value. In the homogeneity study, a statistical evaluation is used to compare the dispersion of the measurements in various subsamples of the material against the measurement method's precision, thus determining the standard deviation between material subsamples. In this sense, the main objective of the homogeneity study was to determine the cadmium concentration variability due to the synthetic matrix's preparation and the acid microwave-assisted digestion procedure.

4.2. Experimental section

4.2.1. Reagents

Standard solutions, samples, and the supporting electrolyte were prepared using type I water. Analytical grade sodium acetate ($\geq 99 \%$, w/w) and glacial acetic acid (Merck, 100 %, w/w) were used to prepare the supporting electrolyte in total acetate concentrations of 0.5 M. The pH of the solution was adjusted to a value equal to 4.3, according to the previous optimization (Section 3.3.2). Preparation of Bi^{3+} and Cd^{2+} stock solutions and glassware cleaning were the same as described in Section 3.2.1.

4.2.2. Samples

The digestion methods for the SWASV-BiFE methodology were tested using a synthetic cocoa matrix (SM). The SM was prepared using oleic acid (PanReac AppliChem), stearic acid, starch (Fisher Scientific), sucrose, and cellulose (Sigma-Aldrich). The composition of the SM was selected according to literature review (Rucker, 2009; Bertazzo et al., 2013) and is shown in Table 4-1.

The solid components were weighed and mixed in a ceramic mortar. Then, the liquid components were added. The mixture was homogenized in the ceramic mortar. Finally, the mixture was separated into halves. The first half was used as a matrix blank, SM-B. The second half was fortified using a 50 mg kg^{-1} Cd^{2+} stock solution to achieve a concentration of 3.20 mg

Table 4-1.: Synthetic cocoa matrix composition used in this work.

Component	% w/w
Humidity	7.0
Oleic acid	5.0
Stearic acid	35.0
Starch	19.0
Sucrose	20.0
Cellulose	14.0

kg⁻¹ of Cd²⁺, SM-Cd.

Hydrogen peroxide solution (Sigma-Aldrich, 30 % w/w), subdistilled nitric acid (70 % w/w), subdistilled hydrochloric acid (37 % w/w), and sodium hydroxide pellets (PanReac Appli-Chem, 98 % w/w) were used for the digestion methods tested in this work.

4.2.3. Instrumentation, electrochemical cell and electrodes

The electrochemical system used and the cleaning procedure for the GCE are the same as described in Section 2.2.2. The experimental parameters for SWASV are those presented and optimized in Chapter 3.

4.2.4. Dry ashing digestion

Samples of approximately 0.5 g of the SM were weighted to the nearest 0.0001 g directly into platinum crucibles (capacity 15 mL). Samples were placed in a muffle furnace, the temperature was stepped to 450 °C over 2 h and then held for 16 h. After cooling, the ashes were dissolved in 50 g of supporting electrolyte. Before measurement, the solution was filtered using a 17mm HPLC Syringe Filter Regenerated Cellulose, 0.45µm.

4.2.5. Alkali microwave-assisted digestion

Samples of approximately 0.3 g of the SM were weighted to the nearest 0.0001 g directly into a teflon microwave digestion tube, 0.6 g of NaOH and 2.5 mL of type I water were added. The digestion tube was placed in a vortex mixer (150 rpm) for 5 min. Then, 3.0 mL of H₂O₂ (30 % w/w) were added, and the tube was stirred in the vortex mixer (150 rpm) for another 5 min. The tubes were immediately capped and placed in the ceramic tubs. An Anton Paar Multiwave 5000 microwave was used to conduct the alkali digestion. The power was stepped to 950 W over 20 min, then lowered to 450 W and held for 20 min. After cooling, the excess NaOH was neutralized with HCl (37 % w/w). Then, the solution was brought to

50 g with the supporting electrolyte. Finally, the SSA-IS calibration curve was prepared, adding the respective aliquot of Bi^{3+} and Cd^{2+} stock solutions to achieve a concentration in the electrochemical cell of $500 \mu\text{g kg}^{-1}$ and $30 \mu\text{g kg}^{-1}$, respectively. Before measurement, the solution was filtered using a 17mm HPLC Syringe Filter Regenerated Cellulose, $0.45\mu\text{m}$.

4.2.6. Acid microwave-assisted digestion

Samples of approximately 0.3 g of the SM were weighted to the nearest 0.0001 g directly into a Teflon microwave digestion tube, 5.0 mL of HNO_3 and 2.0 mL of 30 % w/w H_2O_2 were added. The tubes were immediately capped and placed in the ceramic tubes. Two power programs for acid digestion were tested. The first was the same as that used for alkaline digestion (Section 4.2.5). For the second one, the power was stepped to 450 W over 30 min, then held for 30 min. After cooling, the contents of the tubes were transferred to a 100 mL glass beaker. Then, the solution was heated to dryness on a hot plate. The remaining was dissolved in 50 g of supporting electrolyte. The SSA-IS calibration curve was prepared as described in Section 4.2.5. Before measurement, the solution was filtered using a 17mm HPLC Syringe Filter Regenerated Cellulose, $0.45\mu\text{m}$.

Homogeneity study of the acid microwave-assisted digestion

Twelve SM-Cd replicas were prepared as described in Section 4.2.6 and treated with the second power program. A sample of 5 g of each SM-Cd digestion extract was taken and brought to 50 g with 0.5 % HNO_3 , and a mixture of internal standards (U and Ge) was added at $1 \mu\text{g kg}^{-1}$; then, the diluted extract was measured 12 times by ICP-MS under repeatability conditions. The estimation of the uncertainty due to homogeneity (u_{hom}) of this sample was obtained by determining the variation due to taking the subsamples ($\text{CME}_{\text{subsample}}$) and the measurement (CME_{Med}). The result is expressed in terms of the average of the relative responses between ^{113}Cd and ^{74}Ge .

4.3. Results

4.3.1. Dry ashing

The initial dry ashing experiments were done with a cocoa powder reference material, certified concentration of $3.200 \pm 0.064 \text{ mg g}^{-1}$ of Cd^{2+} , characterized in the INM of Colombia and following the procedure described in Section 4.2.4. A strong interference of copper in the determination of cadmium in cocoa was found, agreeing with the literature (Wise et al., 1983; Lin et al., 2019; Yanagisawa et al., 2015; Yang et al., 2013; Babyak and Smart, 2004). The copper interference study and the treatment strategies for copper removal from cocoa extracts are presented in the validation chapter, Section 5.3.3. Meanwhile, it was decided to prepare a synthetic cocoa matrix to evaluate the most appropriate digestion method for

the electrochemical quantification of cadmium in cocoa. This approach aimed to produce a matrix with characteristics resembling the matrix of interest without copper interference.

Figures 4.1(a), 4.1(b), 4.1(c), and 4.1(d) show the voltammograms for the SM matrix blank (SM-B), the non-spiked and spiked extracts of three fortified (SM-Cd) matrix replicas treated by dry ashing digestion.

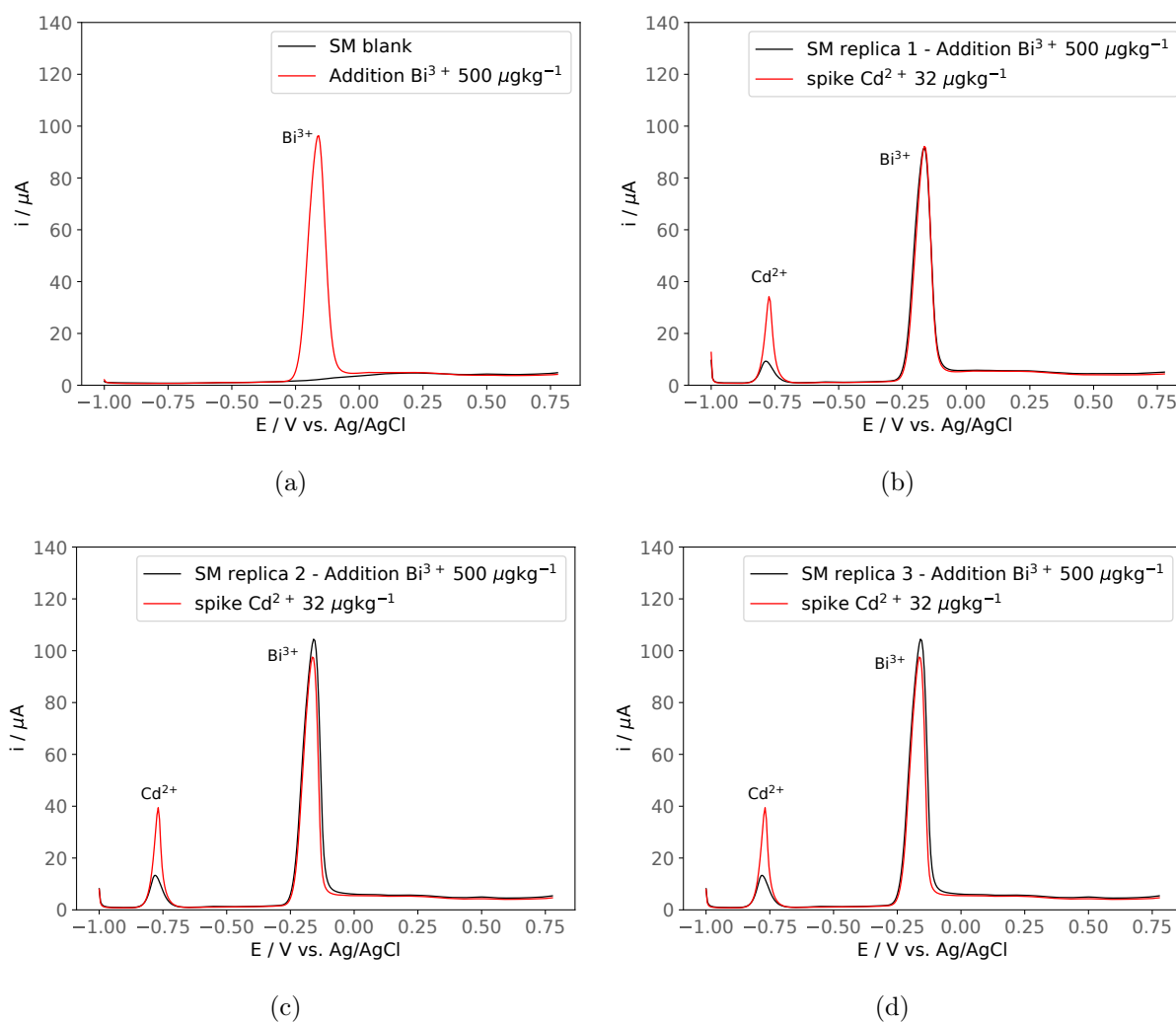


Figure 4-1.: Voltammograms using SWASV in acetate buffer 0.5 M and pH 4.3 obtained by dry ashing digestion of the SM blank (SM-B) and fortified samples (SM-Cd). **(a)** SM-B digestion extract (black line), and addition of Bi^{3+} (red line), **(b)** replica 1, **(c)** replica 2, and **(d)** replica 3 of an SM-Cd digestion extract with Bi^{3+} (black line), and Cadmium spike $[\text{Cd}^{2+}] = 30 \mu\text{g kg}^{-1}$ (red line). In all cases the added Bi^{3+} was $500 \mu\text{g kg}^{-1}$.

Well-defined voltammetric peaks, no interferences, and a clean baseline (almost perfect ho-

rizontals) were obtained after the dry ashing procedure. As reported in the literature, this digestion technique ensures the efficient elimination of organic matter (Hu and Qi, 2014; Munoz et al., 2013; Mamani et al., 2005). Figure 4-2 shows the SSA-IS calibration curves constructed using normalized peak areas from the non-spike and the spike SM-Cd extract.

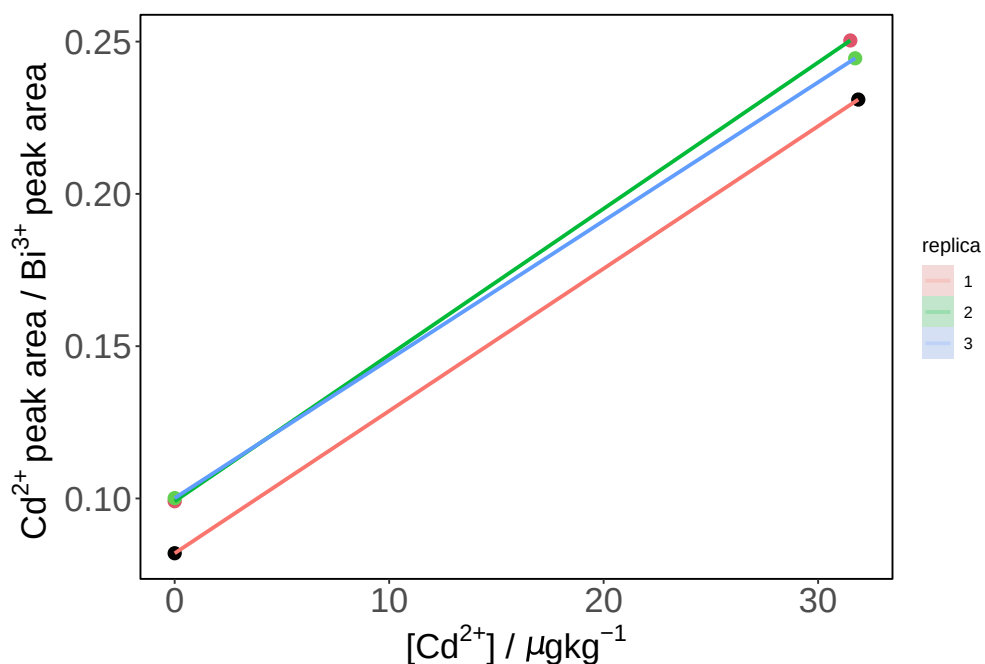


Figure 4-2.: Calibration curves Cd^{2+} peak area / Bi^{3+} peak area vs. $[\text{Cd}^{2+}]$ by single-point standard addition with the internal standard method (SSA-IS) of the SM-Cd treated by dry ashing digestion.

The cadmium concentration in the SM-Cd matrix was determined, and an average cadmium concentration of 2.00 mg kg^{-1} of Cd^{2+} was obtained with a recovery = 63.3% and an RSD = 11.3%. Since it is an open and dry digestion method, we attribute the low recovery percentage obtained to temperature-induced cadmium losses. Despite selecting an appropriate and low ashing temperature to ensure quantitative decomposition of the organic matter ($450 \text{ }^\circ\text{C}$), cadmium is prone to losses by volatilization. When treated by dry ashing, some elements, such as cadmium, are more susceptible to volatilization if certain species are present in the sample matrix (Barnes et al., 2014).

4.3.2. Microwave assisted digestion

Alkali digestion

Figures 4.3(a), 4.3(b), 4.3(c), and 4.3(d) show the voltammograms for the SM-B matrix blank, the non-spiked, and the spiked extract of three fortified SM-Cd replicas treated by alkali microwave-assisted digestion. Lead contamination was observed in the voltammograms

obtained for all the microwave-treated samples. The contamination was found to come from the teflon digestion tubes. Nevertheless, the presence of Pb^{2+} is not an interference in the determination of cadmium in the SM-Cd extracts.

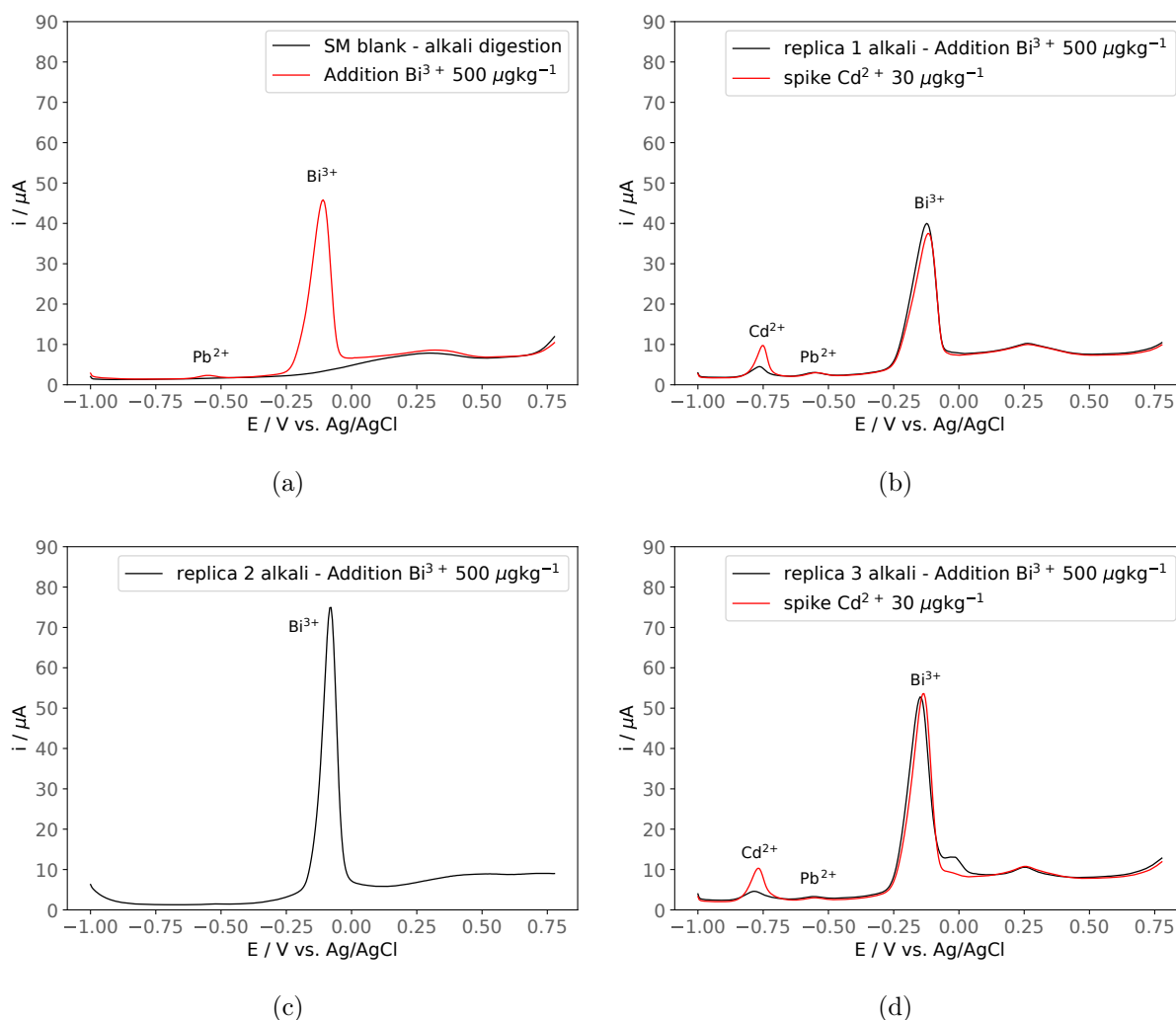


Figure 4-3.: Voltammograms using SWASV in acetate buffer 0.5 M and pH 4.3 obtained by alkali microwave-assisted digestion of SM-B and SM-Cd. **(a)** SM-B (black line), and addition of Bi^{3+} (red line), **(b)** replica 1, **(c)** replica 2, and **(d)** replica 3 of an SM-Cd digestion extract with Bi^{3+} (black line), and Cadmium spike $[\text{Cd}^{2+}] = 30 \mu\text{g kg}^{-1}$ (red line). In all cases the added Bi^{3+} was $500 \mu\text{g kg}^{-1}$.

It is important to mention that in one of the SM-Cd replicas treated by the alkali digestion, it was impossible to distinguish any cadmium signal, Figure 4.3(c). The latter happened because the alkali digestion tubes' temperature ranged between 172 to 192 °C (55 to 64 °C

higher than that registered for the acid digestion), even though the applied power ramp was the same for the acid digestion. These high temperatures led to recurring sample loss in the microwave. Besides, the method required an excess of NaOH and adding HCl (37 % w/w) to the digestion extract to neutralize it. Therefore, less-defined voltammetric peaks were obtained for the solutions treated by the alkali microwave-assisted procedure. Also, observe that the baselines are not as horizontal as in the dry ashing digestion. The latter facts indicate that added chlorides alongside possible residual organic matter affect cadmium voltammetric detection.

Acid digestion

Figures 4.4(a), 4.4(b), 4.4(c), and 4.4(d) show the voltammograms for the SM-B, the non-spiked, and the spiked extract of three fortified SM-Cd replicas treated by acid microwave-assisted digestion.

Similar to the alkali digestion, a lead oxidation signal is observed in all the digestion extracts. Also, the stripping signals and background currents are affected, probably, by residual organic matter or nitrates when compared to the dry ashing baselines, as in the case of the alkali digestion but changing the chlorides by nitrates. Acid digestion does not present the losses observed in alkali digestion because of the lower temperature of the digestion tubes. Figure 4.5(a) shows the calibration curves for both acid (replicas 1, 2, and 3) and alkali digestions (replicas 4 and 5). An average cadmium concentration of 2.87 mg kg^{-1} of Cd^{2+} (recovery = 89.0 % , RSD = 7.7 %) was obtained for acid digestion and 1.69 mg kg^{-1} of Cd^{2+} (recovery = 52.6 % , RSD = 8.0 %) was obtained for alkali digestion. In that way, acid digestion appears more repeatable and with more trueness than alkaline digestion and dry ashing (recovery = 63.3 % , RSD = 11.3 %). Therefore, the acid digestion method was selected as the most appropriate digestion for the electrochemical detection of cadmium in the synthetic cocoa matrix.

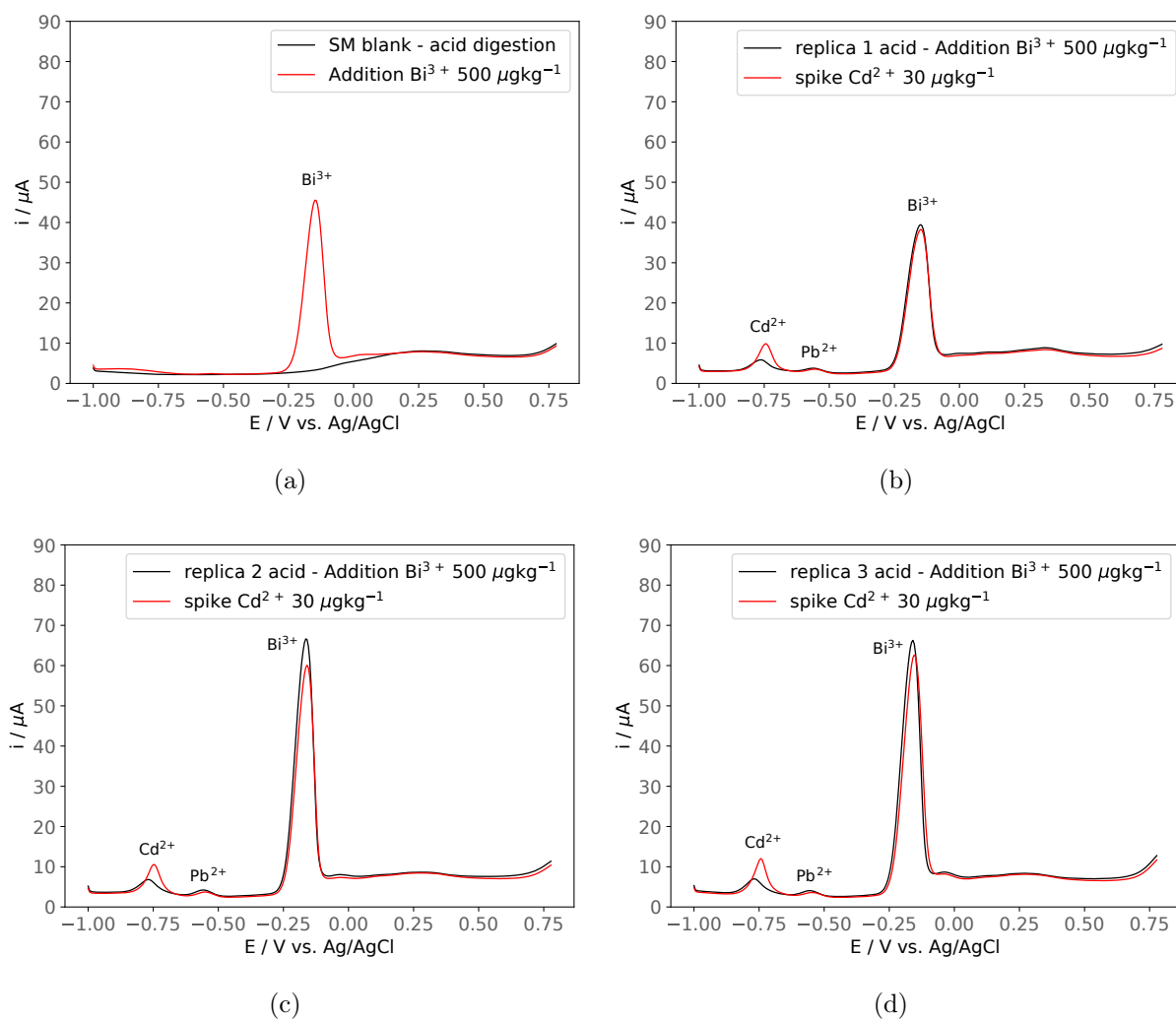


Figure 4-4.: Voltammograms using SWASV in acetate buffer 0.5 M and pH 4.3 obtained by acid microwave-assisted digestion of the SM blank (SM-B) and fortified samples (SM-Cd). (a) SM-B digestion extract (black line), and addition of Bi^{3+} (red line), (b) replica 1, (c) replica 2, and (d) replica 3 of an SM-Cd digestion extract with Bi^{3+} (black line), and Cadmium spike $[\text{Cd}^{2+}] = 30 \mu\text{g kg}^{-1}$ (red line). In all cases the added Bi^{3+} was $500 \mu\text{g kg}^{-1}$.

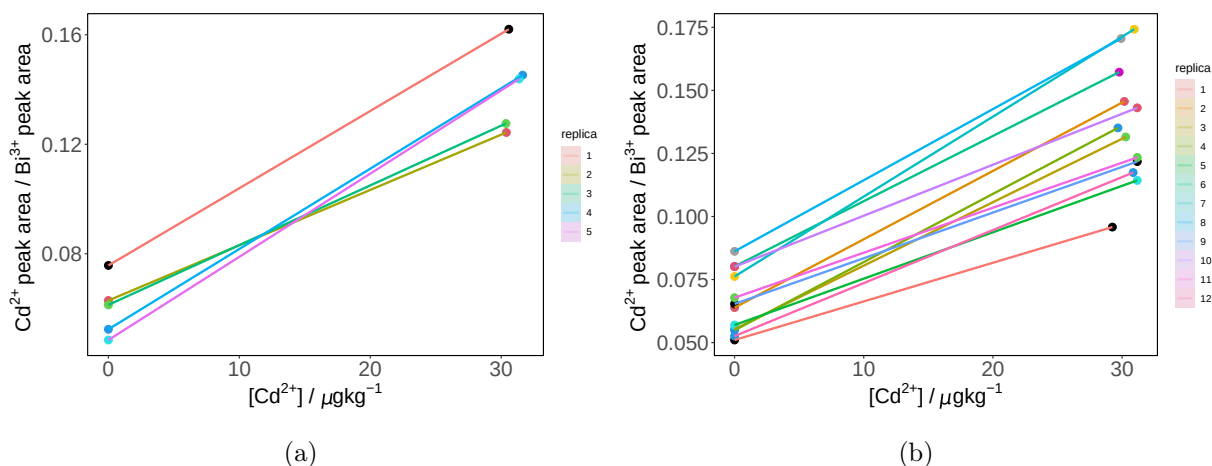


Figure 4-5.: (a) Calibration curves Cd²⁺ peak area / Bi³⁺ peak area vs. [Cd²⁺] by single-point standard addition with the internal standard method (SSA-IS) of the SM-Cd treated by acid (1, 2, and 3) and alkali (4 and 5) microwave-assisted digestion. (b) Calibration curves Cd²⁺ peak area / Bi³⁺ peak area vs. [Cd²⁺] by single-point standard addition with the internal standard method (SSA-IS) of the SM-Cd treated by modified acid microwave-assisted digestion.

Improvement of the acid microwave-assisted digestion

The power ramp initially used in the microwave oven seems too high because of the losses evident in the alkali digestion. Then, a lower power ramp (450 W) was tested to avoid possible losses. Twelve samples of the SM-Cd were treated using the second power ramp described in Section 4.2.6, see Figure 4.5(b). The cadmium concentration and the expanded uncertainties were estimated for each analyzed replica of the SM-Cd following the estimation procedure described in Section 3.3.1 (Table 4-2).

The new power ramp produced a greater homogeneity between digestion tubes, including the color of the digestion extract, the residual organic matter, and the maximum temperature in the digestion tube (between 88 and 106 °C).

Figure 4.5(b) shows the SSA-IS calibration curves obtained for the 12 SM-Cd replicas obtained by SWASV-BiFE. An increase in the average recovery percentage (92.4 %) was achieved, but a greater variability in the cadmium concentration was obtained (RSD = 22.0 %). This is attributed to the complexity of the sample and the residual organic matter and nitrates that affects the electrochemical detection, probably due to adsorption processes on the working electrode (Munoz et al., 2007). Nevertheless, with this result, we have developed an adequate digestion methodology for the SWASV-BiFE measurement method, with acceptable precision and trueness levels (Table 4-3) according to the range of analyte concentration. (Joint

Table 4-2.: Cadmium concentrations and estimated expanded uncertainty (95 %, $k = 1.962$) of the SM-Cd treated by acid microwave-assisted digestion (second power ramp) and measured by SWASV and SSA-IS calibration methodology.

Replica	[SM-Cd] _{measured} (mg kg ⁻¹)	U _(k=1.962) (mg kg ⁻¹)
1	3.34	0.47
2	2.39	0.33
3	2.19	0.30
4	2.07	0.29
5	3.09	0.43
6	3.10	0.44
8	3.02	0.42
9	3.62	0.51
10	3.97	0.57
11	3.81	0.54
12	2.50	0.35
Mean	2.96	0.42
SD	0.65	0.10
RSD(%)	21.90	22.91

FAO/WHO Codex Alimentarius Commission, 1992; Committee et al., 2011).

Table 4-3.: Performance parameters recovery and repeatability of the digestion methods tested in this work.

Digestion method	n	% recovery _{average}	%RSD
Dry ashing	3	63.3	11.3
Alkali microwave-assisted	2	52.6	8.0
Acid microwave-assisted	3	89.0	7.7
Acid microwave-assisted*	12	92.4	22.0

*Modified power ramp.

A One Sample t-test was also performed to compare our electrochemical method with the ICP-MS reference method (Figure 4-6). The mean value for cadmium concentration in the SM-Cd obtained by SWASV (\bar{m}) is compared against the reference value (μ) obtained by ICP-MS.

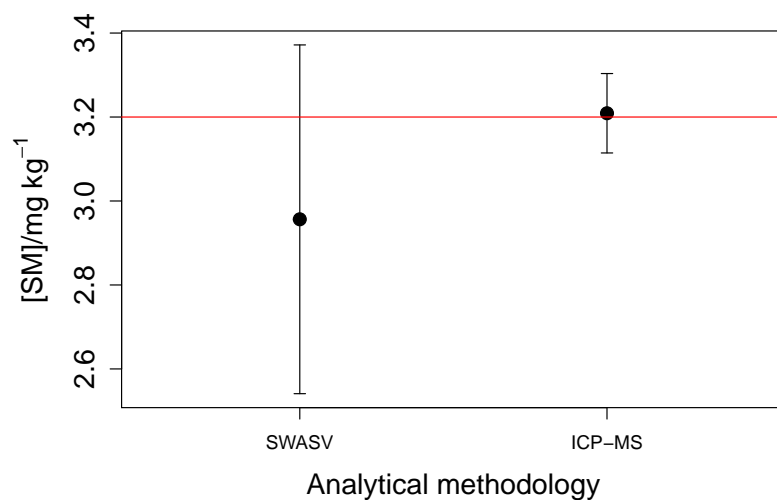


Figure 4-6.: Comparison of the SM-Cd cadmium concentration and expanded uncertainty value (95 %, $k = 1.962$) determined by SWASV and the reference method ICP-MS.

With a p -value = 0.1669 greater than the significance level of 0.05, the t -test fails to reject the null hypothesis ($H_0: m = \mu$). In this way, the cadmium concentration in the synthetic cocoa matrix obtained by the proposed electrochemical methodology in this work is not statistically different from the value obtained by the reference method.

Homogeneity study of the acid microwave-assisted digestion. The results of the homogeneity study reveal an homogeneity uncertainty, u_{hom} , equal to 4.6 %. This percentage is within the measurement capabilities (uncertainty levels) developed by the INM of Colombia to produce certified reference materials and aptitude test items to carry out quality control and validation of Cd measurement methods in cocoa.

4.4. Conclusions

The results of the cadmium concentration in the Cd-enriched synthetic cocoa matrix (SM-Cd) indicated that acid microwave-assisted digestion is the most appropriate digestion procedure in terms of repeatability ($RSD = 22.0\%$) and trueness ($recovery_{average} = 92.4\%$), for the SWASV determination of cadmium in cacao samples. The methodology satisfies the range of the acceptable mean recovery and RSDs according to the AOAC and CODEX Alimentarius criterion. Furthermore, this is an agile and fast alternative for cocoa-similar sample treatment. Although the method's trueness is good enough, the precision must be improved. The precision drawback is attributed to the complexity of the sample and its high content of organic matter and nitrate residuals. The latter substances affect electrochemical detection

due to adsorption processes on the working electrode. In addition, the extra operations performed after acid-microwave digestion needed to condition the extract for its appropriated measurement by SWASV (solution brought to dryness by heating on a hot plate and subsequent redissolution in the supporting electrolyte) are sources of random errors and could negatively influence the precision of the measurements.

4.5. References

- Alexandre, B., Barbara, G., Laure, W., Bruno, D., Adriana, G.-O., and Emmanuelle, V. (2016). Development of a multiple-class analytical method based on the use of synthetic matrices for the simultaneous determination of commonly used commercial surfactants in wastewater by liquid chromatography-tandem mass spectrometry. *Journal of Chromatography A*, 1450:64–75.
- Babyak, C. and Smart, R. B. (2004). Electrochemical detection of trace concentrations of cadmium and lead with a boron-doped diamond electrode: Effect of kcl and kno3 electrolytes, interferences and measurement in river water. *Electroanalysis: An International Journal Devoted to Fundamental and Practical Aspects of Electroanalysis*, 16(3):175–182.
- Barnes, R. M., Júnior, D. S., and Krug, F. J. (2014). Introduction to sample preparation for trace element determination. In *Microwave-assisted sample preparation for trace element analysis*, pages 1–58. Elsevier.
- Bertazzo, A., Comai, S., Mangiarini, F., and Chen, S. (2013). Composition of cacao beans. In *Chocolate in health and nutrition*, pages 105–117. Springer.
- Bertoldi, D., Barbero, A., Camin, F., Caligiani, A., and Larcher, R. (2016). Multielemental fingerprinting and geographic traceability of theobroma cacao beans and cocoa products. *Food Control*, 65:46–53.
- Committee, A. I. M. et al. (2011). Standard method performance requirements-aoac international methods committee guidelines for validation of biological threat agent methods and/or procedures. *J. AOAC Int.*, 94:1359–1381.
- Engbersen, N., Gramlich, A., Lopez, M., Schwarz, G., Hattendorf, B., Gutierrez, O., and Schulin, R. (2019). Cadmium accumulation and allocation in different cacao cultivars. *Science of The Total Environment*, 678:660–670.
- Gramlich, A., Tandy, S., Andres, C., Paniagua, J. C., Armengot, L., Schneider, M., and Schulin, R. (2017). Cadmium uptake by cocoa trees in agroforestry and monoculture systems under conventional and organic management. *Science of The Total Environment*, 580:677–686.

- Hu, Z. and Qi, L. (2014). 15.5—sample digestion methods. *Treatise on Geochemistry (Second Edition)*. Elsevier, Oxford, 1:87–109.
- Joint FAO/WHO Codex Alimentarius Commission (1992). *Codex alimentarius*. Food & Agriculture Org.
- Kingston, H. M., Jassie, L. B., et al. (1988). *Introduction to microwave sample preparation*. American Chemical Society.
- Lin, C.-H., Li, P.-H., Yang, M., Ye, J.-J., and Huang, X.-J. (2019). Metal replacement causing interference in stripping analysis of multiple heavy metal analytes: kinetic study on cd (ii) and cu (ii) electroanalysis via experiment and simulation. *Analytical chemistry*, 91(15):9978–9985.
- Mamani, M. C. V., Aleixo, L. M., de Abreu, M. F., and Rath, S. (2005). Simultaneous determination of cadmium and lead in medicinal plants by anodic stripping voltammetry. *Journal of Pharmaceutical and Biomedical Analysis*, 37(4):709–713.
- Mohamed, R., Zainudin, B. H., and Yaakob, A. S. (2020). Method validation and determination of heavy metals in cocoa beans and cocoa products by microwave assisted digestion technique with inductively coupled plasma mass spectrometry. *Food chemistry*, 303:125–392.
- Munoz, R., Almeida, E., and Angnes, L. (2013). Sample preparation techniques for the electrochemical determination of metals in environmental and food samples. *Reference Module in Chemistry, Molecular Sciences and Chemical Engineering*.
- Munoz, R. A., Correia, P. R., Nascimento, A. N., Silva, C. S., Oliveira, P. V., and Angnes, L. (2007). Electroanalysis of crude oil and petroleum-based fuel for trace metals: evaluation of different microwave-assisted sample decompositions and stripping techniques. *Energy & fuels*, 21(1):295–302.
- Romero-Estévez, D., Yáñez-Jácome, G. S., Simbaña-Farinango, K., and Navarrete, H. (2019). Content and the relationship between cadmium, nickel, and lead concentrations in ecuadorian cocoa beans from nine provinces. *Food control*, 106:106–750.
- Rucker, R. (2009). Appendix 10: Nutritional properties of cocoa. *Chocolate: History, Culture, and Heritage*, pages 943–946.
- Saihua, L., Yunhe, X., Ji, X., Juan, H., Bocharnikova, E., and Matichenkov, V. (2018). Microwave digestion for colorimetric determination of total si in plant and mineral samples. *Communications in Soil Science and Plant Analysis*, 49(7):840–847.

- Wise, J. A., Roston, D. A., and Heineman, W. R. (1983). The effects of copper-zinc and copper-cadmium intermetallic compounds in different systems used for anodic stripping voltammetry. *Analytica chimica acta*, 154:95–104.
- Yanagisawa, H., Kurita, R., Kamata, T., Yoshioka, K., Kato, D., Iwasawa, A., Nakazato, T., Torimura, M., and Niwa, O. (2015). Effect of the sp²/sp³ ratio in a hybrid nanocarbon thin film electrode for anodic stripping voltammetry fabricated by unbalanced magnetron sputtering equipment. *Analytical Sciences*, 31(7):635–641.
- Yang, D., Wang, L., Chen, Z., Megharaj, M., and Naidu, R. (2013). Investigation of copper (ii) interference on the anodic stripping voltammetry of lead (ii) and cadmium (ii) at bismuth film electrode. *Electroanalysis*, 25(12):2637–2644.

5. Validation of the Square Wave Anodic Stripping Voltammetry methodology for cadmium quantification in *Theobroma cacao* L.

5.1. Introduction

Methodology validation is carried out to confirm that the analytical procedure can obtain reliable results under the working conditions available in the laboratory, proving that it is suitable for its purpose. The validation process is accomplished by evaluating the performance parameters. The selection of performance parameters depends on the methodology's characteristics to be validated and the validation level that will be carried out. The Food and Drug Administration has defined that the validation process consists of four hierarchical levels (Figure 5-1) (U.S. Food and Drug Administration, 2019) This investigation aims to carry out a level two or intra-laboratory validation. Single laboratory work will be done at this validation level and contemplates the evaluation of the linearity, detection and quantification limits, selectivity, precision, and trueness. The assessment is done by providing objective evidence to support the claims made about the method's suitability. The objective evidence comprehends the analysis and documentation of experimental results for each of the method's performance parameters.

Intra-laboratory validated methods are not always available or applicable, especially in the case of multi-analyte/multi-substrate methods and new analytes. The criteria to be used to select a method are included in the General Criteria for the Selection of Methods of Analysis (Joint FAO/WHO Codex Alimentarius Commission, 1992). The single-laboratory validated methods should be complemented with information on accuracy demonstrated with:

- Regular participation in proficiency schemes, where available;
- Calibration using certified reference materials, where applicable;

- Recovery studies performed at the expected concentration of the analytes;
- Verification of result with other validated methods, where available.

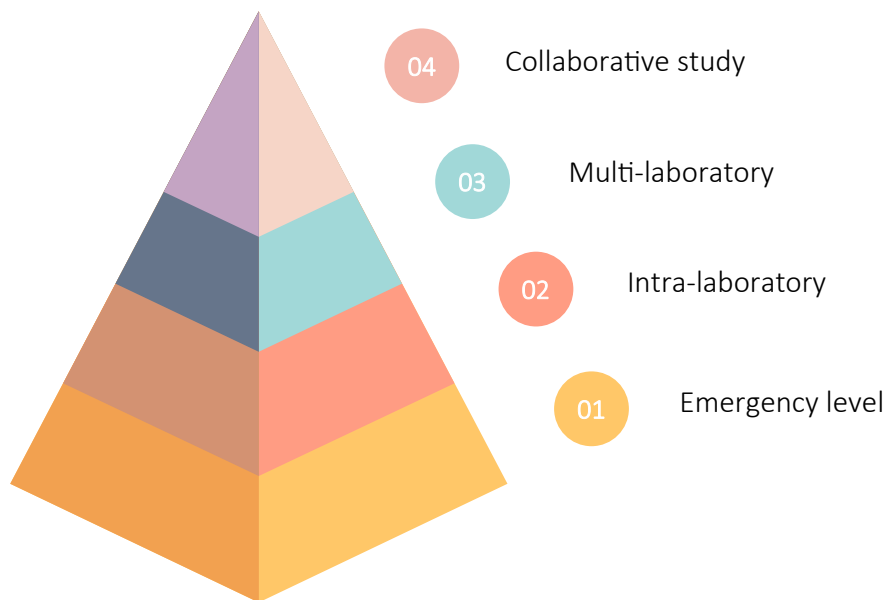


Figure 5-1.: Hierarchical levels of validation for an analytical system. (U.S. Food and Drug Administration, 2019)

Selectivity is defined as the property of a measuring system used with a specified measurement procedure, whereby it provides measured quantity values for one or more measurands such that the values of each measurand are independent of other measurands or other quantities in the phenomenon, body, or substance being investigated (Balazs, 2008). Selectivity studies seek to identify possible interferences that may be present in the matrix. The presence of copper at different concentrations has shown a decrease in the cadmium current signal in the electrochemical determination of this metal. Copper interference studies have been mostly reported in matrices such as standard solutions, tap water, and river water (Table 5-1). Considering that Cu^{2+} and Cd^{2+} are among the most commonly determined metals by ASV and are found in environmental and biological samples like cocoa, an accurate assessment of the magnitude of the interference observed between these metals is worthwhile. The Cd determination by SWASV with BiFE requires to eliminate copper from the solution. Two methods are proposed to eliminate copper from solutions to be tested, one using a chelating ion exchange resin and the other by an electrolysis method. In previous works, the use of chelating resins such as the Chelex 100 has been reported for the separation and preconcentration of the metal ions on resins with different sorbing properties (Pesavento et al., 2001; Schulze and Elsholz, 1989; Yanagisawa et al., 2015). Chelex 100 resin consists

Table 5-1.: Studies of copper interference in determining cadmium by ASV.

Working Electrode	Sample	[Cd ²⁺] / [Cu ²⁺] ($\mu\text{g kg}^{-1}$)	Reference
Mercury film electrode	Standard solution	470 / 1000	(Wise et al., 1983)
Nanocarbon film electrode	Water	50 / 100	(Yanagisawa et al., 2015)
Glassy Carbon electrode	Standard solution	337 / 189	(Lin et al., 2019)
Bismuth Film Electrode	Standard solution	22 / 126	(Yang et al., 2013)
Boron-doped diamond electrode	River water	10 / 5	(Babyak and Smart, 2004)

of styrene divinylbenzene copolymers containing paired iminodiacetate ions which act as chelating groups in binding polyvalent metal ions. Chelex 100 chelating resin is classified as a weakly acidic cation exchange resin by virtue of its carboxylic acid groups, but it differs from ordinary exchangers because of its high selectivity for metal ions and its much higher bond strength (Bio-Rad, 2000). The selectivity factors for different cations of the Chelex 100 are shown in Table 5-2.

Table 5-2.: Chelex 100 resin selectivity factors for divalent cations. Compared to its affinity for a reference cation, Zn²⁺.

Cation	Selectivity factor	Cation	Selectivity factor
Hg ⁺²	1060	Fe ⁺²	0.130
Cu ⁺²	126	Mn ⁺²	0.024
UO ⁺²	5.70	Ba ⁺²	0.016
Ni ⁺²	4.40	Ca ⁺²	0.013
Pb ⁺²	3.88	Sr ⁺²	0.013
Zn ⁺²	1.00	Mg ⁺²	0.009
Co ⁺²	0.615	Na ⁺¹	0.0000001
Cd ⁺²	0.390		

On the other hand, electrolysis methods such as electrogravimetry, coulometry, separation or removal techniques, and electrosynthetic methods are employed when it is desired to alter the composition of the bulk solution. Controlled-potential techniques are usually the most desirable for bulk electrolysis since the working electrode's potential controls the selectivity degree of an electrolytic process in most cases. Constant Potential Electrolysis (CPE) is conducted with large surface area to volume ratios and with the effective mass-transfer conditions as possible (Bard and Faulkner, 2001). CPE working and counter electrodes are 2 to 4 orders of magnitude larger in area than those used in many other electrochemical techniques such as CV and ASV. Typically platinum meshes or high surface area carbon

meshes, foam, felts, and glassy carbon materials are used to increase current (charge) and reduce time to reach exhaustive electrolysis. Often, the goal is to convert the whole analyte from reduced to oxidized form, or vice-versa (Bard and Faulkner, 2001). Here, electrolysis is used to remove Cu^{+2} from the solution selectively.

This chapter assesses the validation parameters, linearity, the limit of detection (LOD), the limit of quantification (LOQ), selectivity, repeatability, and trueness for the quantification of Cd^{2+} in cocoa by SWASV with BiFE under the conditions developed in the previous chapters. Two procedures, Chelex 100 and CPE, are studied for the selective removal of copper from standard solutions and digested extracts of a reference material of cadmium in cocoa powder.

5.2. Experimental section

5.2.1. Reagents

The supporting electrolyte, Bi^{3+} and Cd^{2+} stock solutions were prepared as described in Section 3.2.1. The Cu^{2+} stock solution was prepared using a standard solution of $1.000 \pm 0.002 \text{ g L}^{-1}$ (Sigma-Aldrich Inc.). The cocoa reference material (RM) produced in the Instituto Nacional Metrología de Colombia (Cadmium $3.200 \pm 0.064 \text{ mg kg}^{-1}$, Copper $40.200 \pm 2.100 \text{ mg kg}^{-1}$) was used to validate the electroanalytical method in terms of repeatability and trueness. Chelex 100 Chelating Resin (BIORAD, analytical grade, 200–400 mesh, sodium form) was used to remove Cu^{+2} . The laboratory glassware was cleaned as described in Section 2.2.1. Activated carbon powder (PanReact-AppliChem, technical grade) was used to pretreat the extracts obtained by acid microwave-assisted digestion.

5.2.2. Samples

The cocoa powder reference material (RM) was treated by the acid microwave-assisted digestion selected in Chapter 4. The sample was prepared to obtain a concentration of $32 \mu\text{g kg}^{-1}$ of Cd^{2+} in the electrochemical cell.

5.2.3. Instrumentation, electrochemical cell and electrodes

The electrochemical system used for SWASV measurements and the cleaning procedure for the GCE are the same as described in Section 2.2.2. The experimental parameters for SWASV are those selected and optimized in Chapter 3.

5.2.4. Chelating Ion Exchange Resin

Batch method

The batch method consists of the addition of the Chelex 100 resin directly into the sample, followed by stirring. After a determined stirring time, the sample is filtered or separated by decantation from the resin. The quantity of resin, time of treatment, pH of the solution, and stirring method (vortex or magnetic stirring) were studied and selected using a standard solution of concentration $30 \mu\text{g kg}^{-1}$ of Cd^{2+} and $470 \mu\text{g kg}^{-1}$ of Cu^{2+} .

Column method

The column method involves pouring a column with the Chelex 100 resin and passing the sample through it to achieve the separation. A syringe of 1 mL of capacity was used as a column. The quantity of resin was selected using a standard solution of concentration $30 \mu\text{g kg}^{-1}$ of Cd^{2+} and $470 \mu\text{g kg}^{-1}$ of Cu^{2+} .

The copper removal obtained by both Chelex 100 methods was evaluated by following the oxidation signals of cadmium and copper obtained by SWASV with GCE as the working electrode. Finally, the improved process was employed to treat a cocoa powder RM digestion extract obtained by the acid microwave-assisted digestion (Section 4.2.6).

5.2.5. Constant potential electrolysis (CPE)

A platinum plate electrode and a platinum spiral electrode (99.95 % purity) were used as working and counter electrodes, respectively. The reference electrode was Ag/AgCl, KCl (sat). A potential of -0.4 V was applied to the cocoa powder RM digestion extracts. The solution was kept under stirring to favor mass transport (600 rpm). After some time of treatment, the platinum working electrode was removed from the cell, and the electrochemical system was changed to monitor the Cd^{2+} and Cu^{2+} signals by SWASV using GCE as working electrode. This step was repeated until a significant decrease in the copper signal was observed.

5.3. Results

5.3.1. Linearity

As seen in Chapter 3, Section 3.3.1, a passivation in the GCE surface is observed as a multi-point calibration curve is built. For that reason, polishing and electrochemical cleaning of the GCE between each concentration level is necessary to obtain reliable results. In that sense, the linearity of the method was confirmed with the ESC-IS calibration curve (between 5 and $95 \mu\text{g kg}^{-1}$ of Cd^{2+}), performing the cleaning step of the GCE surface before each

measurement, Figure 3.4(a). According to the regression coefficients of the mentioned ESC-IS calibration curve ($m = 0.00487$, $a = 0.00236$, and $r^2 = 0.9957$) a $t_m = 27.00$, $t_a = 0.16$, and $t_r = 44.09$ were obtained using Eq. 5-1, Eq. 5-2, and Eq. 5-3.

$$\text{Slope (m): } t_m = \frac{|m|}{S_m} \quad (5-1)$$

$$\text{Intercept (a): } t_a = \frac{|a|}{S_a} \quad (5-2)$$

$$\text{Correlation coefficient (r): } t_r = \frac{|r|\sqrt{n-2}}{\sqrt{1-r^2}} \quad (5-3)$$

Now, considering a significance level of 0.05 and a $t_{critical}=2.306$, the H_0 for the slope is rejected, so the slope is significantly different from zero at 95% confidence. The H_0 for the intercept fails to be rejected, so the intercept is not significantly different from zero at 95% confidence. Finally, the H_0 for the correlation coefficient is rejected, so there is sufficient evidence to conclude that there is a significant linear relationship between the Cd^{2+} concentration (x) and the Cd^{2+} peak area/ Bi^{3+} peak area (y). These facts are summarized in Table 5.3.1.

Table 5-3.: t-Student tests for linearity assessment of the ESC-IS calibration curve.

t-Student			
$t_{critical(\alpha=0.05)}=2.306$			
	For the slope	For the intercept	For the correlation coefficient
	$t_m=27.00$	$t_a=0.16$	$t_r=44.09$
H_0	$m = 0$	$a = 0$	There is NOT correlation between x and y
Decision rule	$(t_m > t_{critical})$ Reject H_0	$(t_a < t_{critical})$ Not reject H_0	$(t_r > t_{critical})$ Reject H_0

5.3.2. Limit of detection and limit of quantification

According to the American Chemical Society (ACS), the limit of detection (LOD) expressed as a concentration quantity is derived from the smallest measure that can be detected with reasonable certainty for a given analytical procedure. The limit of quantification (LOQ) refers to the smallest concentration or mass, which can be quantitatively analyzed with reasonable reliability by a given procedure (Loening, 1978). One successful procedure for calculating both limits for electrochemical trace analysis is known as the regression approach,

RA (Mocak et al., 1997). Its basic principles are: (1) the intercept of the regression line (a) is used as the point of reference, and (2) the regression statistic ($S_{y/x}$) is used to express the variation of the signal values around the regression values (Miller, 1988; Mocak et al., 1997). According to the above, the expressions for the signals corresponding to LOD and LOQ (in y units) are given by the following equations:

$$Y_{LOD} = a + 3S_{y/x} \quad (5-4)$$

$$Y_{LOQ} = a + 10S_{y/x} \quad (5-5)$$

Then, the values of LOD and LOQ are calculated using the linear equation and given in x units ($[\text{Cd}^{2+}]/\mu\text{g kg}^{-1}$). Therefore, an ESC-IS calibration curve at low concentrations (1 to $10 \mu\text{g kg}^{-1}$ of Cd^{2+}) with cleaning between the concentration levels was used to estimate the limit of detection and quantification (Figure 5-2). Using the regression parameters, Eq. 5-4 and Eq. 5-5 a value of $\text{LOD} = 0.45 \mu\text{g kg}^{-1}$ and $\text{LOQ} = 1.63 \mu\text{g kg}^{-1}$ were obtained for Cd^{2+} quantification by SWASV with BiFE.

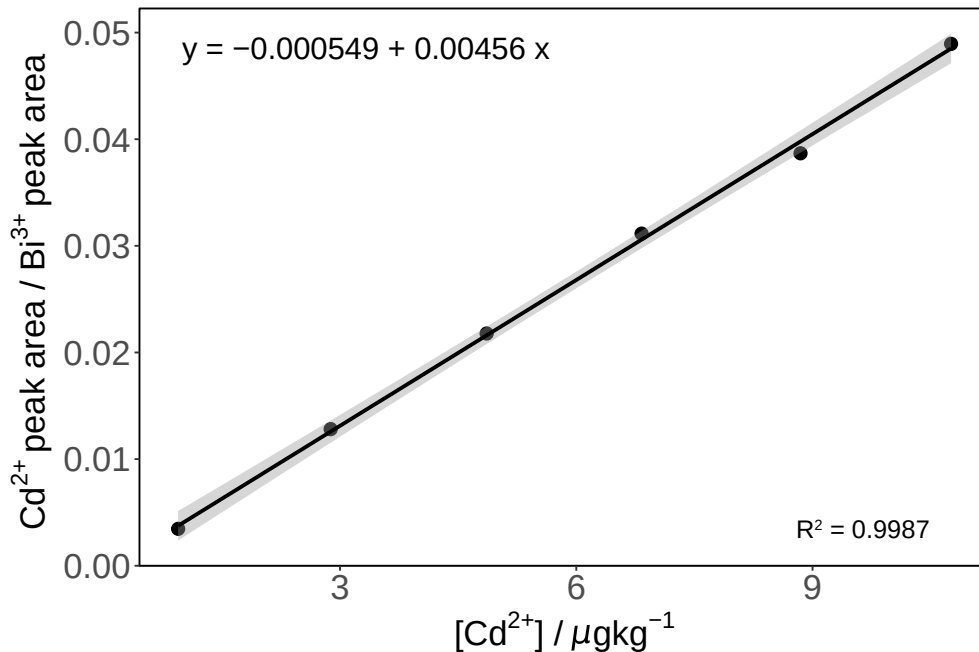


Figure 5-2.: Calibration curve (Cd^{2+} peak area / Bi^{3+} peak area) vs. $[\text{Cd}^{2+}]$ at low concentrations range by external standard calibration with internal standard method (ESC-IS) and cleaning between calibration levels.

5.3.3. Selectivity: Copper interference

The cocoa powder RM was used as a sample and treated by dry ashing digestion following the procedure described in Section 4.2.4. Figure 5.3(a) shows a voltammogram of a digestion extract of the cocoa powder RM. We found a single signal close to 0.06 V (signal A). When the bismuth addition was made to form the bismuth film in the GCE, no cadmium or bismuth signals were observed, only an increase in the A signal. In addition, it was not possible for us to distinguish other signals even when spiking the extract with the cadmium standard solution (Figure 5.3(a), blue line). Then a 1:4 dilution of this spiked extract was made (Figure 5.3(b), black line), and it was possible to distinguish three signals, cadmium oxidation signal at 0.78 V, bismuth oxidation signal at -0.15 V, and the A signal at 0.06 V. According to the reduction potential and the high concentration in which it is found in this matrix (Haynes et al., 2016; Bertazzo et al., 2013), it was most likely that the A signal corresponded to the oxidation of copper. To confirm this, a spike on the diluted extract was made with a standard copper solution (Figure 5.3(b), red line). An increase in the A signal corroborated that this signal corresponds to copper oxidation. In addition, the increase in copper concentration decreased cadmium and bismuth voltammetric signals.

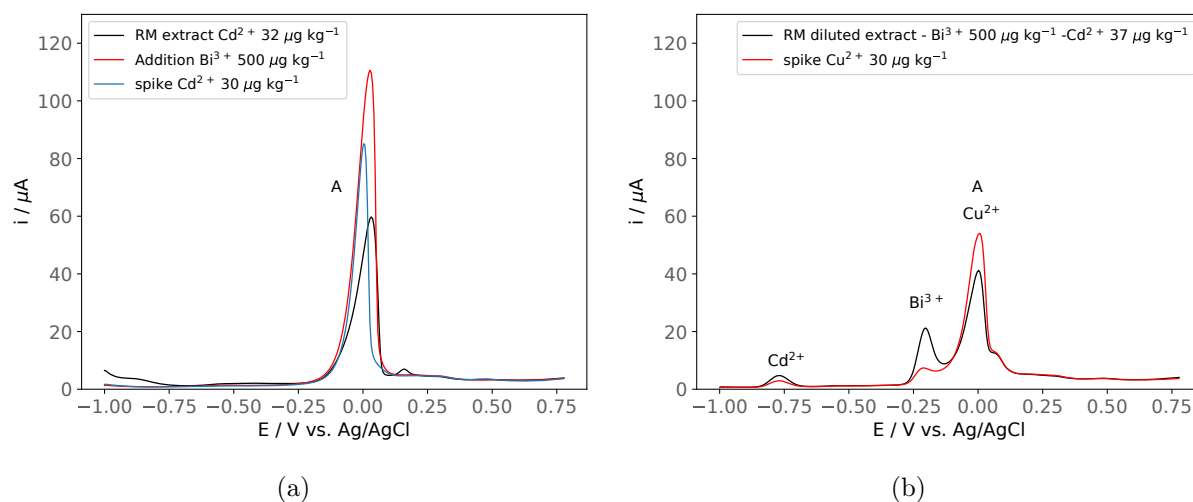


Figure 5-3.: Voltammograms using SWASV of cocoa RM digestion extract in acetate buffer 0.5 M and pH 4.3 obtained by dry ashing digestion, **(a)** raw extract (black line), $[\text{Bi}^{3+}]$ addition (red line), and cadmium spike $[\text{Cd}^{2+}] = 30 \mu\text{g kg}^{-1}$ (blue line); **(b)** dilution 1:4 with Bi^{3+} and $37 \mu\text{g kg}^{-1}$ Cd^{2+} (black line), and $30 \mu\text{g kg}^{-1}$ Cu^{2+} spike (red line). In all cases $[\text{Bi}^{3+}]$ added was $500 \mu\text{g kg}^{-1}$.

As mentioned in the previous chapter (Section 4.1), copper concentrations in cocoa beans range between 10 to 100 mg kg^{-1} , while cadmium has been found between 0.1 to 10 mg kg^{-1} . This significant difference can be explained by the fact that cadmium does not have a function in the plant, and its presence is considered contamination. In contrast, copper

is an essential metal for plants, required in different metabolic pathways. Taking this into account, copper is a strong interference, so in this section, a study of copper interference in the quantification of cadmium by anodic stripping voltammetry using bismuth film electrodes was carried out. Experiments were performed to determine how much the cadmium and bismuth signals are affected in the presence of different concentrations of copper, especially in the range of concentrations in which it would be found in the cocoa matrix.

The interference study started with a standard solution with a constant concentration of cadmium and bismuth ($30 \mu\text{g kg}^{-1}$ and $500 \mu\text{g kg}^{-1}$, respectively), then we added successive aliquots of a copper standard to achieved concentrations from 5 to $240 \mu\text{g kg}^{-1}$ of Cu^{2+} . Reaching a concentration of $15 \mu\text{g kg}^{-1}$ of Cu^{2+} , the cadmium signal begins to decrease, and its shape changes. Both cadmium and bismuth signals are completely suppressed when the copper concentration reaches $240 \mu\text{g kg}^{-1}$, $\text{Cd}^{2+}:\text{Cu}^{2+}$ ratio 1:8 (Figure 5-4).

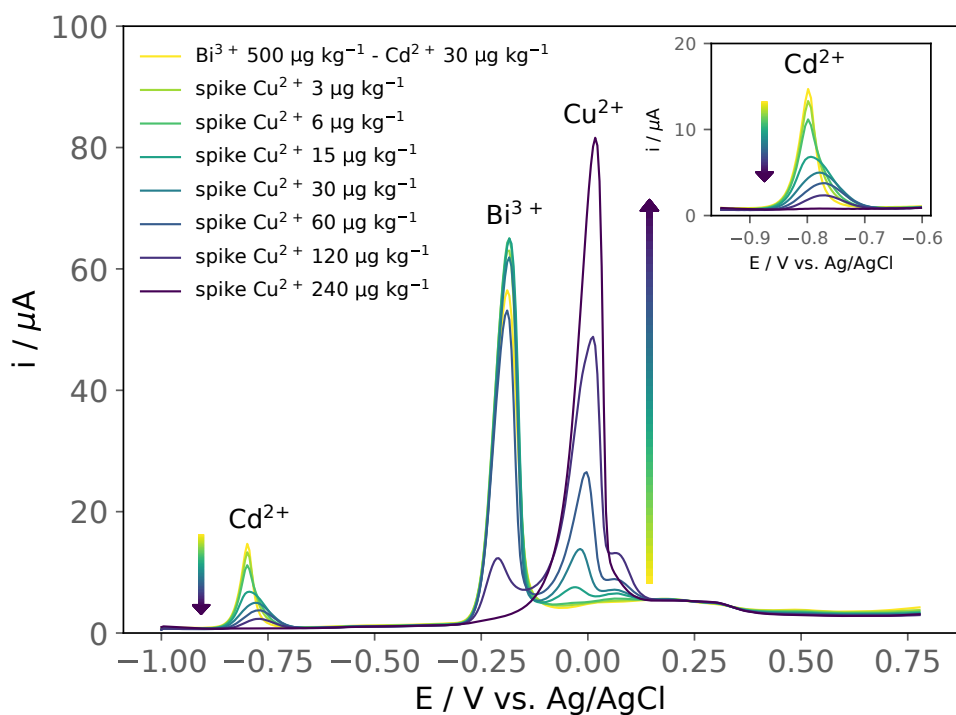


Figure 5-4.: Copper interference on the cadmium quantification in cocoa beans by anodic stripping square wave voltammetry. The solution has $[\text{Bi}^{3+}] = 500 \mu\text{g kg}^{-1}$, $[\text{Cd}^{2+}] = 30 \mu\text{g kg}^{-1}$, and the copper concentrations are from top to bottom 0, 3, 6, 15, 30, 60, 120, $240 \mu\text{g kg}^{-1}$, Cu^{2+} . Inset: close-up of the cadmium peak.

Similar results have been reported in the detection of Cd^{2+} in bare-GCE and BiFE electrodes (Lin et al., 2019; Yang et al., 2013). One possible explanation for the interference effect of Cu^{2+} observed when Cd^{2+} is analyzed on GCE is the replacement of deposited Cd by Cu (Lin et al., 2019). In the bismuth film electrode, two main contributions to the decrease in the cadmium stripping responses by the presence of copper have been suggested: first, competition between cadmium and copper ions for active bismuth sites, and second, the formation of a Cu-Cd intermetallic compound (Yang et al., 2013). Moreover, it has been reported that the decrease of the cadmium signal depends only on the Cu^{2+} concentration and not on the $\text{Cd}^{2+}:\text{Cu}^{2+}$ ratio (Wise et al., 1983). Nevertheless, the most probable reason for the Cu^{2+} interference during the Cd^{2+} determination by SWASV is the fact that Cu^{2+} is reduced at a more positive potential than Bi^{3+} and Cd^{2+} . The latter, together with the high concentration in which copper is found in the cocoa extract, avoids the reduction of Bi^{3+} or Cd^{2+} until enough Cu^{2+} has been reduced. As a result, it is impossible to obtain either the Bi^{3+} or the Cd^{2+} signal on the extracts voltammograms, Figure 5.3(a). According to the above, copper indeed interferes in measuring cadmium by SWASV, and the concentration levels in which it is found in cocoa will not allow cadmium quantification. For the cocoa RM $\text{Cd}^{2+}:\text{Cu}^{2+}$ concentration ratio is 1:13 ($3.20 \text{ mg kg}^{-1}:\text{40.2 mg kg}^{-1}$). In consequence, it is necessary to remove copper from the digestion extracts before cadmium can be quantified. In this work, two procedures were tested to remove Cu^{2+} from the cocoa extracts: **Chelating Ion Exchange Resin** and **CPE**.

Copper elimination from the extracts by Chelating Ion Exchange Resin

The batch method. The experimental conditions for the selective removal of copper from the RM cocoa extracts using the batch method were evaluated by monitoring the normalized area of a reference solution without Cu^{2+} and the normalized area of the solution containing Cu^{2+} and Cd^{2+} treated with Chelex 100 under the specified conditions, according to the Eq. 5-6.

$$\%Recovery_{signal} = \%R_s = \frac{(\text{Cd}^{2+} \text{ peak area} / \text{Bi}^{3+} \text{ peak area})_{treated}}{(\text{Cd}^{2+} \text{ peak area} / \text{Bi}^{3+} \text{ peak area})_{ref}} \times 100 \% \quad (5-6)$$

The amount of resin and treatment time were the first variables studied. Figure 5.5(a) and Figure 5.5(b) show the voltammograms obtained for the treatment of 50 g of a solution containing a concentration of $30 \mu\text{g kg}^{-1}$ of Cd^{2+} and $470 \mu\text{g kg}^{-1}$ of Cu^{2+} in acetate buffer 0.5 M pH = 4.3 with 0.10 g and 0.25 g of Chelex 100; at the three treatment times (15, 35, and 60 minutes) under vortex stirring at 140 rpm. A slight decrease in the intensity of the Cu^{2+} signal is seen, and two barely visible signals, corresponding to the oxidation of bismuth and the oxidation of cadmium, appear. According to this, in both cases, the amount of Chelex 100 is insufficient to remove the copper significantly.

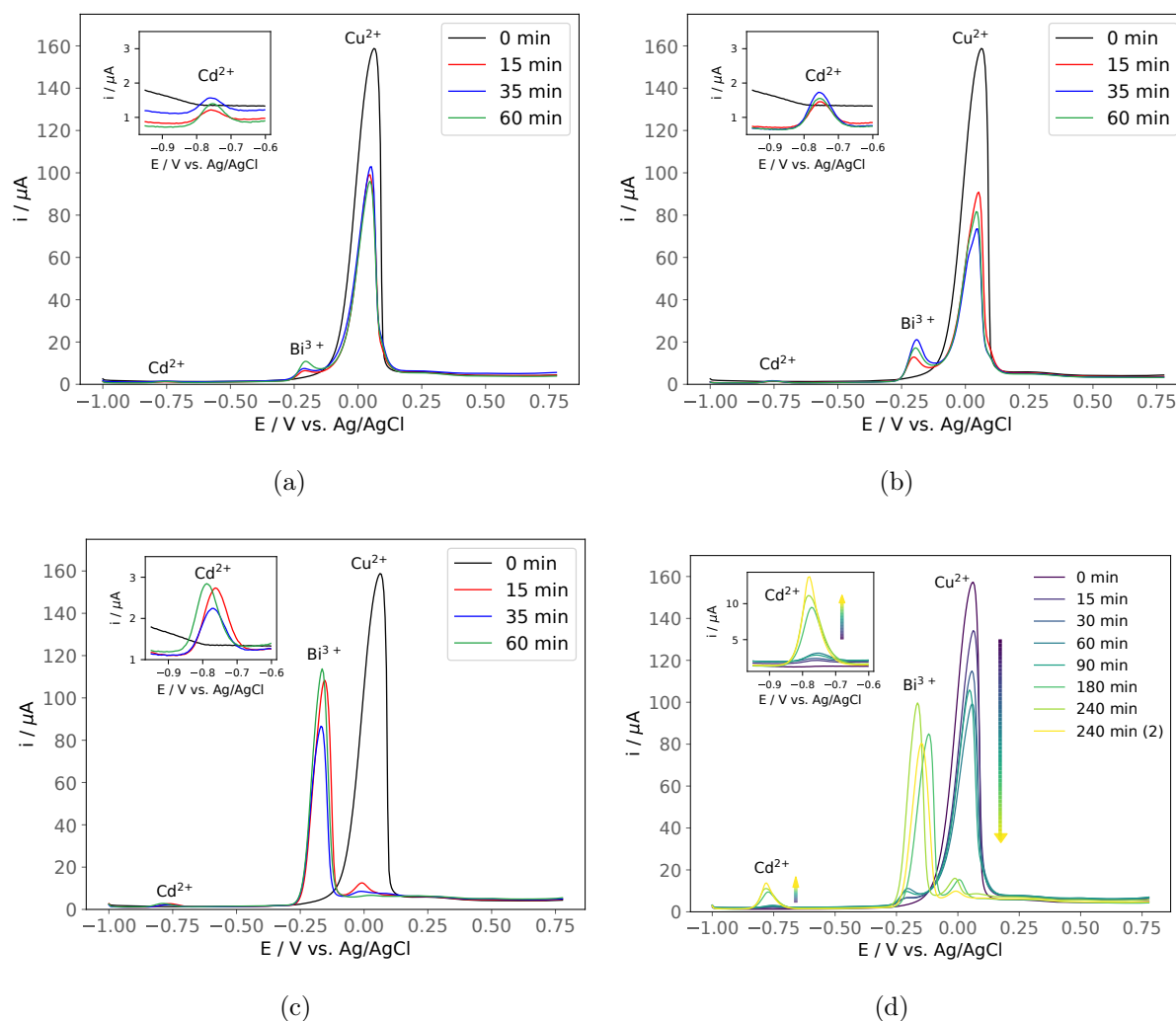


Figure 5-5.: Voltammograms using SWASV of a standard solution, $[\text{Cu}^{2+}] = 470 \mu\text{g kg}^{-1}$, $[\text{Cd}^{2+}] = 30 \mu\text{g kg}^{-1}$ in acetate buffer 0.5 M pH = 4.3, treated by the batch method with (a) 0.1 g, (b) 0.25 g, and (c) 0.5 g of Chelex 100. The treatment times were 0, 15, 35, and 60 min of magnetic stirring at 450 rpm. In (d), the pH changed to 2.5, with 0.1 g of Chelex 100, and the treatment times were 0, 15, 30, 60, 90, 180, and 240 min of magnetic stirring at 450 rpm. Insets: close-up of the cadmium peak. The solutions have $[\text{Bi}^{3+}] = 500 \mu\text{g kg}^{-1}$.

Only by increasing the amount of resin to 0.50 g was it possible to observe a 100% decrease in the Cu^{2+} signal after 35 min of treatment, Figure 5.5(c). Even after removing all the copper from the solution, only a $\%R_s$ of 13, 11, and 11 was obtained for 15, 30, and 60 min of treatment, respectively. Therefore, it is believed that under these experimental conditions, the Chelex 100 is not selectively removing copper from the solution; instead, the Chelex 100 removes both copper and cadmium.

The selectivity of Chelex 100 resin for metal cations corresponds to that of iminodiacetic acid. Table 5-2 shows a list of selectivity factors for several divalent cations (Bio-Rad, 2000). However, the actual selectivity values for any particular system depend on a number of factors, including the pH, ionic strength, and the presence of other complex-forming species. The quantity of cations exchanged is a function of pH. The Chelex 100 ion exchange is very low, below pH = 2; then, it increases sharply from pH = 2 to pH = 4 and reaches a maximum above pH = 4. According to the latter facts, the working pH of 4.3 is within the optimal cation exchange capacity range. The selectivity for copper would increase by limiting the amount of cation exchange, considering the concentration difference between the cations studied. Therefore, to increase the preference for copper over cadmium, the pH was lowered to be in the range of low exchange capacity around pH = 2.5. In that sense, a solution at pH = 2.5 treated with 0.50 g of Chelex 100 shows a % R_s of 17, 24, and 26 for the three treatment times (15, 35, and 60 min). Compared to the % R_s obtained at a higher pH value, lowering the pH value to 2.5 shows an improvement of 15% at 60 min of treatment. Nevertheless, the % R_s = 26 still needs to be improved. Thereby, the quantity of resin was reduced to 0.10 g, and the time treatment was increased to 90, 180, and 240 min. The voltammograms obtained are shown in Figure 5.5(d); where it can be seen that after 180 min, a significant decrease in the copper signal is achieved, and bismuth and cadmium signals begin to be observed. Finally, two solutions were treated for 240 min, and a % R_s of 80 and 94 were achieved. According to the above, the most appropriate parameters for the batch method are pH = 2.5, 0.10 g of Chelex 100, and a treatment time of 240 min.

Finally, it was found that exists a linear relationship between the amount of Chelex 100 and the amount of the solution treated. Then, for later experiments, an amount of 30 g of the standard solution and 0.06 g of Chelex 100 will be used. In addition, the treatment time was reduced to 60 min by changing the stirring method to magnetic stirring at 450 rpm.

The column method. The column method was tested with 15 g of the standard solution at pH = 2.5, the same used for the batch method. Figure 5-6 shows the voltammograms obtained for four solutions treated with 0.10, 0.15, 0.25, and 0.50 g of Chelex 100 packed into a column.

The higher % R_s obtained was for the 0.10 g and 0.15 g experiments with a value of 56 and 57, respectively. According to the voltammograms, a complete decrease in the copper signal is obtained from 0.10 g of resin. However, it seems that the amount of resin is yet too high, and cadmium is also retained. In this case, the selective separation of cations from the solution is based on the time of contact of the solution with the specific quantity of resin packed. Therefore, to increase the % R_s , the amount of resin packed was reduced to 0.05 g.

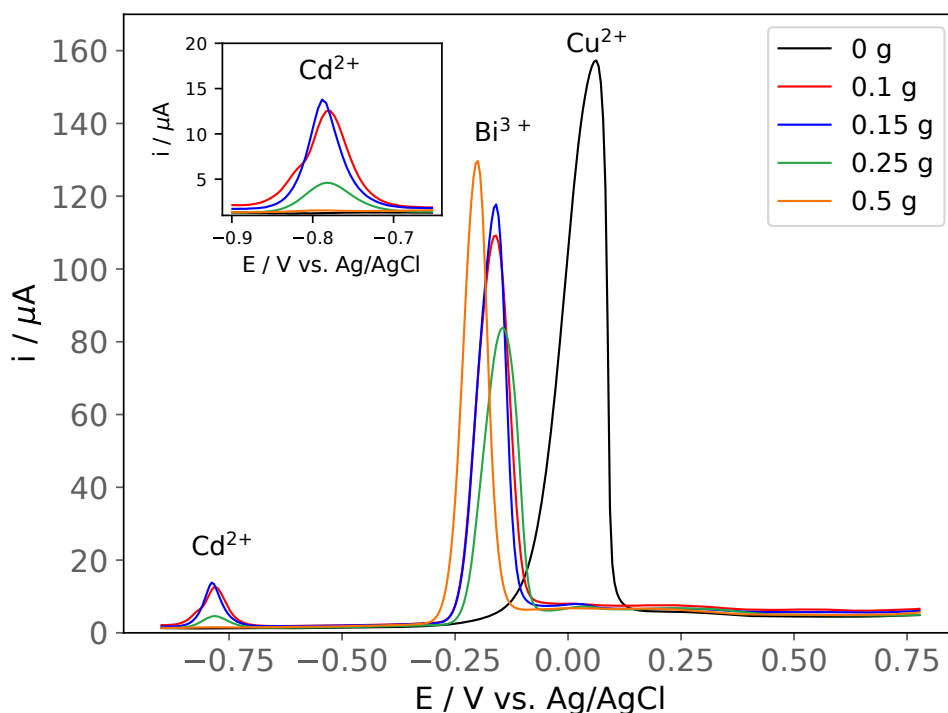


Figure 5-6.: Voltammograms using SWAV of a standard solution, $[\text{Cu}^{2+}] = 470 \mu\text{g kg}^{-1}$, $[\text{Cd}^{2+}] = 30 \mu\text{g kg}^{-1}$ in acetate buffer 0.5 M pH = 2.5, treated by the column method with 0.1, 0.15, 0.25, and 0.5 g of Chelex 100. Inset: close-up of the cadmium peak. The solutions have $[\text{Bi}^{3+}] = 500 \mu\text{g kg}^{-1}$.

Comparison between the batch and column methods. Twelve replicates of the standard solution were used to compare the column and batch methods in terms of $\%R_s$. Six of these replicates were treated by the column method (0.05 g Chelex 100, 15 g of the standard solution at pH = 2.5). The other six replicates were treated by the batch method at previously selected conditions (0.06 g of Chelex 100, 30 g of the standard solution at pH=2.5, 60 min of treatment under magnetic stirring at 450 rpm).

Figure 5.7(a) shows the voltammograms of two solutions, each treated by the batch and column methods, respectively. Figure 5.7(b) shows both methods' $\%R_s$ obtained for the six replicates. The batch and column methods provide acceptable $\%R_s$ values between 80 and 102. Therefore, both methods are suitable for removing copper selectively from the solution.

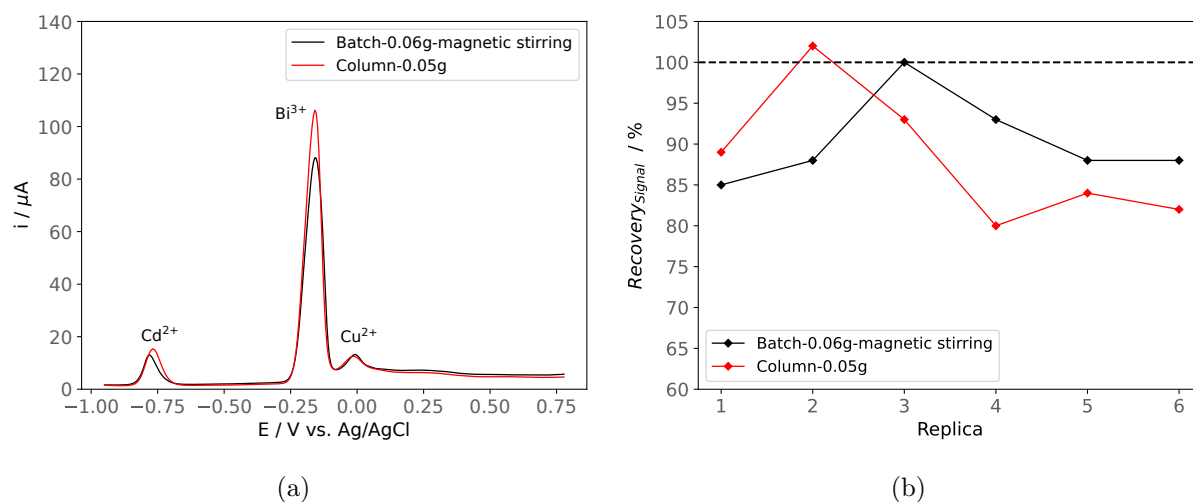


Figure 5-7.: (a) Voltammograms using SWAV of a standard solution, $[\text{Cu}^{2+}] = 470 \mu\text{g kg}^{-1}$, $[\text{Cd}^{2+}] = 30 \mu\text{g kg}^{-1}$ in acetate buffer 0.5 M pH = 2.5, treated by the batch method (black line) and the column method (red line). The solutions have $[\text{Bi}^{3+}] = 500 \mu\text{g kg}^{-1}$. (b) Chelex 100 comparison signal recovery percentages for six replicates treated by the batch (black line) and column (red line) methods.

The selection of one method was based on a compromise between the repeatability results obtained (Table 5-4) and the practicality of the procedure.

Table 5-4.: Recovery percentage of the normalized area of Cd obtained for six replicates of a standard solution containing $30 \mu\text{g kg}^{-1}$ of Cd²⁺ and $470 \mu\text{g kg}^{-1}$ of Cu²⁺ in acetate buffer 0.5 M pH = 2.5 treated by the batch and column methods.

Replica	% Recovery _{signal} (% R _s)	
	Batch method	Column method
1	85	89
2	88	102
3	100	93
4	93	80
5	88	84
6	88	82
Mean	90	88
SD	5.4	8.2
% RSD	6.0	9.3

According to this, the batch method was selected as the most appropriate method for using

Chelex 100 in removing the copper interference and detecting Cd^{2+} by SWASV with BiFE.

Copper removal by chelating ion exchange resin (batch method) from RM digestion extracts of cocoa powder obtained by microwave-assisted acid digestion. The improved batch method was tested on real cocoa powder RM digestion extract obtained by acid microwave-assisted digestion. However, the signal of copper is not diminished by the amount of Chelex 100 and treatment time at the pH value and stirring method previously selected. The complexity of the sample is related to this result. Although Cd^{2+} and Cu^{2+} concentrations are close to those studied in standard solution, other cations present in high concentrations in the extracted cocoa RM, such as Zn^{2+} , and Fe^{2+} , and possible residual organic matter from the digestion methodology, interfere with the Chelex 100 performance to remove copper.

Therefore, increasing the amount of Chelex 100 for the same amount of solution (30 g) was the first strategy to improve the removal of copper from the digestion extracts. Until now, in all the previous Chelex 100 measurements, the resin was used in its sodium form, and given the minimum quantities needed to remove copper from the standard solutions, the pH value of the treated solution was not affected by the Chelex 100. In the new experiments, it was necessary to increase the amount of resin to 4.5 g to treat the 30 g of cocoa powder RM digested extract to remove all copper in the solution. However, this amount of resin caused an increase in the pH value from 2.5 to 4.2. The increase in the pH value decreased the selectivity of the resin, causing the retention of cadmium as well. Chelex 100 resin in the sodium form has a pH of about 11; meanwhile, the pH in the hydrogen form is about 2 to 3 (Bio-Rad, 2000). In that sense, a pre-treatment was applied to the resin before using it in the cocoa powder RM digested extract. The sodium form was transformed to the hydrogen form by rinsing with 0.1 M HCl, followed by consecutive type I water rinses. After drying at 60 °C for 1 h, the resin was ready to be used on the cocoa powder RM extracts without affecting the pH value.

As found in the previous chapter, the main disadvantage of the selected acid microwave-assisted digestion methodology is the residual organic matter. The degree of the residual organic matter is higher in the real cocoa samples than in the synthetic cocoa matrix. Therefore, a pre-cleaning step with activated carbon was added to the procedure. The use of activated carbons in the adsorptive removal of toxic metals and recovering certain metals has been studied in numerous investigations. Activated carbons have a highly developed porosity and an extended interparticulate surface area (Bansal and Goyal, 2005). Adsorption from solutions on activated carbons has wide applications in food to remove undesired components from the solution. The adsorption of a solute from a solution is mainly determined by the nature of the solution's components, the concentration of the species in the solution, and the pH value (Bansal and Goyal, 2005).

Figure 5.8(a) shows the voltammograms obtained from a cocoa powder RM digestion extract before any treatment, after the treatment with activated carbon (cleaning step), and then after the treatment with Chelex 100 by the batch method.

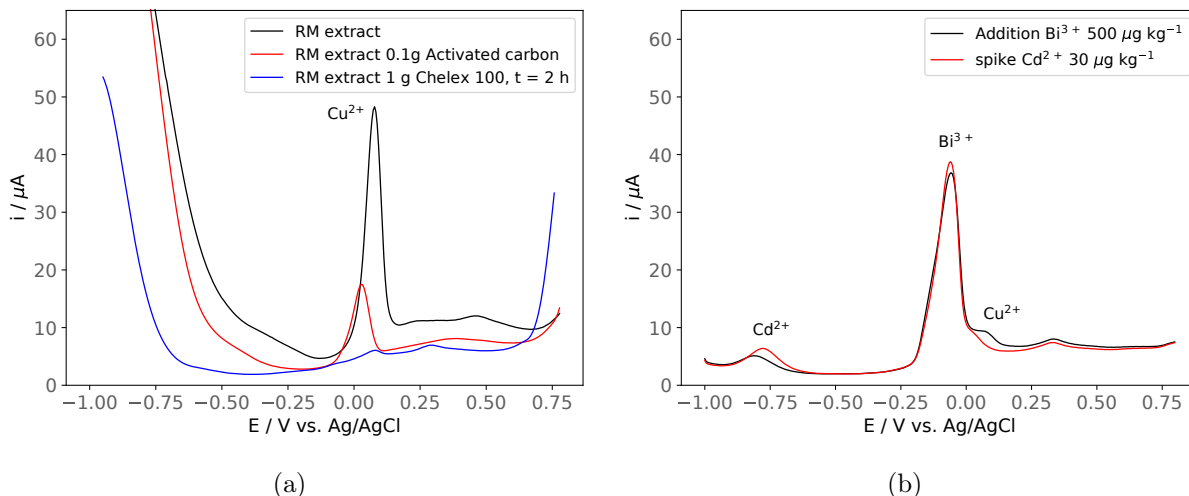


Figure 5-8.: Voltammograms using SWASV of an RM digestion extract in acetate buffer 0.5 M and $\text{pH} = 2.5$. **(a)** before any treatment (black line), after the treatment with 0.1 g of activated carbon, cleaning step (red line), and then after the treatment with 1 g of Chelex 100 by the batch method (blue line); and **(b)** the previous sample cleaned and treated added with $[\text{Bi}^{3+}] = 500 \mu\text{g kg}^{-1}$ (black line), and spiked with $[\text{Cd}^{2+}] = 30 \mu\text{g kg}^{-1}$ (red line).

Pre-treatment with activated carbon consisted of adding 0.1 g of activated carbon to a Falcon® tube containing 30 g of cocoa powder RM digestion extract. Then, the solution was shaken gently for 20 s and filtered using a Whatman® qualitative filter paper, Grade 1. After this treatment, the Cu^{2+} signal is significantly decreased (Figure 5.8(a), red line). In addition, the solution was decolorized, showing that the extract's cleaning was effective. Then, the previously cleaned solution was treated with 1.0 g of Chelex 100 (washed with HCl) and stirred for 2 h. After the treatment, a small signal is observed in the voltammogram (Figure 5.8(a), blue line), meaning that a great portion of the copper in the solution has been eliminated successfully. Subsequently, the bismuth aliquot was added to the treated cocoa powder RM digestion extract to form the film on the glassy carbon electrode, and the SWASV was performed. Figure 5.8(b) shows a distinguishable signal close to -0.80 V. This signal was assigned to cadmium oxidation by adding an aliquot of a standard cadmium solution to the treated cocoa powder RM digestion extract. According to the above, the combined use of activated carbon (cleaning step) and Chelex 100 in the hydrogen form removed the interferences from the cocoa powder RM digestion extract, allowing the Cd^{2+}

voltammetric detection. In Section 5.3.4, the improved Chelex 100 treatment is tested in terms of repeatability and trueness for the quantification of cadmium in the cocoa powder RM.

Copper elimination from the extracts by Constant Potential Electrolysis

Another approach to overcome the copper interference in the cadmium determination by SWASV with BiFE was the removal of Cu^{2+} by CPE. The two-electrode setup is the most common configuration to employ this technique. The main advantage of using only a working electrode and a counter electrode is its low cost and simplicity (Rafiee et al., 2021). However, the ohmic drop and the potentials between the working and the counter electrode oscillate with time. In contrast, in the three-electrode electrochemical setup used in this work, the potential between the working and reference electrodes is controlled while monitoring the current between the working and counter electrodes. The latter allows a selective reduction desired for copper elimination without cadmium losses.

The first test involved applying -0.40 V vs. Ag/AgCl to 30 mL of cocoa powder RM digested extract for 2 h with magnetic stirring (600 rpm). The intensity of the Cu^{2+} signal followed by SWASV remains the same after the treatment. Nonetheless, the solution suffers a decolorization after the treatment, similar to the observed with the Chelex 100 tests. Therefore, the organic matter residues, interfere with the copper reduction. Hence a pre-treatment of the digestion extract with activated carbon is necessary. In addition, considering the reduction potentials of cadmium (-0.80 V vs. Ag/AgCl) and copper (0.06 V vs. Ag/AgCl), it is possible to increase the reduction potential applied to a more negative value than -0.40 V vs. Ag/AgCl. This helps remove copper but still keeps the process selective enough to leave the cadmium extracted in the solution without losses and available to be quantified.

Figure 5.9(a) shows the voltammograms of a cocoa powder RM digestion extract obtained by the acid microwave-assisted digestion before any treatment, after the treatment with activated carbon (cleaning step), and then after 2 h of electrolysis at -0.75 V vs. Ag/AgCl. Similarly to the Chelex 100 procedure, after the addition of 0.1 g of activated carbon, the solution was decolorized, and the copper signal was greatly decreased, Figure 5.9(a), red line. Then, after two hours of electrolysis, the copper signal was wholly suppressed, Figure 5.9(a), blue line. The corresponding bismuth aliquot was added to the treated cocoa powder RM digestion extract to perform the SWASV. As expected, with the formation of the bismuth film on the glassy carbon electrode is possible to distinguish a signal close to -0.80 V vs. Ag/AgCl, Figure 5.9(b), black line. After adding the aliquot of the standard cadmium solution, the current intensity increased; therefore, the signal was assigned to cadmium oxidation.

Accordingly, the CPE at the improved experimental conditions effectively allowed the selective removal of copper from cocoa extracts within a reasonable treatment time and a simple

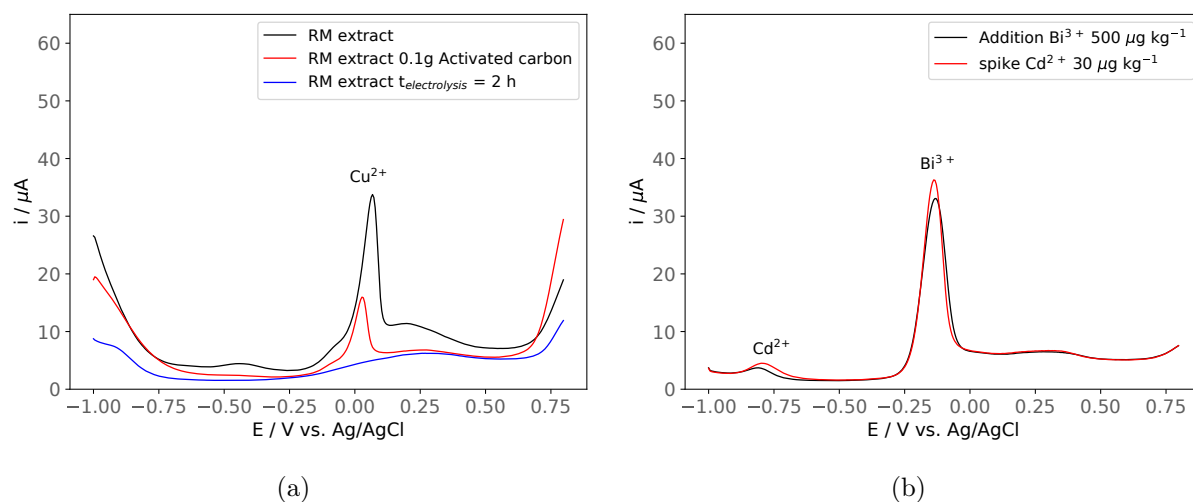


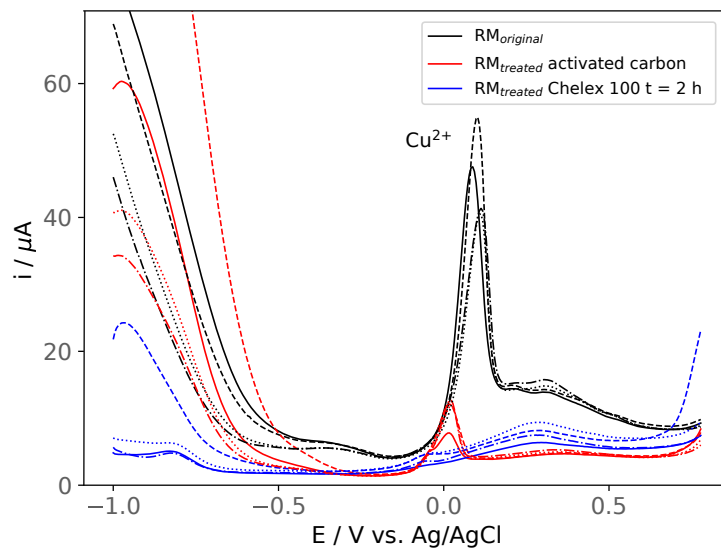
Figure 5-9.: Voltammograms using SWASV of an RM digestion extract in acetate buffer 0.5 M, and pH = 4.3. **(a)** before any treatment (black line), after the treatment with 0.1 g of activated carbon, cleaning step (red line), and then after CPE (blue line); and **(b)** the previous cleaned sample added with $[\text{Bi}^{3+}] = 500 \mu\text{g kg}^{-1}$ (black line), and then spiked with $[\text{Cd}^{2+}] = 30 \mu\text{g kg}^{-1}$ (red line).

and practical experimental procedure.

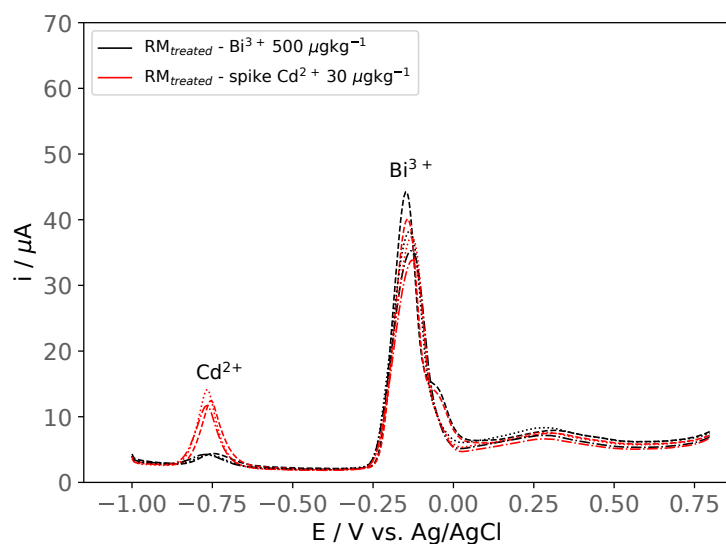
5.3.4. Precision and Trueness

The two procedures, treatment with the chelating resin Chelex 100 and the CPE, are tested to assess the quantification methodology in terms of repeatability and trueness. Four replicates of the cocoa powder RM were used as samples. The replicas were digested by the acid microwave-assisted digestion methodology at the selected conditions (Section 4.3.2). Figure 5.10(a) shows the Cu^{2+} SWASV with GCE for the four cocoa powder RM replicates after the cleaning with activated carbon and treatment with Chelex 100. The voltammetric signals for all replicates were similar, showing almost an entirely Cu^{2+} signal decreases after the treatments.

Subsequently, the quantification of Cd^{2+} in the four treated extracts was performed by the SSA-IS using SWASV with BiFE. The voltammograms of the four calibration curves are presented in Figure 5.10(b). All the replicates show the Cd^{2+} signal and the increment of that signal after the single-point standard addition. In replica 2, a visible shoulder peak at a less negative potential, next to the bismuth oxidation signal, is observed. This signal is assigned to a copper residual in the solution. Then, the respective calibration curves were constructed, Figure 5.11(a), and the concentration of cadmium in the cocoa powder RM was determined and shown in Table 5-5 (columns 3 and 4). An average $[\text{Cd}^{2+}] = 0.82 \text{ mg kg}^{-1}$



(a)



(b)

Figure 5-10.: Voltammograms using SWASV of four RM digestion extracts in acetate buffer 0.5 M, and pH = 2.5: **(a)** before any treatment (black lines), after the treatment with 0.1 g of activated carbon (red lines), and then after the treatment with 1 g of Chelex 100 by the batch method (blue lines); and **(b)** SSA-IS calibration curves using BiFE of the previous four RM digestion extracts with addition of $[\text{Bi}^{3+}] = 500 \mu\text{g kg}^{-1}$ (black lines), and spiked with $[\text{Cd}^{2+}] = 30 \mu\text{g kg}^{-1}$ (red lines).

was obtained with a RSD = 6.72 % and a bias = -74.30 %.

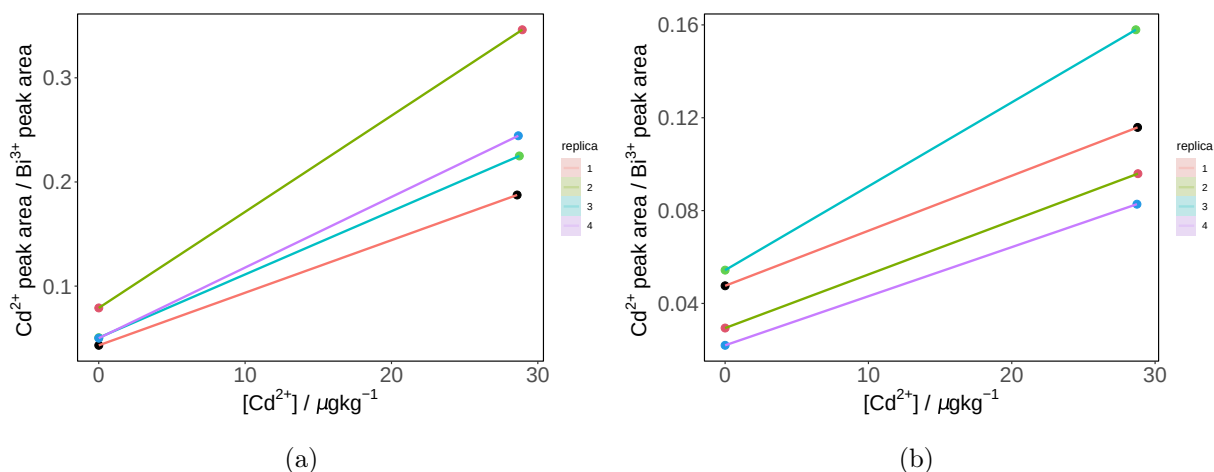


Figure 5-11.: Calibration curves Cd²⁺ peak area / Bi³⁺ peak area vs. [Cd²⁺] by single-point standard addition with the internal standard method (SSA-IS) of four RM replicas treated by (a) the Chelex 100 procedure, and (b) the CPE procedure.

Table 5-5.: Comparison of cadmium concentrations and performance parameters bias and repeatability of the RM cocoa powder (3.2 ± 0.064 mg kg⁻¹) measured by SWASV with BiFE and the SSA-IS methodology, obtained with the two procedures for copper interference elimination: Chelex 100 and CPE.

Replica	Chelex 100			Electrolysis (CPE)	
	[RM] _{true} (mg kg ⁻¹)	[RM] _{measured} (mg kg ⁻¹)	bias (%)	[RM] _{measured} (mg kg ⁻¹)	bias (%)
1	3.20	0.86	-73.13	2.01	-37.19
2		0.86	-73.13	1.28	-60.00
3		0.83	-74.06	1.50	-53.13
4		0.74	-76.88	1.03	-67.81
Mean		0.82	-74.30	1.45	-54.6
SD		0.06	1.77	0.42	13.0
RSD (%)		6.72	2.39	28.7	23.9

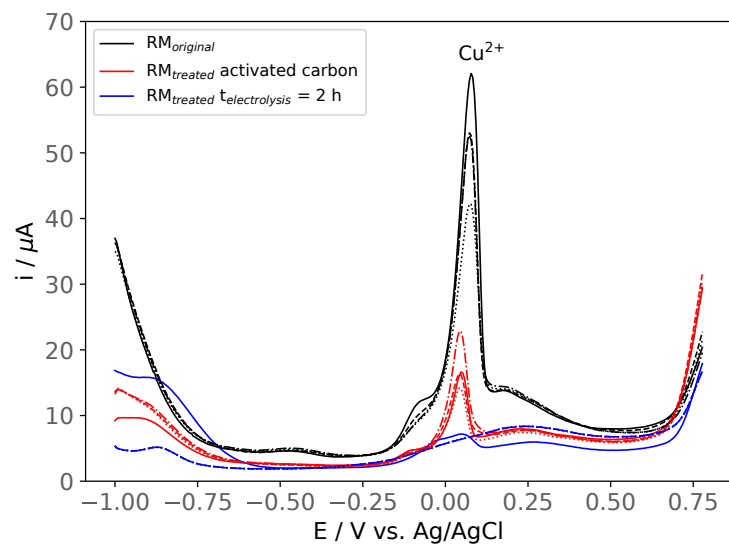
Figure 5.12(a) shows the Cu²⁺ signal before and after the improved electrolysis treatment. In the same way, as for the replicas treated with Chelex 100, the Cu²⁺ signal is significantly decreased after applying the procedure, although replica 1 has a clear residual signal. As

expected, a shoulder signal is observed for this replica after the bismuth addition, Figure 5.12(b). Nevertheless, it was possible to distinguish a cadmium oxidation signal with the bismuth film electrode for all the replicas, and the signal increases after the standard addition of Cd^{2+} , Figure 5.12(b). As before, the peak areas for cadmium and bismuth were calculated, and the normalized areas were used to construct the SSA-IS calibration curves, Figure 5.11(b). The cadmium concentration in the cocoa powder RM was determined and shown in Table 5-5 (Columns 5 and 6). An average $[\text{Cd}^{2+}] = 1.45 \text{ mg kg}^{-1}$ was obtained with a $\text{RSD} = 28.7\%$ and a $\text{bias} = -54.6\%$.

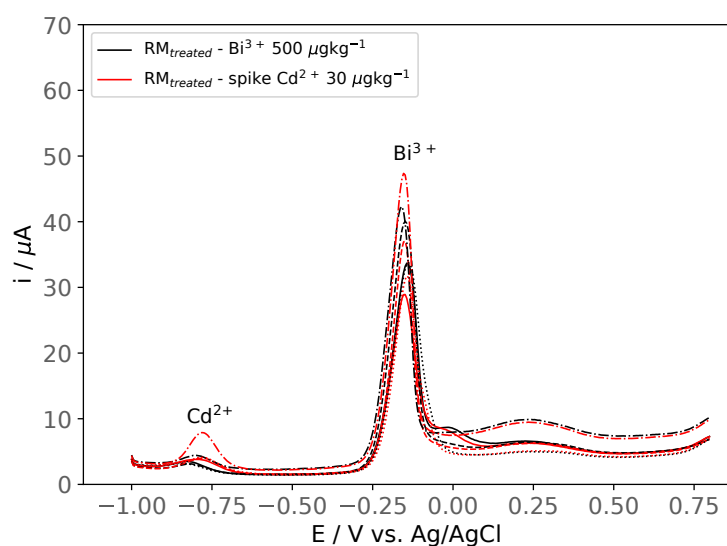
According to the results of repeatability and trueness, both methods need to be improved. The expected precision (repeatability) as a function of the analyte concentrations reported by the AOAC (Committee et al., 2011) and the Codex Alimentarius (Joint FAO/WHO Codex Alimentarius Commission, 1992) for an analyte concentration level of $10 \mu\text{g kg}^{-1}$ an acceptable RSD value must be $\text{RSD} < 22\%$. Therefore, the Chelex 100 procedure satisfies the repeatability criteria with an $\text{RSD} = 6.72\%$. Unlike the CPE procedure, $\text{RSD} = 28.7\%$ fails to meet the requirements of acceptable RSD values. Although the same treatment was performed on all four replicates, the variations in the copper and/or other cations contents in each solution may come from the digestion procedure, as seen in the previous chapters. Also, the variation between replicates could come from the interference elimination treatment. Several steps, such as two filtrations procedures, must be followed to clean the extract before possible cadmium detection. These multiple steps could increase the final variability in the result. Nevertheless, the variation between replicates could be minimized by improving the control in the experimental conditions. For instance, the contact time with the activated carbon. Different filtration fluxes between the replicas were observed when the solutions were filtered with the Whatman filter. Therefore, improving the filtration method for this cleaning step could homogenize the results, as all the solutions will have the same contact time with the activated carbon.

Regarding bias, both methodologies fail because the percentages range between -73.13 and -76.88% for Chelex 100 procedure and -37.19 and -67.81% for CPE. The purpose of using activated carbon was to remove the organic matter from the extract and decrease the levels of the interfering cations, Zn^{2+} , Fe^{2+} , and Cu^{2+} . It seems that no selective retention between cations, as Cd^{2+} , Zn^{2+} , Fe^{2+} and Cu^{2+} , is obtained when using the activated carbon under our experimental conditions. Then, part of the cadmium losses is attributed to this cleaning step. Despite its insufficient selective adsorption, using activated carbon is a cheaper and simpler proposal to make the necessary cleaning step of the digested extract before the more selective procedures (Chelex 100 and CPE) and then be able to quantify cadmium in cocoa by SWASV with BiFE.

Therefore, more experiments are needed to improve these results. Nevertheless, it is impor-



(a)



(b)

Figure 5-12.: Voltammograms using SWASV of four RM digestion extracts in acetate buffer 0.5 M, and pH = 4.3: **(a)** before any treatment (black lines), after treatment with 0.1 g of activated carbon (red lines), and then after 2h of CPE at -0.75 V vs. Ag/AgCl (blue lines); and **(b)** SSA-IS calibration curves using BiFE of the previous four RM digestion extracts treated by the CPE procedure with $[\text{Bi}^{3+}] = 500 \mu\text{g kg}^{-1}$ (black lines), and spiked with $[\text{Cd}^{2+}] = 30 \mu\text{g kg}^{-1}$ (red lines).

tant to highlight that both procedures possess a significant potential for eliminating the copper and other cations interferences, alongside removing the organic matter residuals, for the cadmium quantification by SWASV with BiFE. Then, a deeper study that includes optimizing the quantity of activated carbon, time of contact, and filtration procedures would allow us to improve the validation parameters and obtain more accurate results.

5.4. Conclusions

A linear working range between 5 to 95 $\mu\text{g kg}^{-1}$ of Cd^{2+} was obtained for the calibration curve Cd^{2+} peak area / Bi^{3+} peak area vs. $[\text{Cd}^{2+}]$ with cleaning between calibration levels, complying with the evaluation statistics for the parameters slope, intercept, and correlation coefficient. Limits of detection (LOD) and quantification (LOQ) were found to be 0.45 $\mu\text{g kg}^{-1}$ of Cd^{2+} and 1.63 $\mu\text{g kg}^{-1}$ of Cd^{2+} , respectively. The present investigation found that the high concentrations of copper in cocoa interfere with the quantification of cadmium by SWASV with BiFE. The study of copper interference allowed the development and validation of a new methodology for this determination. At concentration levels of 30 $\mu\text{g kg}^{-1}$ of Cd^{2+} , the cadmium stripping signal is diminished starting from a $\text{Cd}^{2+} : \text{Cu}^{2+}$ concentration ratio of 2 : 1 (30 : 15 $\mu\text{g kg}^{-1}$), and the signal is wholly suppressed when the ratio exceeds 1 : 8 (30 : 240 $\mu\text{g kg}^{-1}$). Consequently, removing copper from the digestion extracts is mandatory before cadmium can be quantified.

Due to the complexity of the cocoa matrix, residual organic matter is obtained after the acid microwave-assisted digestion methodology. A pre-treatment with 0.10 g of activated carbon is proposed to clean the digestion extracts of the cocoa powder RM samples. After this first treatment, two procedures were found suitable for the selective removal of copper from the solution: i-) the addition of 1.0 g of chelating resin Chelex 100 in the hydrogen form by the batch method for 2 h and ii-) the constant potential electrolysis for 2 h at -0.75 V vs. Ag/AgCl under magnetic stirring. The two methodologies remove the interferences, mainly Cu^{2+} , and allow the quantification of cadmium by SWASV using BiFe in a cocoa reference material. Further studies and optimization of the proposed procedures must be carried out to improve the performance parameters bias and repeatability of the quantification of cadmium in a cocoa matrix by SWASV with BiFE.

5.5. References

Babyak, C. and Smart, R. B. (2004). Electrochemical detection of trace concentrations of cadmium and lead with a boron-doped diamond electrode: Effect of kcl and kno3 electrolytes, interferences and measurement in river water. *Electroanalysis: An International Journal Devoted to Fundamental and Practical Aspects of Electroanalysis*, 16(3):175–182.

- Balazs, A. (2008). International vocabulary of metrology-basic and general concepts and associated terms. *Chemistry International*, 25.
- Bansal, R. C. and Goyal, M. (2005). *Activated carbon adsorption*. CRC press.
- Bard, A. J. and Faulkner, L. R. (2001). *Electrochemical methods. Fundamentals and applications*. John Wiley & Sons, Inc.
- Bertazzo, A., Comai, S., Mangiarini, F., and Chen, S. (2013). Composition of cacao beans. In *Chocolate in health and nutrition*, pages 105–117. Springer.
- Bio-Rad, L. (2000). Chelex®-100 and chelex®-20 chelating ion exchange resin instruction manual. *Bio-Rad Laboratories*.
- Committee, A. I. M. et al. (2011). Standard method performance requirements-aoac international methods committee guidelines for validation of biological threat agent methods and/or procedures. *J. AOAC Int.*, 94:1359–1381.
- Haynes, W. M., Lide, D. R., and Bruno, T. J. (2016). *CRC handbook of chemistry and physics*. CRC press.
- Joint FAO/WHO Codex Alimentarius Commission (1992). *Codex alimentarius*. Food & Agriculture Org.
- Lin, C.-H., Li, P.-H., Yang, M., Ye, J.-J., and Huang, X.-J. (2019). Metal replacement causing interference in stripping analysis of multiple heavy metal analytes: kinetic study on cd (ii) and cu (ii) electroanalysis via experiment and simulation. *Analytical chemistry*, 91(15):9978–9985.
- Loening, K. L. (1978). Acs committee on nomenclature annual report for 1977. *Journal of Chemical Information and Computer Sciences*, 18(2):87–90.
- Miller, J. (1988). Jn miller statistics for analytical chemistry.
- Mocak, J., Bond, A. M., Mitchell, S., and Scollary, G. (1997). A statistical overview of standard (iupac and acs) and new procedures for determining the limits of detection and quantification: application to voltammetric and stripping techniques (technical report). *Pure and Applied Chemistry*, 69(2):297–328.
- Pesavento, M., Biesuz, R., Gnecco, C., and Magi, E. (2001). Investigation of the metal species in seawater by sorption of the metal ion on complexing resins with different sorbing properties. *Analytica chimica acta*, 449(1-2):23–33.
- Rafiee, M., Mayer, M. N., Punchihewa, B. T., and Mumau, M. R. (2021). Constant potential and constant current electrolysis: An introduction and comparison of different techniques for organic electrosynthesis. *The Journal of Organic Chemistry*, 86(22):15866–15874.

- Schulze, G. and Elsholz, O. (1989). Ion-exchange micro columns for on-line preconcentration of heavy metals i. a rapid voltammetric screening test of ion-exchange kinetics. *Fresenius' Zeitschrift für analytische Chemie*, 335(7):721–727.
- U.S. Food and Drug Administration (2019). Guidelines for the validation of chemical methods in food, feed, cosmetics, and veterinary products.
- Wise, J. A., Roston, D. A., and Heineman, W. R. (1983). The effects of copper-zinc and copper-cadmium intermetallic compounds in different systems used for anodic stripping voltammetry. *Analytica chimica acta*, 154:95–104.
- Yanagisawa, H., Kurita, R., Kamata, T., Yoshioka, K., Kato, D., Iwasawa, A., Nakazato, T., Torimura, M., and Niwa, O. (2015). Effect of the sp²/sp³ ratio in a hybrid nanocarbon thin film electrode for anodic stripping voltammetry fabricated by unbalanced magnetron sputtering equipment. *Analytical Sciences*, 31(7):635–641.
- Yang, D., Wang, L., Chen, Z., Megharaj, M., and Naidu, R. (2013). Investigation of copper (ii) interference on the anodic stripping voltammetry of lead (ii) and cadmium (ii) at bismuth film electrode. *Electroanalysis*, 25(12):2637–2644.

6. Conclusions and Recommendations

The validation of the Square Wave Anodic Stripping Voltammetry methodology for cadmium quantification in *Theobroma cacao* L. beans started with the electrochemical study of the bismuth reduction onto the glassy carbon electrode. The formation of the bismuth film is a non-reversible complex process. Multiple oxidation signals of bismuth in cyclic voltammetry are related to the formation of bismuth hydroxides due to the surface pH. As well, the presence of oxygen affects the reproducibility, properties, and performance of the bismuth film in SWASV measurements. Thereby, it is recommended to remove oxygen before performing a measurement. Using the Scharifker-Hills' models and chronoamperometry experiments, it was possible to attribute the nucleation mechanism of bismuth deposition in GCE to a progressive nucleation and 3D growth mechanism. The electrode area and electrochemical rate constant for the $[\text{Fe}(\text{CN})_6]^{3-}/[\text{Fe}(\text{CN})_6]^{4-}$ redox couple were estimated, and compared, using electrochemical impedance spectroscopy when using GCE with and without bismuth film modification. The improvement in the current intensity when using BiFE in SWASV for cadmium determinations is attributed to a larger electrochemical rate constant.

It was also found that the surface conditions of the BiFE working electrode during the quantification of Cd^{2+} by SWASV directly affect the precision and trueness of the methodology. Then, the internal standard *in situ* calibration and the single-point standard addition was selected as the most outstanding, practical and faster calibration method. The proposed methodology satisfy the required levels of precision and trueness with an RSD = 6.77 %, and bias = 5.16 % for cadmium quantification of a reference material NIST 3108 Cd^{2+} in solution. Additionally, using the simplex optimization method, the experimental conditions pH = 4.3, $E_d = -1.2$ V, and $t_d = 198$ s were found to be the optimal values for Cd^{2+} detection by SWASV with BiFE.

Moreover, the acid microwave-assisted digestion is the most appropriate digestion procedure, in terms of repeatability and trueness, for the electrochemical determination of cadmium in a synthetic cocoa matrix with an RSD = 22 % and a recovery_{average} = 92 %. The methodology satisfies the range of the acceptable mean recovery and RSDs according to the AOAC and CODEX Alimentarius criterion. The complexity of the sample and its high content of organic matter appears to affect the electrochemical detection due to adsorption processes on the working electrode. In addition, the extra operations performed after acid-microwave digestion, needed to condition the extract for its appropriated measurement by SWASV are

sources of random errors and could negatively influence the precision of the measurements.

The linear working range for the calibration curve Cd^{2+} peak area / Bi^{3+} peak area vs. $[\text{Cd}^{2+}]$ were found between 5 to $95 \mu\text{g kg}^{-1}$ of Cd^{2+} in standard solution. A $\text{LOD} = 0.45 \mu\text{g kg}^{-1}$ of Cd^{2+} , and $\text{LOQ} = 1.63 \mu\text{g kg}^{-1}$ of Cd^{2+} in standard solution were determined. In addition, it was found that high concentrations of copper in cocoa interfere with the quantification of cadmium by SWASV with BiFE. At concentration levels of $30 \mu\text{g kg}^{-1}$ of Cd^{2+} , the cadmium stripping signal is diminished starting from a $\text{Cd}^{2+} : \text{Cu}^{2+}$ concentration ratio of 2 : 1 ($30 : 15 \mu\text{g kg}^{-1}$). In consequence, it is necessary to remove copper from the digestion extracts before cadmium can be quantified. Also, an activated carbon pre-treatment was necessary to clean the digestion extracts of the cocoa powder RM samples. After this pre-treatment, two procedures were satisfactory for the selective removal of copper from the solution. The first is adding the extracts with 1.0 g of chelating resin Chelex 100 in the hydrogen form by the batch method for 2 h. The second applies 2 h of constant potential electrolysis at -0.75 V vs. Ag/AgCl under magnetic stirring. Both procedures allowed the quantification of cadmium by SWASV with BiFE.

On the other hand, as a research center, the Instituto Nacional de Metrología de Colombia is always searching for new and more suitable methodologies to support existing and traditional quantification methodologies, such as AAS and ICP-MS, to verify and characterize certified reference materials. In this sense, the developed and optimized method in this investigation represents a valuable and practical alternative to produce certified reference materials of cadmium in solution. As far as the present investigation was able to go, it is ready to provide an accurate determination of cadmium with and without interference cations such as Zn^{2+} , Fe^{2+} and Cu^{2+} , in standard solutions and other matrices such as water. Additionally, the scope of the methodology could be extended for the detection of other cations of interest, like Pb^{2+} and Cu^{2+} in standard solutions, water, and cocoa beans matrices.

Regarding the quantification in the cocoa matrix, the method shows remarkable potential for cadmium quantification. However, based on the results found in this research, the following recommendations are proposed for future work. First, continue optimizing the acid microwave-assisted digestion methodology for cocoa samples to improve digestion quality and eliminate interferences during the electrochemical analysis. The power ramp and sample weight would be the main parameters to be optimized. In addition, to improve the performance parameters, bias, and repeatability of the electroanalytical methodology, it is necessary to optimize the pre-treatment with activated carbon to remove interferences, residual organic matter, and the most abundant cations. Finally, the proposed electrochemical method should be tested in a portable system (portable potentiostat module and graphite sensors electrodes setup, See Appendix A) for field application of cadmium determination in different environmental matrices, including cocoa beans.

A. Appendix: Portable potentiostat experiment

A.1. Introduction

A potentiostat is an analytical and electronic instrument designed to control the working electrode's potential and measure the current flow through an electrochemical cell in the performing of electroanalytical measurements (Sun and Hall, 2019; Bezuidenhout et al., 2018). The commercially available potentiostats most used in analytical laboratories are large and expensive (Krorakai et al., 2021) limiting their application in studies with limited resources or/and field experiments. As a solution to the above, electrochemical sensing has been developed and applied in fields such as food control, environmental measurements, and clinical studies, as a low-cost and easy-to-use electrochemical setting (Kurbanoglu et al., 2020; Yan et al., 2021; Mohankumar et al., 2021). In recent years, different studies have developed reasonable cost and open-source potentiostats (Krorakai et al., 2021; Dobbelaere et al., 2017; Lopin and Lopin, 2018). In addition, the coupling of smartphones in electrochemical detection systems is increasingly used. In these systems, potentiostats are connected to the smartphone through Wi-Fi, USB, or Bluetooth to accomplish data collection and processing, result display, and sharing (Xu et al., 2019).

On the other hand, screen-printed electrodes (SPEs) are electrochemical devices manufactured by printing different types of ink, such as carbon, silver, gold, and platinum, on plastic or polymeric substrates. Fast in-situ analysis with high reproducibility, sensitivity, and accuracy can be accomplished using SPEs (Renedo et al., 2007). The selection of ink used in the manufacture of the SPE depends on its purpose and determines its performance parameters.

The Sensit BT electrochemical sensor, alongside with ItalSens IS-C sensors by PalmSens, are used to present a demonstration of the application of the SWASV with BiFE methodology in the quantification of cadmium in a certified reference material of cadmium in solution, using the single-point standard addition with internal standard calibration method, developed in this thesis.

A.2. Experimental

A.2.1. Reagents

Standard solutions, samples, and the supporting electrolyte were prepared using type I water. Analytical grade sodium acetate ($\geq 99\%$, w/w) and glacial acetic acid (Merck, 100%, w/w) were used to prepare the supporting electrolyte in a total acetate concentration of 0.5 M. The pH of the solution was adjusted to a value equal to 4.3 with a solution of 1 M NaOH. The Cd^{2+} and Bi^{3+} stock solutions were prepared gravimetrically using a Cd^{2+} standard solution of $1.000 \pm 0.002 \text{ g L}^{-1}$ (Sigma-Aldrich Inc.), $\text{Bi}(\text{NO}_3)_3 \cdot 5\text{H}_2\text{O}$ (PanReac AppliChem, $\geq 98\%$, w/w) and the supporting electrolyte as the solvent. The standard reference material (RM) NIST 3108 (Cadmium $10.007 \pm 0.027 \text{ mg g}^{-1}$ in 1.3 M HNO_3 solution) was used as a sample to test the portable potentiostat. The two points of the calibration curve were prepared gravimetrically in Falcon® tubes (50 mL).

A.2.2. Samples

The RM, certified concentration of $10.007 \pm 0.027 \text{ mg g}^{-1}$ of Cd^{2+} , was used to prepare a sample in concentration of $35 \mu\text{g kg}^{-1}$ of Cd^{2+} . The latter required two intermediate solutions, one of $221.32 \text{ mg kg}^{-1}$ and the other of 4.77 mg kg^{-1} of Cd^{2+} . The cadmium concentration in the RM was estimated using the proposed single-point standard addition with the internal standard calibration method (Section 3.3.1).

A.2.3. Instrumentation, electrochemical cell and electrodes

The experiment was carried out using the Sensit BT (PalmSens BV Inc.) electrochemical sensor and Android app PStouch (version 2.8, PalmSens BV Inc.). Italsens Sensors IS-C (carbon material as the counter and the working electrode, and silver as the reference electrode, PalmSens BV Inc.) were employed in the measurement. A new IS-C Sensor was employed for every single measurement. The PStouch software (version 5.9.3803, PalmSens BV Inc.) was used to analyze the voltammograms and calculate the corresponding peak areas. The experimental setup is shown in Figure A-1. The bismuth film was formed by the *in situ* method using $500 \mu\text{g kg}^{-1}$ of Bi^{3+} in the electrochemical cell. The optimized SWASV parameters obtained in Chapter 3 were used in this experiment, except for the deposition potential that had to be increased to -1.7 V vs. Ag , and the SWASV potential limits, -1.7 V to 0.4 V vs. Ag . These changes were made considering the change of the reference electrode from Ag/AgCl to Ag . The experimental parameters for SWASV are shown in Table A-1.

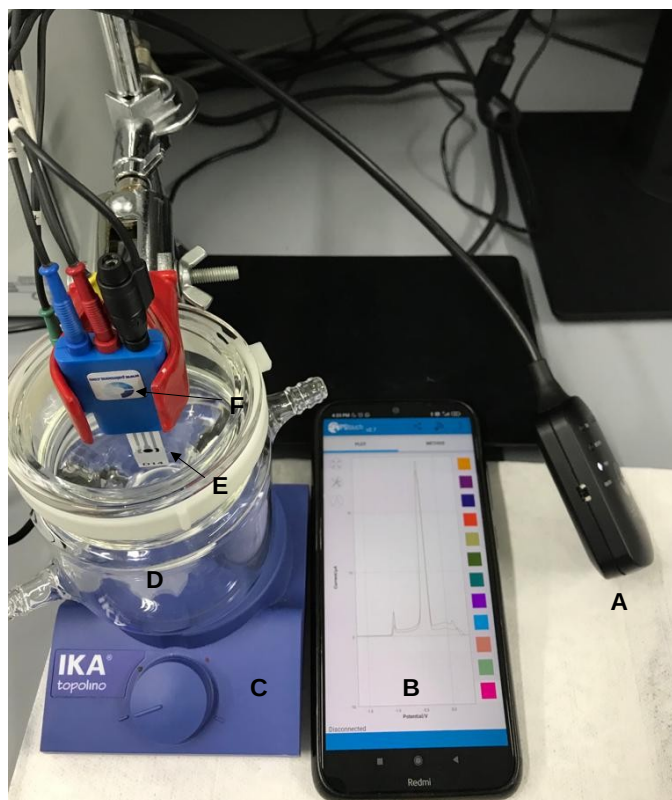


Figure A-1.: Experimental setup for SWASV measurement for portable potentiostat experiment. (A) Sensit BT electrochemical sensor; (B) Smartphone with PSTouch App for data collection; (C) Magnetic stirrer; (D) Electrochemical cell; (E) ItalSens Sensor IS-C; (F) Sensor Connection.

Table A-1.: Electrochemical parameters used in the determination of cadmium using SWASV with the Sensit BT electrochemical sensor and ItalSens Sensors.

Parameter	Value
Deposition potential	-1.70 V vs. Ag
Deposition time	120 s
Rest time	20 s
Agitation rate	500 rpm
Pulse amplitude	20 mV
Pulse frequency	25 Hz
Square wave voltammetry potential limits	-1.70 to 0.40 V vs. Ag

A.3. Results

The SSA-IS calibration method implemented in this work was tested in a portable system to quantify cadmium in the RM NIST 3108 by SWASV with BiFE. Figure A-2 shows the voltammograms obtained for the non-spiked and the spiked RM solution. Well-defined cadmium and bismuth oxidation signals are observed at approximately -0.99 and -0.39 V vs. Ag, respectively. The calibration curve was constructed using the Bi signal as an *in situ* internal standard (Cd^{2+} peak area / Bi^{3+} peak area vs. $[\text{Cd}^{2+}]$). Then, the concentration of cadmium, $[\text{RM}]_{\text{measured}}$, was calculated by extrapolation and considering the corresponding dilution factors. A $[\text{RM}]_{\text{measured}} = 8.20 \text{ mg g}^{-1}$ was obtained with a bias of -18 %.

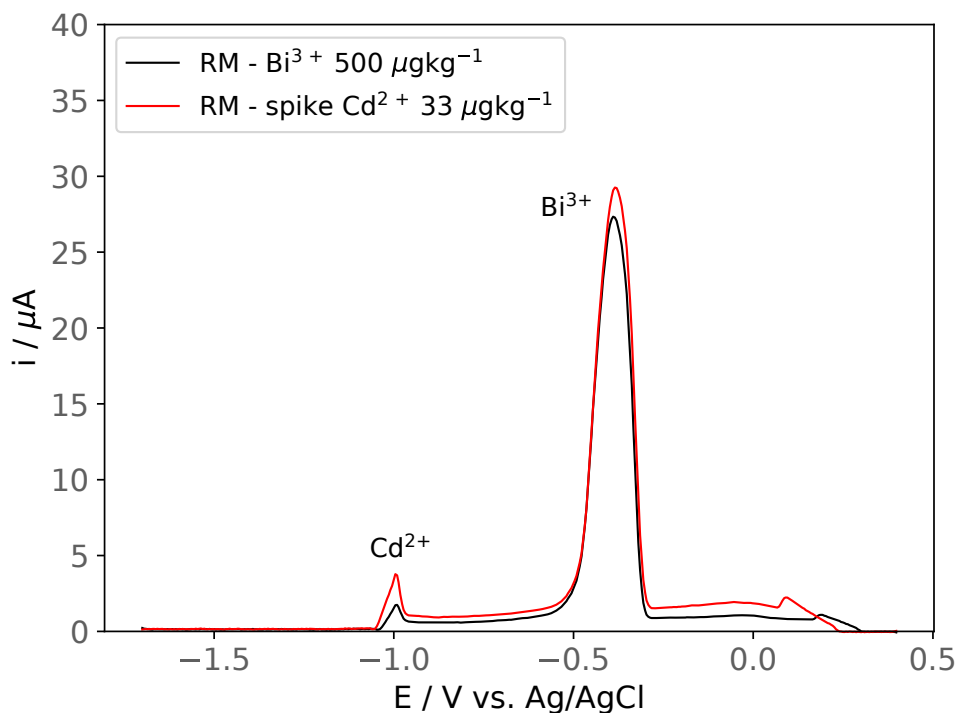


Figure A-2.: Voltammograms using SWASV of a calibration curve by SSA-IS calibration method of an RM solution in acetate buffer 0.5 M, and $\text{pH} = 4.3$ with $[\text{Bi}^{3+}] = 500 \text{ } \mu\text{g kg}^{-1}$ (black line), and then spiked with $[\text{Cd}^{2+}] = 33 \text{ } \mu\text{g kg}^{-1}$ (red line).

The trueness level is within the acceptable criteria according to the concentration range (Joint FAO/WHO Codex Alimentarius Commission, 1992; Committee et al., 2011). This result shows the potential of the analytical technique in portable systems.

A.4. Conclusions

The cadmium concentration in an RM in solution was satisfactorily quantified by the SSA-IS calibration method by SWASV with BiFE in the Sensit BT portable system, using screen-printed electrodes. The trueness results showed that the technique has great potential for field applications. In addition, using a portable potentiostat alongside screen-printed electrodes complements the developed electroanalytical methodology and creates a simple, agile, and effective protocol for quantifying cadmium in solution. Further experiments and optimization studies will improve the method and its application in different matrices.

A.5. References

- Bezuidenhout, P., Smith, S., and Joubert, T.-H. (2018). A low-cost inkjet-printed paper-based potentiostat. *Applied Sciences*, 8(6):968.
- Committee, A. I. M. et al. (2011). Standard method performance requirements-aoac international methods committee guidelines for validation of biological threat agent methods and/or procedures. *J. AOAC Int.*, 94:1359–1381.
- Dobbelaere, T., Vereecken, P. M., and Detavernier, C. (2017). A usb-controlled potentiostat/galvanostat for thin-film battery characterization. *HardwareX*, 2:34–49.
- Joint FAO/WHO Codex Alimentarius Commission (1992). *Codex alimentarius*. Food & Agriculture Org.
- Krorakai, K., Klangphukhiew, S., Kulchat, S., and Patramanon, R. (2021). Smartphone-based nfc potentiostat for wireless electrochemical sensing. *Applied Sciences*, 11(1):392.
- Kurbanoglu, S., Erkmen, C., and Uslu, B. (2020). Frontiers in electrochemical enzyme based biosensors for food and drug analysis. *TrAC Trends in Analytical Chemistry*, 124:115809.
- Lopin, P. and Lopin, K. V. (2018). Psoc-stat: A single chip open source potentiostat based on a programmable system on a chip. *PloS one*, 13(7):e0201353.
- Mohankumar, P., Ajayan, J., Mohanraj, T., and Yasodharan, R. (2021). Recent developments in biosensors for healthcare and biomedical applications: A review. *Measurement*, 167:108293.
- Renedo, O. D., Alonso-Lomillo, M., and Martínez, M. A. (2007). Recent developments in the field of screen-printed electrodes and their related applications. *Talanta*, 73(2):202–219.
- Sun, A. C. and Hall, D. A. (2019). Point-of-care smartphone-based electrochemical biosensing. *Electroanalysis*, 31(1):2–16.

- Xu, G., Cheng, C., Yuan, W., Liu, Z., Zhu, L., Li, X., Lu, Y., Chen, Z., Liu, J., Cui, Z., et al. (2019). Smartphone-based battery-free and flexible electrochemical patch for calcium and chloride ions detections in biofluids. *Sensors and Actuators B: Chemical*, 297:126743.
- Yan, K., Karthick Kannan, P., Doonyapisut, D., Wu, K., Chung, C.-H., and Zhang, J. (2021). Advanced functional electroactive and photoactive materials for monitoring the environmental pollutants. *Advanced Functional Materials*, 31(12):2008227.

B. Appendix: Published article

González-Basto, M. C., España-Sánchez, C. A., Ágreda, J. A., & del Pilar Sandoval-Rojas, A.(2022). Improving precision and trueness in the quantification of cadmium using square wave anodic stripping voltammetry and bismuth film electrodes. *Results in Chemistry*, 100630.

C. Appendix: Participation in academic events

1. Electrochemical study of bismuth deposition on the glassy carbon electrode. *IV Colombian Congress of Electrochemistry. Medellín, Colombia.*



2. Cadmium quantification by square wave anodic stripping voltammetry using bismuth film electrode: “in situ” internal standard calibration and single-point standard addition. *34th Latinoamerican Congress of chemistry. Cartagena de Indias, Colombia*



3. Copper interference in cadmium quantification by square wave anodic stripping voltammetry. *1st Regional Meeting of the International Society of Electrochemistry, Prague, Czech Republic.*



1st Regional Meeting
of the International Society of Electrochemistry
August 15th to 19th 2022, Prague, Czech Republic

CERTIFICATE

This is to certify that **Maria Camila Gonzalez Basto** has participated in the 1st Regional Meeting of the International Society of Electrochemistry on August 15th to 19th 2022 in Prague, Czech Republic. She delivered an Oral presentation entitled "Copper interference in cadmium quantification by square wave anodic stripping voltammetry"

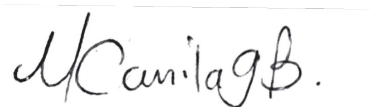
A handwritten signature in blue ink, which appears to read 'Navrátil'.

Prof. Tomáš Navrátil
OC Chair

Declaración

Me permito afirmar que he realizado la presente tesis de manera autónoma y con la única ayuda de los medios permitidos y no diferentes a los mencionados en la propia tesis. Todos los pasajes que se han tomado de manera textual o figurativa de textos publicados y no publicados, los he reconocido en el presente trabajo. Ninguna parte del presente trabajo se ha empleado en ningún otro tipo de tesis.

Bogotá, D.C., 10 de enero de 2023

A handwritten signature in black ink, enclosed in a thin black rectangular border. The signature is written in a cursive style and reads "M Camila GB."

Maria Camila González Basto